Doctoral theses at NTNU, 2022:21

E-Ming Rau

Utilizing inhibitors and genetic engineering to study the biosynthesis of unsaturated fatty acids and lipids in two thraustochytrid strains

Doctoral thesis

NTNU
Norwegian University of Science and Technology
Thesis for the Degree of
Philosophiae Doctor
Faculty of Natural Sciences
Department of Biotechnology and Food Science

NTNU
Norwegian University of
Science and Technology

E-Ming Rau

Utilizing inhibitors and genetic engineering to study the biosynthesis of unsaturated fatty acids and lipids in two thraustochytrid strains

Thesis for the Degree of Philosophiae Doctor

Trondheim, January 2022

Norwegian University of Science and Technology
Faculty of Natural Sciences
Department of Biotechnology and Food Science

NTNU
Norwegian University of
Science and Technology

NTNU
Norwegian University of Science and Technology

Thesis for the Degree of Philosophiae Doctor

Faculty of Natural Sciences
Department of Biotechnology and Food Science

ISBN 978-82-326-5984-5 (printed ver.)
ISBN 978-82-326-5272-3 (electronic ver.)
ISSN 1503-8181 (printed ver.)
ISSN 2703-8084 (online ver.)

Doctoral theses at NTNU, 2022:21

Printed by NTNU Grafisk senter

Acknowledgements

The work in this thesis was financed by the Norwegian Research Council and carried out at the Department of Biotechnology and Food Science (IBT), Norwegian University of Science and Technology (NTNU). The work was a part of the project "AurOmega" (Project No. 90230601) of the Centre for Digital Life Norway, collaborating with SINTEF.

First, I am profoundly grateful to my supervisor Prof. Helga Ertesvåg who has guided me with positive encouragement and constructive advice. She has a great passion for sharing her insightful thoughts and substantial expertise, and always finding time to discuss and help with various issues.

I would like to thank all my other co-authors in my manuscripts, including my co-supervisor Prof. Per Bruheim, Inga Marie Aasen, Zdenka Bartosova and Kåre Andre Kristiansen. Their experimental contributions and thoughtful comments were critical in shaping my research. I would like to acknowledge all the other project team members, collaborators and other people participating in or helping the project, especially Simone Balzer Le, Tonje Marita Bjerkan Heggeset, Prof. Jackie L. Collier and Tone Haugen, for their assistance and willingness to impart their knowledge.

Special thanks belong to all the current and previous members in my research group, especially Garima Jain and Ingerid Onsager, my fellow PhD candidates, and postdocs at IBT. I cherished the time we spent together in the lab, at lunch, at 'payday beer' and in many other indoor and outdoor social settings. I also appreciate all other employees at IBT, who have contributed to a supportive and friendly work environment.

I would like to express my gratitude to my mom, dad, brother, and close friends for their encouragement and unconditional support, providing me a solid foundation and motivation to pursue my personal goals. To conclude, very special thanks belong to my beloved Wei, who is always there with me.

December 2021, Trondheim

E-Ming Rau

Abstract

Thraustochytrids are oleaginous heterotrophic marine eukaryotic microbes known to produce large amounts of docosahexaenoic acid (DHA)-containing triacylglycerols (TAGs), and they also synthesize terpenoids like squalene. These compounds have great economic value and are in high demand. However, DHA produced from thraustochytrids is still more costly than from fish oil whose availability is limited and unstable. Hence, a deeper understanding of the lipid metabolism and genetic manipulation tools in thraustochytrids is vital to developing high productive strains for profitable biomanufacturing. In thraustochytrids, since the fatty acid synthase (FAS) pathway and the DHA synthesizing polyketide synthase-like pathway (PKS) share the same precursors, the first part of this thesis characterized the fatty acid and lipid accumulation between *Aurantiochytrium* sp. T66 (T66) and *Aurantiochytrium limacinum* SR21 (SR21) and studied how it is affected by FAS inhibition. The result showed that the DHA proportion, but not the DHA productivity, was greater under FAS inhibition in the two strains. This suggests that precursor availability for the PKS pathway is not the rate-limiting factor for DHA synthesis. FAS inhibition could also enrich DHA-rich TAG TG(22:6/22:6/22:6) production. Moreover, the conversion of DG(22:6/22:6) to TAGs is potentially a bottleneck for DHA-rich TAGs synthesis. This work then reviewed the genetic engineering methods employed for different thraustochytrid strains and the relevant experience in other organisms to support research on strains that have yet to be successfully transformed. The variables being considered are the transformation methods, genomic integration of DNAs, the elements that regulate gene expression and transformant selection. Genetic engineering was then utilized to characterize genes potentially related to fatty acid (FA) and lipid metabolism, including one

Δ12-desaturase-like gene, *T66des9*, and two type-2 Acyl-CoA:diacylglycerol acyltransferases (DGAT2)-like genes of T66, *T66ASATa* and *T66ASATb*, and their homologs in SR21, *AlASATa* and *AlASATb*. The expression of *T66des9* via genomic knockin in SR21 produced palmitoleic acid (C16:1 n-7) and vaccenic acid (C18:1 n-7), while both FAs were not detected in the control strains. This indicates that T66Des9 is a Δ9-desaturase accepting palmitic acid (C16:0) as a substrate. Genomic knockout of *AlASATa* and *AlASATb* or knockin of the four genes in SR21 showed that the expression of *AlASATb* and *T66ASATb*, and in less extent, *AlASATa* and *T66ASATa*, elevated the accumulation of total steryl esters (SEs), the SEs of C16:0, SE(16:0), and DHA, SE(22:6), and, on the other hand, did not significantly change the level of TAGs or other lipid classes. The results suggest that the four genes encoded proteins possessing acyl-CoA:sterol acyltransferase (ASAT) activity. Furthermore, the expression and overexpression of *T66ASATb* and *AlASATb* enhanced squalene production in SR21. The functional discoveries of the above-mentioned genes pave the way to enhance C16:1 n-7, C18:1 n-7, and squalene production in thraustochytrids through metabolic engineering, and highlight the functional diversity of desaturases and acyl-CoA acyltransferases, which are important to consider when attempting to deduce the function of these proteins solely based on their sequence.

List of Papers

Paper I:

E-Ming Rau, Zdenka Bartosova, Inga Marie Aasen, Per Bruheim and Helga Ertesvåg **Utilizing lipidomics and fatty acid synthase inhibitors to explore lipid accumulation in two *Aurantiochytrium* species** *Manuscript prepared for submission*

Paper II:

E-Ming Rau, Helga Ertesvåg (2021) **Method development progress in genetic engineering of thraustochytrids**. *Marine Drugs,* 19(9), 515

Paper III:

E-Ming Rau, Inga Marie Aasen, Helga Ertesvåg (2021) **A non-canonical Δ9-desaturase synthesizing palmitoleic acid identified in the thraustochytrid *Aurantiochytrium* sp. T66.** *Applied Microbiology and Biotechnology,* 105, 5931–5941

Paper IV:

E-Ming Rau, Zdenka Bartosova, Kåre Andre Kristiansen, Inga Marie Aasen, Per Bruheim**,** Helga Ertesvåg ***Aurantiochytrium* species encode two acyl-CoA:diacylglycerol acyltransferase 2 like acyl-CoA:sterol acyltransferases whose overexpression facilitate squalene accumulation.** *Manuscript prepared for submission*

Abbreviations

CLA	*cis9*, *trans*11-conjugated linoleic acid
ACC	acetyl-CoA carboxylase
ACL	ATP:citrate lyase
ACP	acyl carrier protein
ASAT	acyl-CoA:sterol acyltransferase
AT	acyl transferase
Cas9	CRISPR-associated protein 9
CLF	chain length factor
CRISPR	clustered regularly interspaced short palindromic repeats
D/I	dehydrase/isomerase
DAG	diacylglycerol
DE	Desaturase-Elongase
DGAT	and four acyl-CoA:diacylglycerol acyltransferase
DH	dehydratase
DHA	docosahexaenoic acid
EPA	eicosapentaenoic acid
ER	enyolreductase
FAO	The Joint Food and Agriculture Organization of the United Nations
FAS	fatty Acid Synthase
FPP	farnesyl pyrophosphate
GAPT	glycerol-3-phosphate acyl transferase
g_{CDW}	gram cell dry weight
HMGR	β-Hydroxy β-methylglutaryl-CoA reductase
HR	homologous recombination
IDH	isocitrate dehydrogenase
IDH	isocitrate dehydrogenase
KR	keto reductase
KS	β-ketoacyl synthase

LPAAT	five lysoPA acyl transferase
MAG	monoacylglycerol
MAT	malonyl-CoA:ACP transacylase;
MBOAT	membrane-bound O-acyl transferase
ME	malic enzyme
MGAT	acyl-CoA:monoacylglycerol acyltransferase
MUFA	monounsaturated fatty acid
MVA	mevalonate
PAP	three phosphatidic acid phosphatase
PC	Phosphatidylcholine
PE	phosphatidylethanolamine
PES	phytyl ester synthase
PITP	phosphatidylinositol transfer protein
PKS	polyketide synthase
PSAT	phosphatidylcholine-sterol O-acyltransferase
PUFA	polyunsaturated fatty acid
SE	steryl ester
SM	mono-oxygenase
SQS	Squalene synthase
SR21	*Aurantiochytrium limacinum* SR21
T66	*Aurantiochytrium* sp. T66
TAG	triacylglycerol
TCA	tri-carboxylic acid
TMD	transmembrane domain
UFA	unsaturated fatty acid
WS	wax ester synthase

Table of Contents

1 Introduction

This thesis provides new insights on lipid and unsaturated fatty acid biosynthesis in thraustochytrids, a group of microbes with promising properties to be utilized in sustainable biomanufacturing. The biology and biotechnological applications of thraustochytrids include a wide range of topics. Hence, to provide a context for this study, the biological features and classification of thraustochytrids are first summarized. This is followed by presenting the application and metabolism of the selected unsaturated fatty acids and terpenoids in thraustochytrids. Relevant research in other species is also highlighted.

1.1 Thraustochytrids: biological features and classification

Thraustochytrids are marine unicellular protists, belonging to the stramenopiles (also known as heterokonts). With few exceptions, thraustochytrids have general features that include 1) non-cellulosic cell walls; 2) the 'rhizoid-like' structures, ectoplasmic nets; and 3) biflagellate zoospores (Alderman et al., 1974; Marchan et al., 2018). They are present in a wide range of marine habitats, covering tropical (Ramaiah et al., 2005), temperate and cold waters (Bahnweg and Sparrow Jr., 1974; Rosa et al., 2011). Since they are obligate heterotrophic organisms and require the presence of organic matter to grow, thraustochytrids are more abundant in habitats like the photic zone of shallow coastal water or mangroves (Raghukumar, 2002). Most thraustochytrid species contain multi-hydrolytic enzymes at the ectoplasmic net localized at the outer surface of the plasma membrane. These enzymes can be excreted to digest organic materials for the cell growth (Raghukumar et al., 1994; Bongiorni et al., 2005). Thus, thraustochytrid plays a prominent ecological role by recycling nutrients in marine and

coastal ecosystems (Raghukumar, 2002; Raghukumar and Damare, 2011). The life cycle of thraustochytrids is quite complex and may vary from one genus to another. The common feature of all the genera is the present of a core cycle from vegetative cells that produce multinucleated cells and transform into sporangia (multinucleated cells). After cytokinesis, zoospores are released and then colonize new areas, settle and start the cycle over again (Morabito et al., 2019).

Thraustochytrids consist of at least ten genera (Figure 1). However, their genera and species are frequently reassigned according to the updated analytical results. Based on phylogenetic, morphologic and metabolic analyses, the genus *Schizochytrium* was divided into three genera: *Schizochytrium*, *Aurantiochytrium*, and *Oblongichytrium.* The colonies and ectoplasmic nets of *Aurantiochytrium* are smaller and less developed than those of *Schizochytrium*, respectively. *Aurantiochytrium* also has a more diverse carotenoid profile than *Schizochytrium*. Consequently, *Schizochytrium limacinum* SR21 was renamed *Aurantiochytrium limacinum* SR21 (Yokoyama and Honda, 2007).

Aurantiochytrium limacinum SR21 (hereafter called SR21) was isolated from the mangrove area of Yap Islands, Micronesia, in the western Pacific Ocean (Nakahara et al., 1996; Honda et al., 1998). *Aurantiochytrium* sp. T66 (hereafter called T66) was isolated from the coast of Madeira, Portugal, in the eastern Atlantic Ocean (Jakobsen et al., 2007). In this work, the metabolic pathways of T66 and SR21 related to their biotechnological potentials are selected to be investigated.

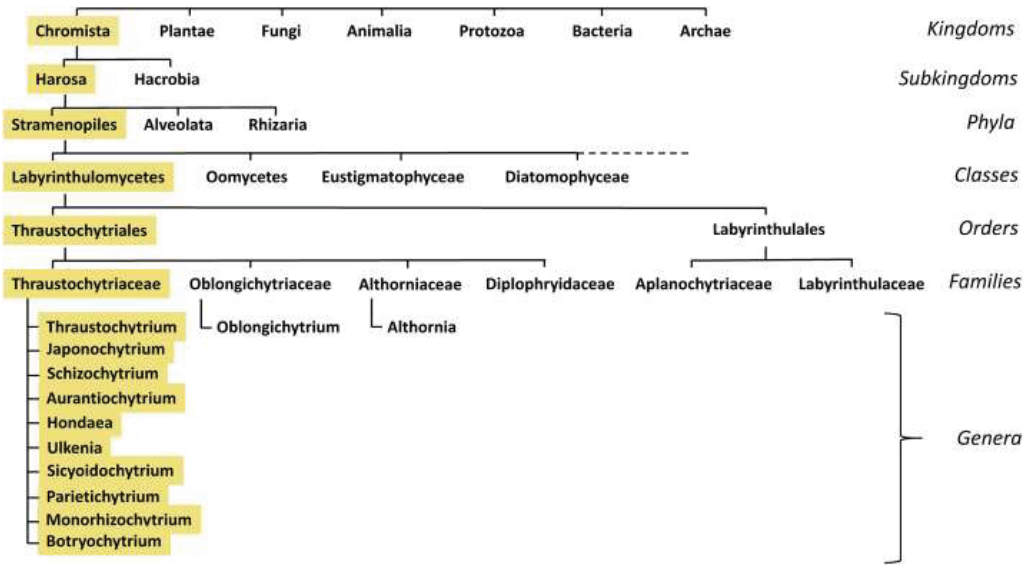

Figure 1. Taxonomy of thraustochytrids and the ten genera. Adapted fromMorabito et al. (2019).

1.2 Thraustochytrids: biotechnological potentials

Thraustochytrids are known to be able to accumulate high levels of docosahexaenoic acid (DHA, C22:6 n-3), squalene and carotenoids. Although less mentioned, palmitoleic acid (C16:1 n-7) and vaccenic acid (C18:1 n-7) are also produced in some thraustochytrid strains. All these compounds are interesting for commercial markets and the demand is a rapidly growing. This section summarizes the application of DHA, C16:1 n-7, C18:1 n-7, squalene and their production in thraustochytrids.

1.2.1 ω-3 polyunsaturated fatty acids

1.2.1.1 Application, demands and sources

ω-3 polyunsaturated fatty acids (PUFAs) are PUFA with a double bond at the ω-3 (also called n-3) position (Figure 2). DHA and eicosapentaenoic acid (EPA) are two ω-3 PUFAs usually considered essential fatty acids since they are unable to be sufficiently synthesized in human bodies and have to be supplied majorly from diets (Finco et al., 2017). Due to the antagonistic properties, increasing the ratio of DHA and EPA to n-6 PUFAs decreases inflammation (Calviello et al., 2013). Since DHA is one of the main structural components distributed in the cellular membrane of the nervous system, it has been considered crucial to infant development of retina and brain (Bazinet and Layé, 2014; DiNicolantonio and O'Keefe, 2020). For adults, recent evidence showed that sufficient DHA and EPA decreased the risk of cardiovascular disease (Mozaffarian and Wu, 2011; Rimm et al., 2018), neurodegenerative disorders, such as Parkinson's disease and Alzheimer's disease (Sinn et al., 2012; Cardoso et al., 2016; Moore et al., 2018) and major depressive disorder (Gertsik et al., 2012; Mocking et al., 2016) Dietary intakes of DHA and EPA may also enhance attention, processing speed, and immediate recall (Mazereeuw et al., 2012).

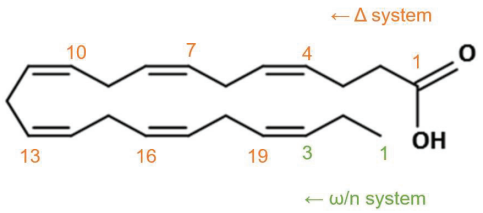

Figure 2. Nomenclature of docosahexaenoic acid, DHA, C22:6 $^{\Delta 4, 7, 10, 13, 16, 19}$ n-3/ω-3. Copied and modified from Silva et al. (2020).

According to the Joint Food and Agriculture Organization of the United Nations (FAO) and Grand View Research, the global demand for ω-3 FAs is projected to grow 16% annually from 2015 to 2025 (Finco et al., 2017). Today, ω-3 FAs are most widely supplied from fish oil, which was produced around 1 million tonnes annually in the world (Sakthivel, 2016). FAO and the World Health Organization recommended 0.3 g/day EPA plus DHA uptake for pregnant and lactating adult, and 0.25 g/day of EPA plus DHA uptake for the rest of the adults (FAO, 2010). Supplements for humans based on fish oil are sold for about €0.12 – €0.26 per 300 mg DHA/EPA containing softgel/capsule (van der Voort et al., 2017). Similar to humans, marine fish in aquaculture like salmon require DHA but do not produce it themselves (Tocher, 2015). Globally, fish farming by aquaculture has shown a continuously growing trend, with an estimated annual growth rate of 2.1% from 2017 to 2030 (FAO, 2018). Aquaculture is the segment that consumes most fish oil, accounting for about 70% of the global demand. However, the wild fish catch peaked in the early 1990s and has been constant ever since, indicating that it might have met the maximum capacity (Salem and Eggersdorfer, 2015; Tocher et al., 2019). In addition, fish oil might be contaminated by heavy metals and mutagenic substances (Castro-González and Méndez-Armenta, 2008). It may have an unpleasant smell and taste, due to the generation of oxidation products from ω -3 PUFA, such as aldehydes, ketones, alcohols, alkanes and alkenes (Hamre et al., 2001). Furthermore, it cannot be used in vegetarian diets.

1.2.1.2 Thraustochytrid production

Thraustochytrids are known for their ability to produce large amount of DHA. Still, thraustochytrid DHA content and productivity can differ, depending on the strains and cultivation conditions. T66 and SR21 can have DHA content up to 35.76 % and 67.76 %,

respectively, of total fatty acids (Patel et al., 2019; Patel et al., 2020). The productivity of DHA in T66 can be around 75 mg/l/h by using glycerol as the carbon source (Jakobsen et al., 2008), while SR21 can have the DHA productivity up to 337 mg/l/h through using glucose and glycerol as the mixed carbon sources (Li et al., 2015).

1.2.2 Palmitoleic and vaccenic acid

1.2.2.1 Application and demands

Palmitoleic acid, C16:1$^{\Delta 9}$ n-7 (C16:1 n-7) and vaccenic acid, C18:1$^{\Delta 11}$ n-7 (C18:1 n-7), are monounsaturated fatty acids (MUFAs).

C16:1 n-7 have a variety of application. C16:1 n-7 plays an important role in the pathophysiology of insulin resistance in humans. (Maedler et al., 2003; Dimopoulos et al., 2006; Stefan et al., 2010). Another application of C16:1 n-7 is for the production of 1-octene, which is highly demanded as co-monomer in the production of polyethylene (Rybak et al., 2008; Nguyen et al., 2010). C16:1 n-7 can also improve biodiesel properties, as methyl palmitoleate has a lower melting point while still considered oxidative stable (Knothe, 2010; Nguyen et al., 2015).

Recent knowledfe of C18:1 n-7 on benefiting human health is emerging. *Trans*-C18:1 n-7 is a precursor for the endogenous synthesis of *cis9*, *trans*11-conjugated linoleic acid (CLA) (c9, t11-C18:2) in both humans and animals (Reynolds et al., 2008). CLA shows health benefits because of its anticarcinogenic, antiobesity, antidiabetic and antihypertensive properties (Koba and Yanagita, 2014). Dietary uptake of *trans*-C18:1 n-7 reduces adipocyte size, induces hypolipidemic effects and alleviates metabolic syndrome in animal model (Wang et al., 2008; Mohankumar et al., 2013; Jacome-Sosa et al., 2014). Higher levels of *cis*-C18:1 n-7 in plasma

may be linked to a lower risk of heart failure in people who have already had coronary heart disease (Djoussé et al., 2014). As a potential fetal hemoglobin therapeutic inducer, *Cis*-C18:1 n-7 directly modulates mammalian cell differentiation and gene expression (Aimola et al., 2016).

Table 1. Prescence (marked '+') or absence (marked '-') of C16:1 n-7 and C18:1 n-7 in different thraustochytrid species/strains.

Strains/Species	C16:1 n-7	C18:1 n-7	Reference
Hondaea fermentlagiana CCAP 4062/3	+	+	(Dellero et al., 2018)
*Aurantiochytrium sp.*T66	+	+	(Jakobsen et al., 2008)
Aurantiochytrium sp. SD116	+	-	(Gao et al., 2013)
Schizochytrium sp. HX308	+	-	(Ren et al., 2018)
Thraustochytrium sp. ATCC 20889	+	-	(Jiang et al., 2004)
Aurantiochytrium limacinum CCAP 4062/1	-	+	(Dellero et al., 2018)
Aurantiochytrium limacinum SR21	-	-	(Yokochi et al., 1998)
Aurantiochytrium mangrovei Sk-02	-	-	(Chodchoey and Verduyn, 2012)

1.2.2.2 Thraustochytrid production

C16:1 n-7 and C18:1 n-7 are present only in some thraustochytrid strains (Table 1). In T66, C16:1 n-7 and C18:1 n-7 can accumulate up to 13% and 8%, respectively, of the total fatty acid under nitrogen starvation (Jakobsen et al., 2008). C16:1 n-7 and C18:1 n-7 have not been detected in strains like SR21 (Yokochi et al., 1998).

1.2.3 Squalene

1.2.3.1 Application and demands

Squalene is a linear polyunsaturated dehydro-triterpene with 30 carbons ($C_{30}H_{50}$) (Figure 3). It is used widely in the food, cosmetics and medicine industries due to its multiple functions. Squalene is a powerful natural antioxidant that can protect cells from free radicals and reactive oxygen species (Güneş, 2013). It is also anti-tumorigenic, inhibits chemically induced tumorigenesis (De Stefani and Ronco, 2013). Moreover, squalene can modulate fatty acid metabolism (Ravi Kumar et al., 2016), and reduce serum cholesterol levels (Chan et al., 1996). Due to its potential capability of increasing immune responses, squalene can be used as an adjuvant in vaccines such as flu vaccines (Giudice et al., 2006). With a compound annual growth rate of 7.8%, the squalene market is expected to increase swiftly from $140 million in 2019 to $204 million in 2024 (Meng et al., 2020).

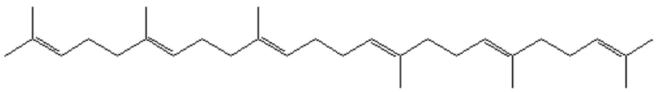

Figure 3. Squalene. Copied from Fox (2009).

Traditionally, squalene is majorly isolated from the liver oil of deep-sea sharks for commercial purposes, with the mean price around $45.75/kg (Xu et al., 2016; Macdonald and Soll, 2020). However, shark populations are decreasing because of the uncontrolled killing, which has endangered shark species and led to ecological concerns (Alexa, 2020). As a result, an urgent need has been raised to produce squalene in a renewable and sustainable approach.

1.2.3.2 Thraustochytrid production

Thraustochytrids can accumulate relatively high amounts of squalene (Aasen et al., 2016), although squalene mainly do not accumulate in large amount in the cell, as it is an intermediate in the biosynthesis of sterols and carotenoids (Gohil et al., 2019). Similar to FA composition, the squalene content of many thraustochytrids varies from one strain to another. Generally, *Aurantiochytrium* has higher squalene than other thraustochytrid genera. *A. limacinum* could produce five times more squalene than *H. fermentalgiana* (Dellero et al., 2018). SR21 and T66 have been shown to produce squalene with the highest yields recorded as 930 mg/L (32 mg/g_{CDW}) and 1.0 g/L (88 mg/g_{CDW}), respectively, through utilizing low-cost feedstock (Patel et al., 2019; Patel et al., 2020).

1.2.4 Thraustochytrids as commercial producers

Currently, several companies have developed commercial DHA production via thraustochytrids. In 2020, as the market leader for microbial DHA production from thraustochytrids, DSM launched 'life'sDHA® SF55-O200DS' with 550 mg/g DHA produced from *Schizochytrium*, as a supplement to maternal people and infants (DSM, 2020). The dietary supplement DHAid™ of Lonza contains DHA ≥400 mg/g, originating from *Ulkenia* sp. (Freitas and Leblanc, 2008). Aquafauna Bio-Marine, Inc. has developed the product Algamac™-enrich as an aquaculture feed, containing whole-cell *Schizochytrium* (aka *Aurantiochytrium*) with a formulation of 8-10% DHA and 30-33% total lipids (Aquafauna_Bio-Marine, 2019). However, the current price of microbial DHA is more expensive than DHA from fish oil. For instance, supplements based on fish oil are sold for about €0.12-€0.26 per 300 mg DHA/EPA containing softgel/capsule, while the microbial supplements are sold for about €0.34-€0.46 per 300 mg

DHA/EPA containing softgel/capsule (van der Voort et al., 2017). Hence, the urgent task is to produce thraustochytrid DHA more competitively than animal-source production.

1.2.5 Genetic engineering in thraustochytrids

Genetic engineering methods are important to understand the function of genes in metabolic pathways. They are also essential to build strains through rational designs that produce valuable compounds at higher rates and titers (Riley and Guss, 2021). Genetic engineering technologies have been established in some thraustochytrid species and strains. Electroporation, biolistic transformation (also called particle bombardment) and *Agrobacterium*-mediated transformation are among the most prevalent methods that have been applied in thraustochytrids (Aasen et al., 2016; Morabito et al., 2019).

Different electroporation conditions have been used to transform the expression cassettes with various designs into SR21 cells, which are mostly eventually integrated into the genomes through homologous recombination (HR). Engineered SR21 strains have been obtained by knock-in of a cassette composed of the Zeocin resistance gene *ble* or the fusion of *ble* and the enhanced green fluorescent protein gene, driven by 1.3kb promoter and 1.0kb terminator regions of the endogenous glyceraldehyde-3-phosphate dehydrogenase gene and placed next to the partial sequences of endogenous 18S ribosomal RNA gene (Faktorová et al., 2020). The transformation efficiency to SR21 cells could be improved by agitating with glass beads or the assistance from the clustered regularly interspaced short palindromic repeats (CRISPR) and CRISPR-associated protein 9 (Cas9) system via the homology-directed repair mechanism (Watanabe et al., 2020). In SR21, genetic engineering was used to demonstrate the function of

the genes contributing to fatty acid production (Li et al., 2018a; Li et al., 2018b; Ling et al., 2020; Watanabe et al., 2020) or the function of signal peptides (Okino et al., 2018).

Still, for some thraustochytrid strains, including T66, genetic engineering methods have not been developed.

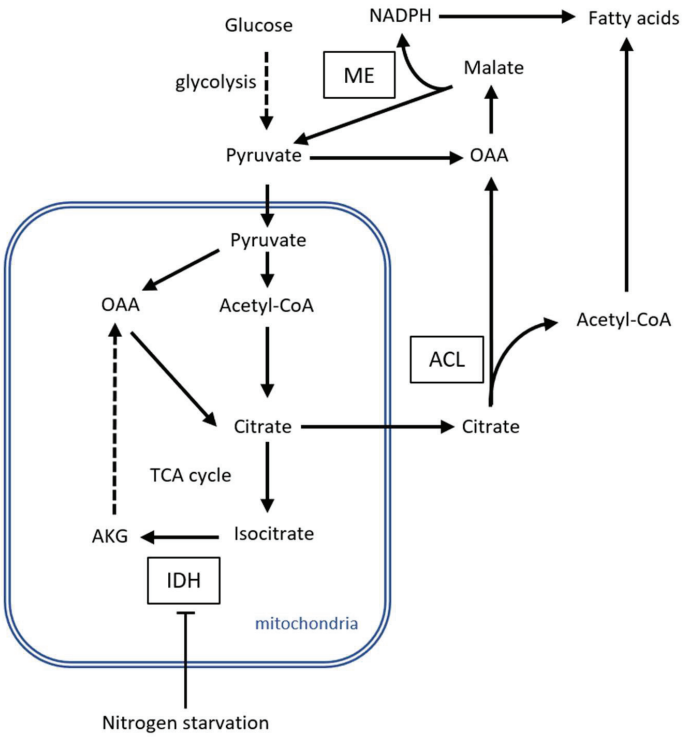

Figure 4. Pathway for generating fatty acids during nitrogen starvation in oleaginous microorganisms. Under nitrogen limitation, the cellular content of AMP is reduced, leading to a reduction in the activity of the AMP-dependent isocitrate dehydrogenase (IDH) of the tri-carboxylic acid (TCA) cycle. As a result, isocitrate and citrate accumulate, with the latter increasingly efflux from mitochondrion to cytosol. Citrate is split into oxaloacetic acid and acetyl-CoA by ATP:citrate lyase (ACL). Oxaloacetic acid converts to malate, which is used to generate NADPH by malic enzyme (ME). Acetyl-CoA and NADPH are the building block and the reducing power provider, respectively, for fatty acid synthesis (Ratledge, 2004). ACL was not found in T66 based on sequence homologies to known ACL (Heggeset et al., 2019). AKG, α-ketoglutaric acid; OAA, oxaloacetic acid. Adapted from Heggeset et al. (2019).

1.3 Thraustochytrids: fatty acid, lipid and terpenoid synthesis

Different culture conditions, such as carbon source, oxygen concentration, salinity, temperature and nutrient availability, affect the synthesis and accumulation of fatty acids, lipids and terpenoids in thraustochytrids. These compounds are also synthesized by metabolic pathways with various genes and enzymes involved (Aasen et al., 2016). This section describes the current knowledge of lipid accumulation triggered by nitrogen starvation as well as the roles or influences of desaturases, acyl-CoA:acyltransferases and cerulenin treatment in desaturase-elongase (DE), triacylglycerol (TAG), steryl ester (SE) and squalene synthesis pathways.

1.3.1 Nitrogen and lipid accumulation

Nitrogen limitation triggers a series of reactions that result in the enhanced FA synthesis, which has been elucidated in oleaginous microbes like yeasts and filamentous fungi (Figure 4). Although this regulatory mechanism has not been substantially studied in thraustochytrid, N-starvation has been shown to enhance lipid accumulation in various thraustochytrid species/strains, including T66 and SR21 (Yokochi et al., 1998; Jakobsen et al., 2008; Ren et al., 2010; Janthanomsuk et al., 2015). Similarly, when considering the availability of both carbon and nitrogen sources, a high C:N ratio was suitable to obtain high DHA yields in SR21 (Yokochi et al., 1998; Rosa et al., 2010). In fed-batch fermentation, the starting time of nitrogen starvation phase is closed to the leveling out of CO_2-emission rate (Figure 5) (Heggeset et al., 2019).

DHA and C16:0, followed by C14:0 and docosapentaenoic acid (DPA), are the most abundant FAs in thraustochytrids, while the presence of other FAs may vary from one strain to another. Based on the PUFA composition, thraustochytrids can be roughly separated into 5 groups: DHA/DPA, DHA/DPA/EPA, DHA/EPA, DHA/DPA/EPA/arachidonic acid (ARA), and DHA/DPA/EPA/ARA/docosatetraenoic acid (Huang et al., 2003). Both T66 and SR21 are classified in the DHA/DPA group.

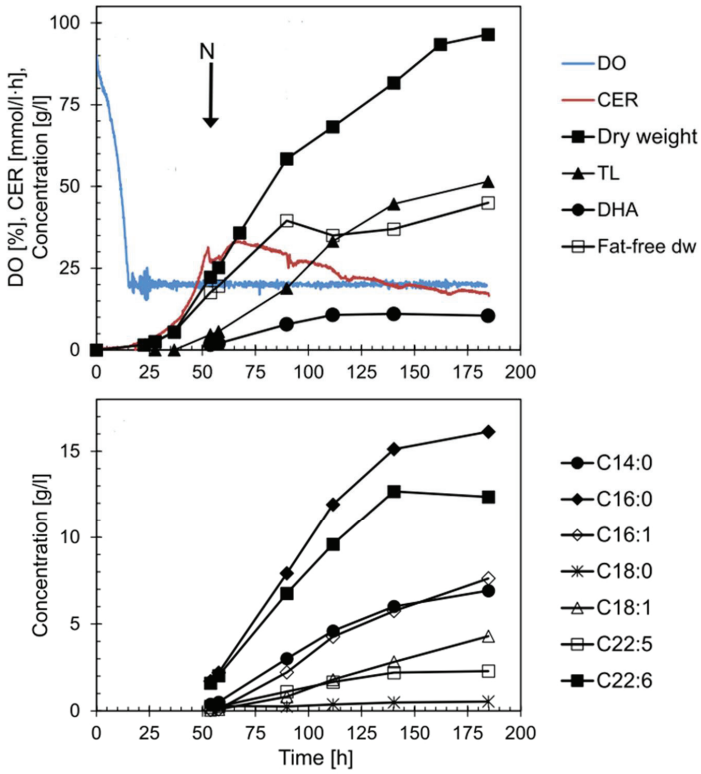

Figure 5. T66 cell growth, lipid and fatty acid production in fermentations with N-starvation. N: N-depletion indicated via the CER peak; TL, total lipid; DHA, C22:6; DO, dissolved oxygen; CER, CO_2 emission rate. Copied and modified from Heggeset et al. (2019).

1.3.2 Fatty acids

Acetyl-CoA and NADPH are the common precursors for all FAs. Acetyl-CoA is converted into malonyl-CoA by acetyl-CoA carboxylase (ACC). Afterwards, saturated fatty acids (SFAs) are synthesized exclusively by Fatty Acid Synthase (FAS). In contrast, unsaturated fatty acid (UFA) can be synthesized by two different pathways that function independently: the aerobic elongase-desaturase (DE) pathway, and the anaerobic polyketide synthase-like (PKS) pathway (Figure 6) (Hauvermale et al., 2006; Sun et al., 2020; Patel et al., 2021).

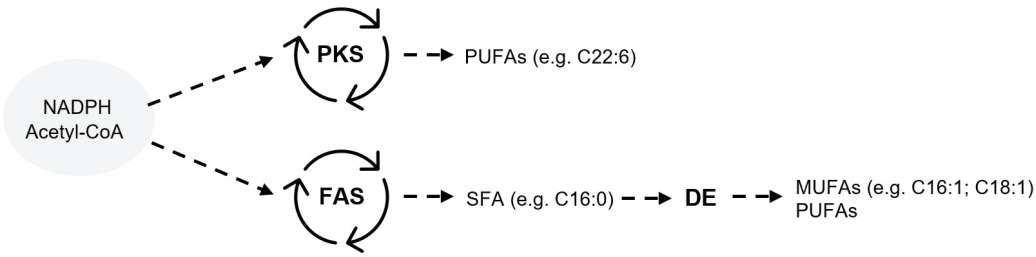

Figure 6. Summary of the main FA pathways in thraustochytrids. PKS generates ω-3 FAs like DHA (C22:6) exclusively, and some ω-6 FAs like DPA. FAS synthesize SFA exclusively. DE produce MUFA and most ω-6 FAs. Adapted from Li et al. (2018a).

1.3.2.1 Fatty Acid Synthase (FAS) pathway

The domains of the multi-subunit enzyme type I FAS complex catalyze a series of ordered and repetitive reactions that result in the production of the SFA C16:0 by adding two carbons at each cycle (Figure 7).

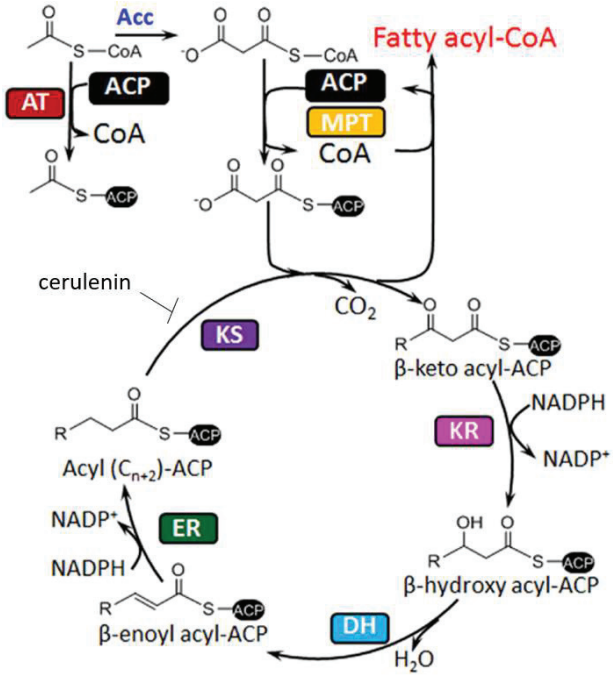

Figure 7. Typical FAS I catalytic reaction cycle and the target of cerulenin inhibition. ACC: acetyl-CoA carboxylase. Acyl carrier protein (ACP) acyltransferase (AT) activates acetyl-CoA, while malonyl/palmitoyl transferase (MPT) constantly feeds malonyl-CoA into the reaction cycle. The elongation process is catalyzed by ketoacyl reductase (KR), dehydratase (DH), and enoyl reductase (ER) in that order. Fatty acyl-CoA (usually C16:0) is released from the enzyme after several rounds of elongation. Copied and modified from Zhou et al. (2014).

1.3.2.2 Desaturase-Elongase (DE) pathway

MUFAs and PUFAs can be produced from C16:0 through series of desaturation and elongation by the DE pathway (Figure 8). The FAS and DE pathway collectively called the FAS-DE pathway. Desaturases are enzymes that introduce double bonds to fatty acids. The length of the fatty acyl chain is increased by adding a two-carbon acetyl group to the carboxyl end of the fatty acid by elongases.

1.3.2.2.1 Desaturase properties and classification

Desaturases are nonheme, di-iron-containing mixed-function oxidases, requiring molecular oxygen and electrons flow via cytochrome b_5, cytochrome b_5 reductase, and NAD(P)H for their catalytic activities (Nagao et al., 2019). Desaturases can be classified as either soluble or integral membrane desaturases. Soluble desaturases are primarily found in plastids of higher plants and specifically desaturate stearoyl-ACP (acyl carrier protein) to produce oleoyl-ACP. On the other hand, integral membrane desaturases show a high diversity of protein sequence, substrate range and regioselectivity (Nachtschatt et al., 2020). Integral membrane desaturases have three conserved histidine boxes that collectively bind two iron ions: $[H(X)_{3-4}H]$, $[H(X)_{2-3}HH]$ and $[H/Q(X)_{2-3}HH]$ (H, histidine; X, variable amino acid; Q, glutamine). The desaturases mentioned in the content below are all integral membrane desaturases.

1.3.2.2.2 Desaturase diversity and evolution

Integral membrane desaturases can be classified into two groups. The first group accepts SFAs as substrates, such as Δ9-desaturase that introduces a *cis*-double bond at the Δ9 position of saturated C16 or C18 acyl-CoA (Figure 8). Another group introduces a double bond on MUFAs or PUFAs, including Δ12-desaturase that introduces a *cis*-double bond at the Δ12 position of C18:1 n-9 acyl-CoA (Figure 8) (Matsuda et al., 2012; Nagao et al., 2019; Nachtschatt et al., 2020).

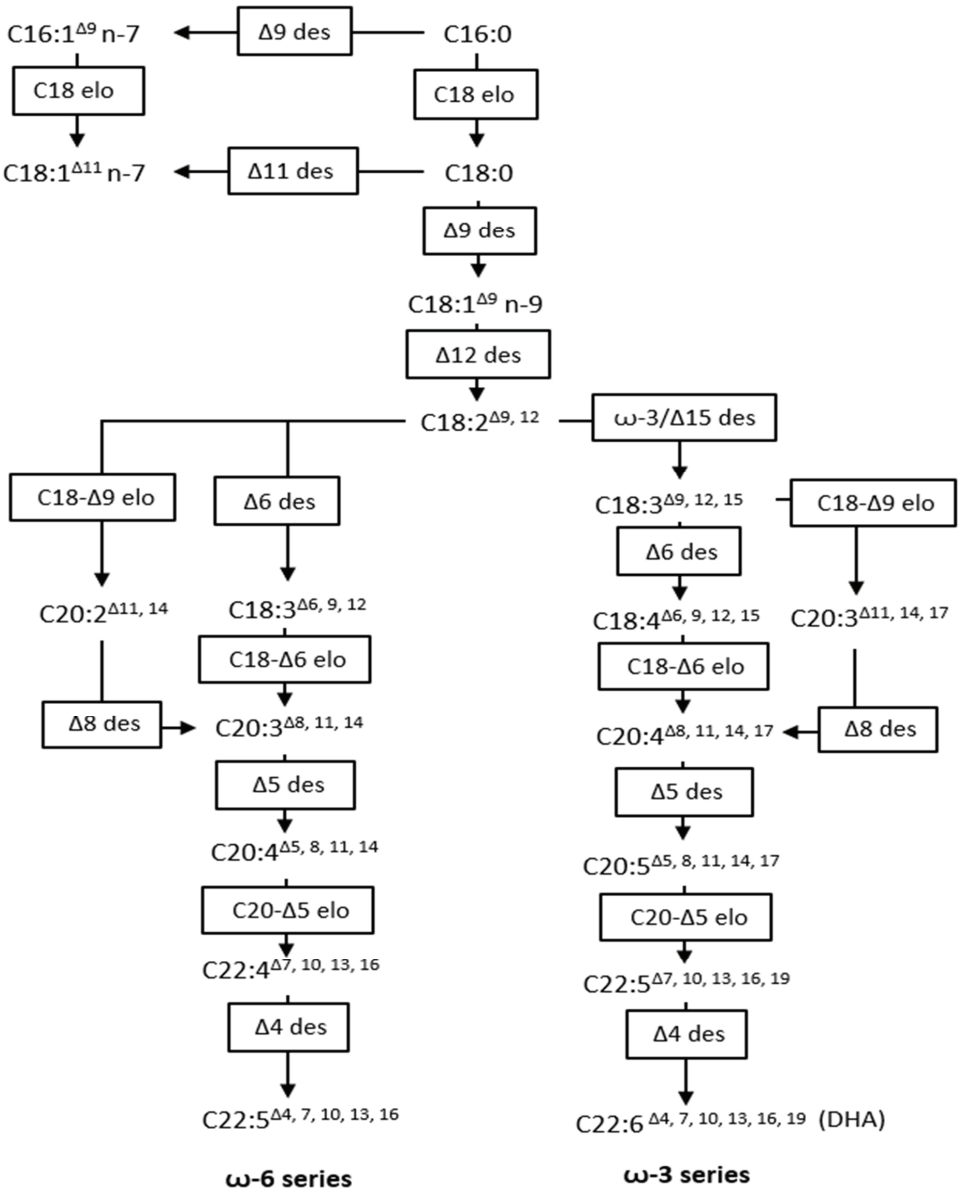

Figure 8. Typical Desaturase-Elongase (DE) pathway. Des, desaturase; elo, elongase. Adapted from Dellero et al. (2018).

Phylogenetic studies of desaturases have shown that desaturase sequences are highly diverse and can be grouped into different clades (Figure 9) (Sperling et al., 2003; Wilding et al., 2017). For example, Δ9-desaturases and Δ12-desaturases are located at different clades. However, it has been emphasized that some of the amino acids now found to be specific for one clade of desaturases might not be necessary for their specific functions since these genes presumably duplicated fairly early in evolution, and then new mutations changed their functions (Sperling et al., 2003). Indeed, some desaturases show activities that were not predicted by sequence homologies to proteins with known functions. TaNe in *Thraustochytrium aureum* ATCC 34304 was originally cloned by primers based on Δ6-desaturase and share only 5% homology with Δ5-desaturase of *Burgia malayi*, but was found to have Δ5 desaturase activity when expressed in yeast (Kang et al., 2010). Another example, the house cricket (*Acheta domesticus*) encodes a bifunctional Δ12/Δ9-desaturase AdD9des with low Δ9 desaturation activity that presumably evolved from a Δ9-desaturase (Zhou et al., 2008). Point mutations acquired by directed evolution enhanced the Δ9 desaturation activity of AdD9des, implying that the Δ12 regioselectivity of AdD9des could have been gained gradually by an ancestral Δ9-desaturase (Vanhercke et al., 2011).

1.3.2.2.3 Desaturases in thraustochytrids

Genome mining has been used to find enzymes in the DE pathway (Figure 8) and to show that the DE pathway is mostly incomplete in thraustochytrids. Δ9-desaturase is not found in the genome of *Thraustochytrium* sp. 26185 (Meesapyodsuk and Qiu, 2016), *Aurantiochytrium limacinum* CCAP 4062/1, *Hondaea fermentalgiana* (Dellero et al., 2018) and T66 (Heggeset et al., 2019). However, determining the presence of desaturases by genome analysis is likely to be inaccurate as discussed above. In SR21, the presence of Δ4, Δ6, Δ8, Δ9, Δ12-desaturases were

suggested by Song et al (Song et al., 2018), while Liang et al (Liang et al., 2020) also suggested the presence of a Δ5-desaturase. Moreover, some of the predicted desaturases show unclear roles in the FA profile of the cells. Genes putatively encoding Δ12-desaturase, Δ6-desaturase and Δ8-desaturase were predicted in T66, but their expected substrates and products were not found (Heggeset et al., 2019).

Experimental studies have also demonstrated that some thraustochytrid strains lack certain desaturase activities. In *Schizochytrium* sp. 20888, the Δ12 desaturation activity is absent, as shown by in vivo labeling experiments with radioactive FAs (Lippmeier et al., 2009). In contrast, the Δ12-desaturase of *Thraustochytrium aureum* ATCC 34304 is functional, verified by heterologous expression in yeast. (Kobayashi et al., 2011), and gene disruption (Matsuda et al., 2012). Δ5-desaturase activity is absent in *A. limacinum* mh018 as the addition of free 20:4$^{\Delta 8,11,14,17}$ in the culture medium of *A. limacinum* mh018 did not increase the EPA production, while EPA was produced when these cells expressed the Δ5-desaturase from *Thraustochytrium aureum* ATCC 34304. This showed that Δ5-desaturase in *Thraustochytrium aureum* ATCC 34304 is functional (Kobayashi et al., 2011), with the evidence strengthened further by gene disruption (Sakaguchi et al., 2012). Both T66 and *Thraustochytrium* sp. ATCC 26185 encodes putative Δ12-desaturases with an identical amino acid sequence, which displayed no Δ12-desaturase activity when it was expressed in *Escherichia coli* (Meesapyodsuk and Qiu, 2016).

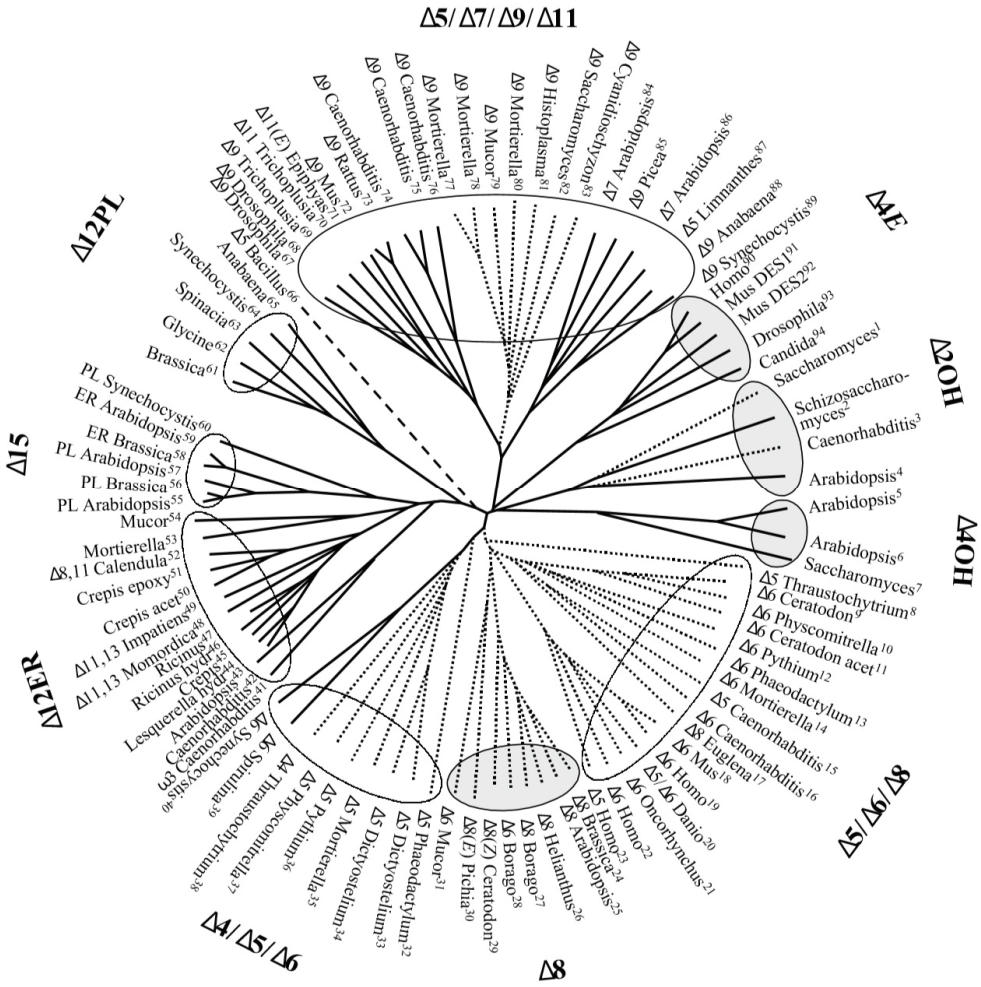

Figure 9. Phylogeny of desaturases. The regioselectivities are marked by Δ with numbers;PL, plastidial; ER, microsomal; Δ2OH and Δ4OH, sphingolipid acyl amide a-hydroxylases and sphingolipid sphingoid C4-hydroxylases; Δ4E, sphingolipid sphingoid desaturases. Gray backgrounds mark all sphingolipid-modifying enzyme groups. Dotted branches indicate cytochrome b5 fusion proteins. The prokaryotic desaturase from *B. subtilis* is indicated by a dashed branch. Copied from Sperling et al. (2003).

1.3.2.3 Polyketide synthase (PKS) pathway

PKS was first identified as the pathway for producing polyketides, which are secondary metabolites with a chemistry and structure related to FAs (Xu et al., 2021a). Several marine and soil bacteria and a few eukaryotes later had been found to synthesize PUFAs utilizing PKS (called PKS-like or PUFA synthase) (Metz et al., 2001; Sasso et al., 2012; Yoshida et al., 2016). The PKS reaction does not require oxygen and can synthesize PUFAs with 20 to 22 carbons by several cycles of two-carbon addition involving a sequential reaction of reduction, dehydration, reduction and condensation in each cycle (Figure 10) (Metz et al., 2001). The PKS in thraustochytrids is comprised of three subunits, PfaA, B and C (also called PKS1, 2 and 3), each containing multiple catalytic domains (Figure 11) (Jovanovic et al., 2021). Some of the PKS catalytic domains have been shown to play a positive role in PUFA accumulation in thraustochytrids. Overexpression of keto reductase (KR) or dehydratase (DH) encoding genes in PfaC slightly enhanced the proportion of some PUFAs in *A. limacinum* OUC168 (Liu et al., 2018). Disruption of the enyolreductase (ER) on PfaB in SR21 and the second DH in PfaC genes reduced the proportion of PUFAs in SR21(Li et al., 2018a; Ling et al., 2020). Still, the function of some catalytic domains remains elusive. Disruption of the ER on PfaC reduced the proportion of SFAs , instead of PUFAs, in SR21 (Ling et al., 2020). Moreover, disruption of the dehydrase/isomerase (D/I) in *Aurantiochytrium* sp. PKU#SW7 reduced cell growth substantially (Liang et al., 2018).

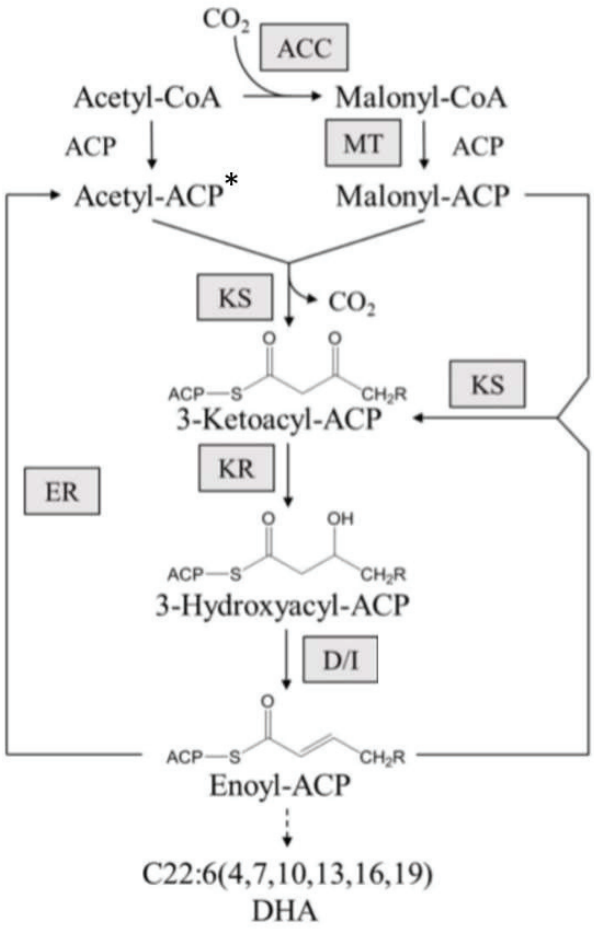

Figure 10. Typical PKS pathway for DHA synthesis. ACC, acetyl-CoA carboxylase; ACP, acyl carrier protein; MT, malonyl-CoA:ACP transacylase; KS, β-ketoacyl synthase; KR, keto reductase; D/I, dehydratase (DH)/isomerase; ER, enoyl reductase. *Becomes Acyl-ACP after the first cycle. Copied and modified from Liang et al. (2018).

Figure 11. PKS subunits (PfaA, PfaB and PfaC, from left to right) and catalytic domains in *A. limacinum* SR21. ACP, acyl carrier protein; AT, acyl transferase; MAT, malonyl-CoA:ACP transacylase; KS, β-ketoacyl synthase; KR, keto reductase; DH, dehydratase; ER, enoyl reductase; CLF, chain length factor. Copied and modified from Ling et al. (2020).

Table 2. The studies utilizing cerulenin for FAS inhibition in thraustochytrids.

	Conc.	Growth stage treated			Analysis	Reference
		Add	End	Length		
Schizochytrium sp. ATCC 20888	1-5 uM (optimal)	Early log	Early log	< 1hr	Labeling	Hauvermale et al. (2006)
Thraustochytrium sp. 26185	20 uM	Log	Log	< 1.5hr	Labeling	Zhao and Qiu (2018)
Aurantiochytrium mangrovei BL10	25 uM (optimal)	From start	Early stationary	> 24hr	FA Profiling	Chaung et al. (2012)
Schizochytrium sp. S056	8 mg/l	Beginning	Stationary	5 days?	FA Profiling	Chen et al. (2016)
Aurantiochytrium sp. SD116	0.5 uM	na	na	na	FA Profiling	Wang et al. (2020)

Conc., concentration; Length, the time length between adding cerulenin and the result analyses; Labeling, Analyzing the incorporation of radio-labeled acetate or propionate into FA; na, not available

1.3.2.4 Contribution and competition between fatty acid synthesis pathways

The PKS and FAS-DE pathways cannot complement each other for growth and the synthesis of some PUFAs in thraustochytrids. Mutants with dysfunctional PKS in *Schizochytrium* sp. 20888 cannot grow and are PUFA auxotrophs (Lippmeier et al., 2009). The addition of free $20{:}4^{\Delta 8,11,14,17}$ and the expression of the Δ5 desaturase in *A. limacinum* mh018 did not increase DHA and DPA level (Kobayashi et al., 2011). In *Thraustochytrium aureum* ATCC 34304, the destruction of Δ12-desaturase gene did not reduce DHA level (Matsuda et al., 2012). Cerulenin

is an antifungal antibiotic derived from the fungus *Cephalosporum caerulens* (Ruth and Javier, 2006). It inhibits fatty acid biosynthesis by irreversibly binding to the KS domain of FAS (Figure 7). Cerulenin treatment has been shown to reduce SFA production more significantly than PUFAs in thraustochytrids, indicating PUFAs were mostly produced by the PKS pathway (Table 2) (Hauvermale et al., 2006; Chaung et al., 2012; Chen et al., 2016; Zhao and Qiu, 2018; Wang et al., 2020).

Reducing or eliminating the flux of competing pathways is one approach to improve the production of a specific pathway (Lee et al., 2012). Since both the PKS and FAS pathways require acetyl-CoA and NADPH as precursors, decreasing FAS could potentially distribute more acetyl-CoA and NADPH for the PKS pathway to consume. In T66, it has been shown that O_2 limitation could hinder the O_2-dependent desaturase(s) in the DE pathway and favor the O_2-independent PKS pathway. As a result, in N and O_2-limited cells, there were no detectable C16:1 n-7 and C18:1 n-7 synthesized, while DHA and total lipid content increased compared to the N starved, well-oxygenated cells (Jakobsen et al., 2008; Heggeset et al., 2019). FAS inhibition via cerulenin treatment increased the proportion of DHA in total FA in *Aurantiochytrium mangrovei* BL10, *Schizochytrium* sp. S056 and *Aurantiochytrium* sp. SD116 (Table 2). However, the production of neither total lipid nor PUFAs was increased (Chaung et al., 2012; Chen et al., 2016; Wang et al., 2020).

1.3.3 Lipids

Thraustochytrids are known for their ability to accumulate high amounts of lipids. Typically, T66 and SR21 contain up to 84% and 52%, respectively, lipids compared to cell dry

weight (CDW) (Li et al., 2015; Patel et al., 2019). Thraustochytrids contain two major lipid groups: neutral lipids and phospholipids.

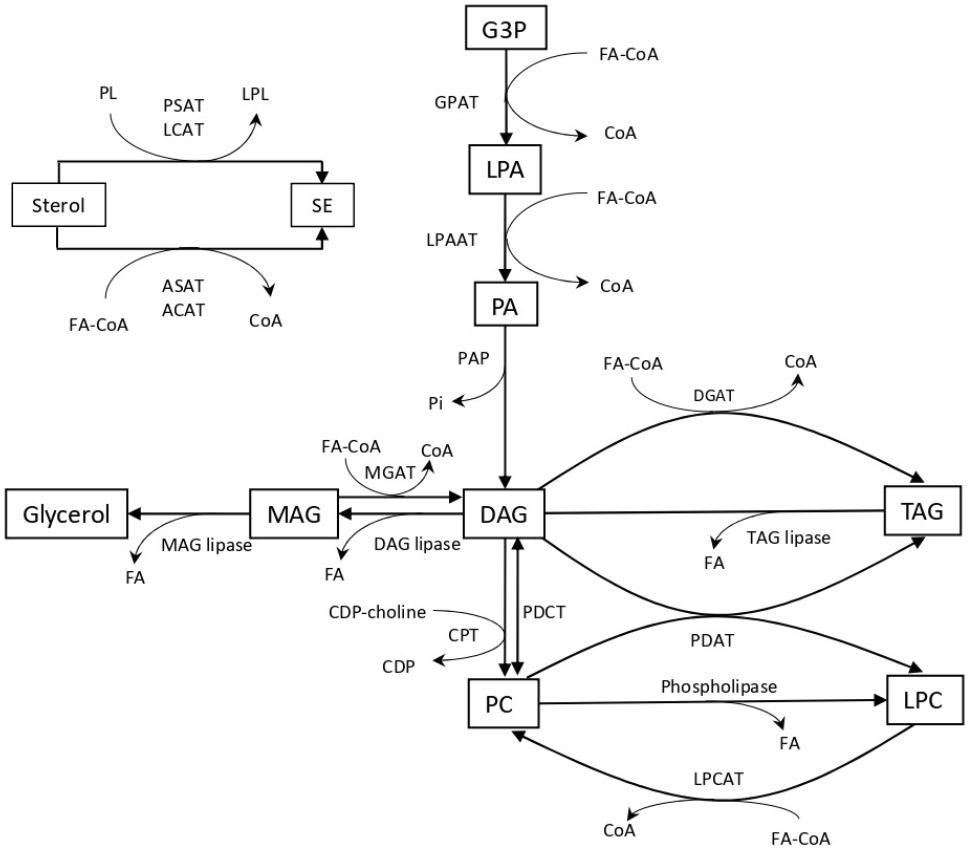

Figure 12. Possible lipid synthesis pathways. ACAT, acyl-CoA cholesterol acyl transferase; ASAT, acyl-CoA:sterol acyltransferase; CPT, CTP:phosphocholine cytidylyltransferase; DAG, diacylglycerol; DGAT, acyl-CoA:diacylglycerol acyltransferase; FA-CoA, fatty acyl-coenzyme A; G3P, glycerol-3-phosphate; GPAT, glycerol-3-phosphate acyl transferases; LCAT, lecithin-cholesterol acyltransferase; LPA, lysophosphatidic acid; LPAAT (AGPAT), lysoPA acyl transferases; LPCAT, lyso-phosphatidylcholine acyltransferase; PLC, lyso-phosphatidylcholine; LPL, lysophospholipid; MAG, monoacylglycerol; MGAT, acyl-CoA:monoacylglycerol acyltransferases PA: phosphatidic acid; PAP, phosphatidic acid phosphatase; PC, phosphatidylcholine; PDAT, Phospholipid:Diacylglycerol Acyltransferase; PDCT, diacylglycerol cholinephosphotransferase; Pi, phosphate; PL, phospholipid; PSAT, phosphatidylcholine-sterol O-acyltransferase; SE, steryl ester; TAG, triacylglycerol. (Liu et al., 2012; Korber et al., 2017).

Neutral lipids include triacylglycerol (TAG), diacylglycerol (DAG), monoacylglycerol (MAG) and steryl ester (SE). They lack charged groups so that they are storage lipids rather than membrane lipids. MAG, DAG and TAG are the esters of glycerol with one, two, and three FA(s) to hydroxy group(s), respectively, while SE is the ester of one FA to a hydroxy group at the C-3 position of a sterol backbone. TAG and SE play a role in the storage of sterols, free FAs and DAGs to buffer the concentration of these compounds in the cell. FAs and DAGs stored in neutral lipids can be used for phospholipid synthesis or energy production via β-oxidation. DAG also acts as a second messenger in signal transduction, regulating kinase activities (Athenstaedt and Daum, 2006; Czabany et al., 2007). In the late lipid accumulation phase, the total lipid can consist of 70-95% neutral lipid (Fan et al., 2007; Liu et al., 2014; Ren et al., 2014). The dominant neutral lipid class is TAG, with a proportion greater than 95% of the total neutral lipid, while DAG, MAG and SE are formed in smaller amounts (Fan et al., 2007; Dellero et al., 2018).

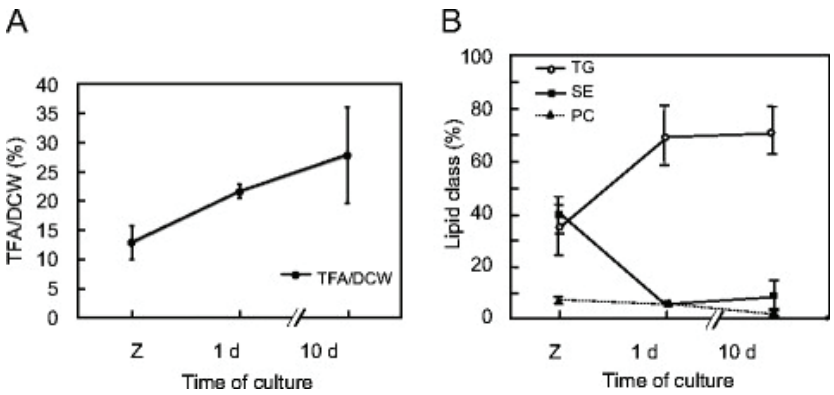

Figure 13. Change of fatty acid contents and lipid components after 1–day and 10–day culture in SR21. Mean values (±SD) of three independent experiments are shown. (A) Total fatty acids (TFAs)/ dry cell weight (DCW). (B) The proportion of main lipid classes in the total lipid. TG, triacylglycerol; SE, steryl ester; PC, phosphatidylcholine. Copied and modified from Morita et al. (2006).

Phospholipids are amphiphilic molecules consisting of a hydrophilic head group and a hydrophobic tail. They are essential components of cell membrane bilayers. Phosphatidylcholine (PC) is a glycerolipid containing two fatty acids attached to two hydroxy groups and a phosphate group and choline linked to the third hydroxy group at a glycerol backbone (Lordan et al., 2017). It is the most abundant phospholipid of all mammalian cells (van der Veen et al., 2017) as well as in thraustochytrid strains (Morita et al., 2006; Fan et al., 2007; Dellero et al., 2018; Bartosova et al., 2021a).

The proportion of different lipid classes alters during cultivation in thraustochytrids. In SR21, TAG and SE constituted a similar proportion in total lipid in zoospores. After one day of culture, TAG and SE substantially increased and decreased, respectively. On the other hand, PC proportions in the total lipids gradually decreased after one day of culture (Figure 13) (Morita et al., 2006).

1.3.3.1 Lipid species

TAG, DAG, MAG and PC are all glycerolipid (Figure 14). Different TAG species can be formed by linking combinations of three identical or different fatty acids as R1, R2 and R3 at stereospecific positions, *sn*-1, *sn*-2 and *sn*-3, respectively. In the same principle, DAG, MAG and PC can have different species, except the R3 in DAG and PC, and the R2 and R3 in MAG are not variable. For SE, different sterol backbones also form different SE species.

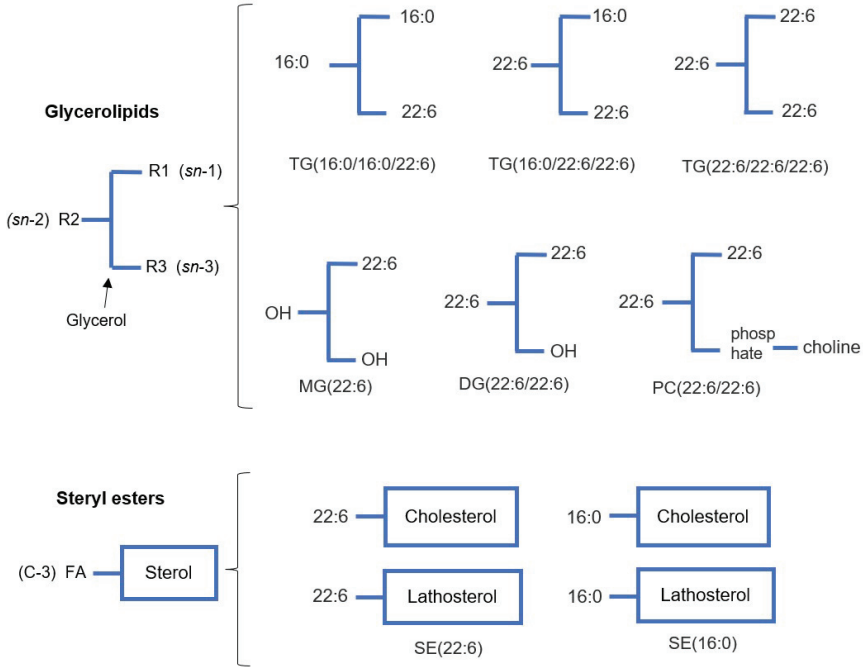

Figure 14. Examples of different species of glycerolipids and steryl esters.

The abundance of different lipid species is strain specific and life cycle dependent in thraustochytrids. The ten most abundant lipid species composed almost 40% of overall lipid abundance in T66 at the start of cultivation and declined to 25–30% after that, with half of this portion made up of the two most abundant lipids, the TAG species TG(16:0/16:0/22:6) and TG(16:0/22:6/22:6) (Bartosova et al., 2021a). In SR21, the two most abundant lipids species are also TG(16:0/16:0/22:6) and TG(16:0/22:6/22:6), representing around 44% of total TAG (Nakahara et al., 1996). The major PC species in *Schizochytrium* sp. A-2 are PC(20:5/22:6) and PC(22:6/22:6) (Yue et al., 2019), while in T66, they are PC(16:0/22:6) and PC(22:6/22:6) (Bartosova et al., 2021a). The proportion of DHA-rich TAG species (TAGs with two or three

DHA) in total TAG is often found to increase during lipid accumulation in thraustochytrids, such as TG(22:6/22:6/22:6), TG(16:0/22:6/22:6) in *Schizochytrium* sp. A-2 and *Schizochytrium* sp. S31 (Yue et al., 2019; Chang et al., 2021). Up to date, although several sterols have been detected in thraustochytrids (see 1.3.4.1), SE species in thraustochytrids have not been described.

1.3.3.2 Enzymes in the lipid synthesis pathways

Lipid synthesis mostly involves a series of incorporation of FAs to the lipid head groups (Figure 12). Most lipid synthesis enzymes have been found through genome mining using a reciprocal BLAST approach to identify orthologous genes in thraustochytrids. In *Aurantiochytrium limacinum* CCAP 4062/1 and *Hondaea fermentalgiana* CCAP 4062/3, almost all the genes involved in synthesizing glycerolipids have been identified (Dellero et al., 2018). In T66, four glycerol-3-phosphate acyl transferases (GAPTs), five lysoPA acyl transferases (LPAATs), three phosphatidic acid phosphatases (PAPs) and four acyl-CoA:diacylglycerol acyltransferases (DGATs) were annotated (Heggeset et al., 2019). In animals, it has been shown that DAGs can also be produced from MAGs by acyl-CoA:monoacylglycerol acyltransferases (MGATs), but such enzymes have not been predicted or characterized in thraustochytrids (Liu et al., 2012).

The expression of enzymes involved in lipid metabolism may change according to growth stage, cultivation condition and the expression of FA synthesis genes. In *Aurantiochytrium* sp. SD116, *DGAT* expression was upregulated under nitrogen limitation. Under low temperatures, the expression of *DGAT*, *GPAT*, *PDAT* and the phospholipase gene was downregulated, while the expression of *LPAAT* and the phosphatidylinositol transfer protein (PITP) gene, which

transports the phospholipids from their site of synthesis to the cell membranes, increased (Ma et al., 2015; Ma et al., 2017). In T66, the genes of one GAPT, one PAP, two DGATs, two TAG lipases, one DAG lipase and one MAG lipase were transcriptionally upregulated during the lipid accumulation phase (Heggeset et al., 2019). In SR21, the expression levels of *GPAT*, *LPAAT* and *PAP,* were significantly upregulated in the PKS DH-overexpression strain compared to the wild-type strain (Shi et al., 2021).

Some acyltransferases in thraustochytrids have been functionally characterized and show substrate preference. The GAPT PLAT2 preferentially incorporates DHA to G3P in *Aurantiochytrium limacinum* F26-b. Overexpression of *PLAT2* increased the production of the lipids with two DHA, DAG, PC, TAG and the lipids with three DHA, TAG, but not DHA-free DAG, TAG and PC (Nutahara et al., 2019). The enzyme LPCAT PLAT1 is responsible for generating one, but not two, DHA-containing PC and phosphatidylethanolamine (PE) in *Aurantiochytrium limacinum* F26-b (Abe et al., 2014).

SEs are known to be synthesized by two enzyme families, acyl-CoA:sterol acyltransferase (ASAT) and phosphatidylcholine-sterol O-acyltransferase (PSAT) (Figure 12). ASATs catalyze the synthesis of SE through transferring FAs to sterols from acyl-CoA. In mammals, two ASAT isoenzymes, ACAT1 and ACAT2, encoded by two different genes were identified. Both ASATs play important roles in cellular cholesterol homeostasis (Chang et al., 2009). In *Saccharomyces cerevisiae*, the ASAT Are1p and Are2p (ACAT related enzymes) are homologous to ACAT1 and ACAT2, respectively, and are the only SE synthesizing enzymes in the yeast. Still, the growth of the *are1are2* double mutant was not affected under the tested conditions (Yu et al., 1996; Sandager et al., 2000). Are1p and Are2p have a significant preference for lanosterol and

ergosterol as a substrate, respectively (Zweytick et al., 2000). In *Arabidopsis thaliana*, the ASAT AtASAT1 is homologous to the animal and yeast ASATs, preferring saturated FA-CoAs as acyl donors and cycloartenol as acceptor molecule (Chen et al., 2007). A PSAT, also called LCAT, synthesizes cholesteryl esters by esterifying free cholesterol with a fatty acid donated from the *sn*-2 position of PC (Jonas, 2000). In *A. thaliana*, the PSAT AtPSAT1 was homologous to the mammalian LCAT, transferring unsaturated FAs from the *sn*-2 position of PC and PE to campesterol, sitosterol and cholesterol (Banaś et al., 2005). Nevertheless, no ASAT or PSAT family members in thraustochytrids has yet been annotated or characterized.

1.3.3.3 Diversity and relations of acyltransferases

Eukaryotic DGATs can be classified into five families with sequences and structures distinct from each other (Figure 15). DGAT1 and DGAT2 are the two families that have been identified in most species, while DGAT3, wax ester synthase/DGAT (WS/DGAT) and phytyl ester synthase (PES) families are only prevalent in plants or bacteria. All DGATs but the soluble DGAT3s are integral membrane proteins (McFie et al., 2010; Liu et al., 2011; Hernández et al., 2012; Xu et al., 2021b). These enzyme families are believed to have originated independently but subsequently became functionally convergent (Turchetto-Zolet et al., 2011). Some DGAT families are homologous to other acyltransferase families. DGAT1s and ASATs belong to the membrane-bound O-acyl transferase (MBOAT) family, while DGAT2s are homologous to MGATs (Figure 15) (Chang et al., 2011; Liu et al., 2012).

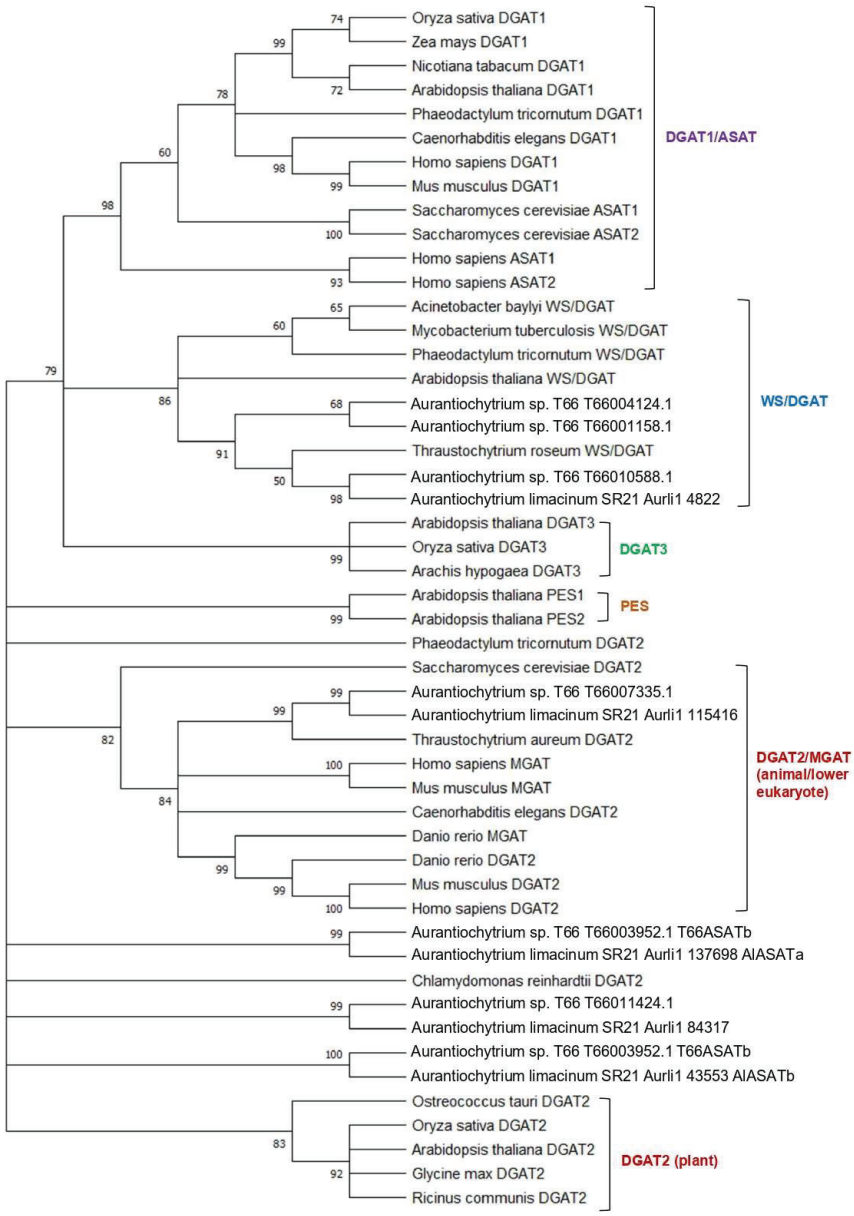

Figure 15. Phylogenetic analysis of DGAT2s, WS/DGATs and DGAT2-like proteins in T66 and SR21, and acyl-CoA:acyltransferases in representative model organisms. The five DGAT families are indicated in color. Modified from Paper IV in this thesis.

DGAT1 polypeptides are predicted to have between 8 and 10 transmembrane domains (TMDs), while DGAT2 polypeptides have one or two putative TMDs in the N-terminus. The hydrophilic N-terminus preceding the first putative TMD has a quite variable length, being much greater in the proteins from fungi than those from animals and plants (Liu et al., 2012). Although the removal of the N-terminus substantially decreases the activity of *S. cerevisiae* DGAT2 (Liu et al., 2011), deletion of the N-terminus of a murine DGAT2 has no effect on its DGAT activity but affects its association with mitochondria membrane (Stone et al., 2009). The motif RXGFX(K/R)XAXXXGXX(L/V)VPXXXFG(E/Q), positioned roughly 150 residues after the first hydrophobic putative TMD, is the most conserved region in DGAT2 and was proposed to be important for DGAT catalysis (Liu et al., 2010). The motif HPHG is conserved in both animal and fungi DGAT2 and was shown to be essential for murine DGAT2 activity (Stone et al., 2006; Liu et al., 2011). Moreover, six highly conserved motifs were identified by analyzed DGAT2 sequences from 70 organisms (Cao, 2011).

Most microalgal species contain multiple *DGAT* genes. Interestingly, those multiple DGATs usually include one *DGAT1* gene and multiple *DGAT2* and *DGAT2*-like genes. These DGAT2s were proposed to be evolved from multiple origins of the various DGAT2 isoforms, and, consequently, are very divergent from each other, even among isoforms from the same species. In fact, some homologous DGAT2s are more closely related to those from other algal species than they are to other DGAT2s within their own genomes (Figure 16). Algal DGAT2 protein sequences could be related to the sequences of either plant DGAT2s, animal DGAT2s, or unrelated to the DGAT2s from higher eukaryotes. At least one DGAT2 from every algal species is found associated with the clades of animal-like DGAT2s (Chen and Smith, 2012).

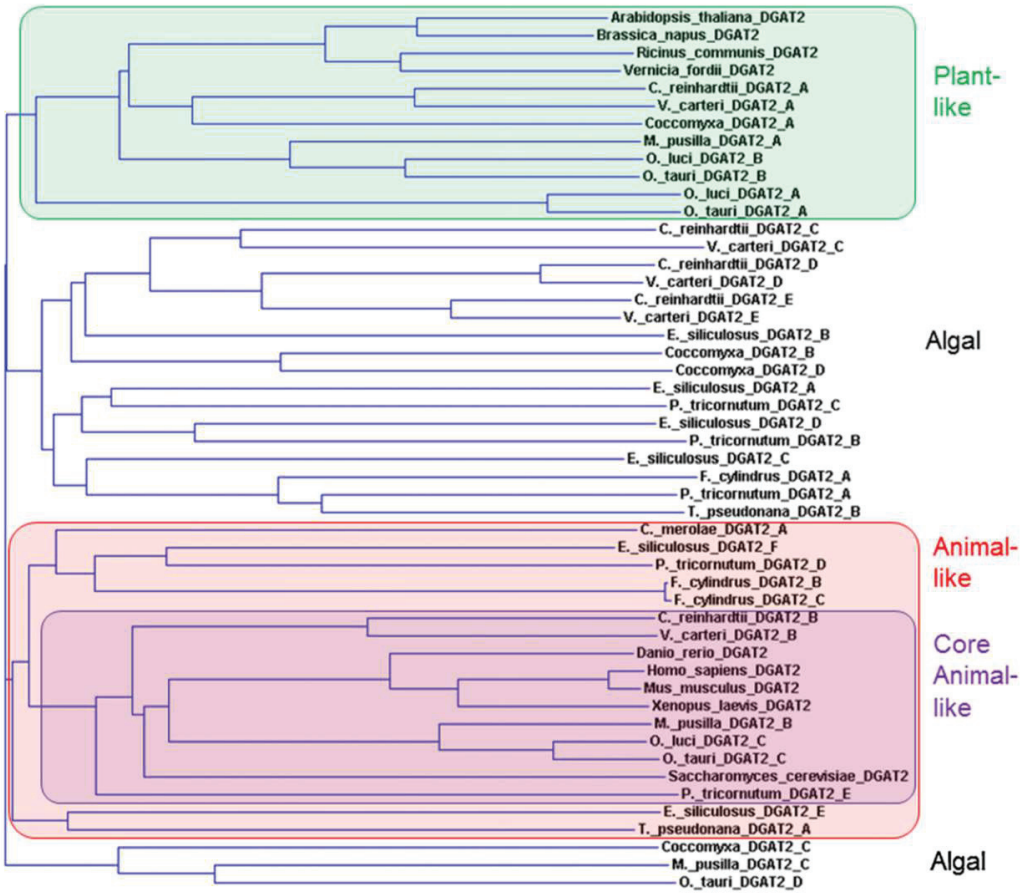

Figure 16. Dendrogram of selected DGAT2s based on the protein sequence. Adapted from Chen and Smith (2012).

1.3.4 Terpenoids

The mevalonate (MVA) pathway is utilized by most eukaryotes and thraustochytrids to synthesize terpenoids, including carotenoids, sterols and the intermediate compound squalene

(Figure 17). Farnesyl pyrophosphate (FPP) is the branch point for the sterol and carotenoid synthesis pathways.

1.3.4.1 Squalene and sterol

The pathway for squalene synthesis in thraustochytrids is far from being fully unraveled. The pathway has been tentatively reconstructed from the genome of *A. limacinum* CCAP 4062/1 and *H. fermentalgiana* CCAP 4062/3 (Dellero et al., 2018). In these species, no squalene mono-oxygenase (SM), one regulatory point for sterol synthesis in yeasts and mammals (Figure 18), was identified, potentially due to the high sequence variability of this enzyme in eukaryotes. Terbinafine treatment, which inhibits SM, led to increased accumulation of squalene in *Aurantiochytrium mangrovei* FB3 (Fan et al., 2010). Squalene synthase (SQS) has been characterized in *Aurantiochytrium sp.* KRS101, showing its activity of converting FPP to squalene in the presence of NADPH and Mg^{2+} (Won-Kyung et al., 2013).

Squalene levels in thraustochytrids usually depends on growth condition and life stage. In some cases, it is reduced when lipids accumulates. The squalene content dropped during the lipid accumulation stage in *Schizochytrium* sp. HX-308 and SR21 (Ren et al., 2014; Patel et al., 2020). The expression of an ω-3 desaturase increased PUFA but reduced squalene and sterol contents by 37.19% and 22.31% in *Schizochytrium* sp. HX-308 (Ren et al., 2015). SR21 and T66 have been shown to utilize low-cost feedstock to produce DHA and squalene simultaneously, indicating that they are potentially competitive for coproduction of squalene together with DHA for the low-cost market (Patel et al., 2019; Patel et al., 2020).

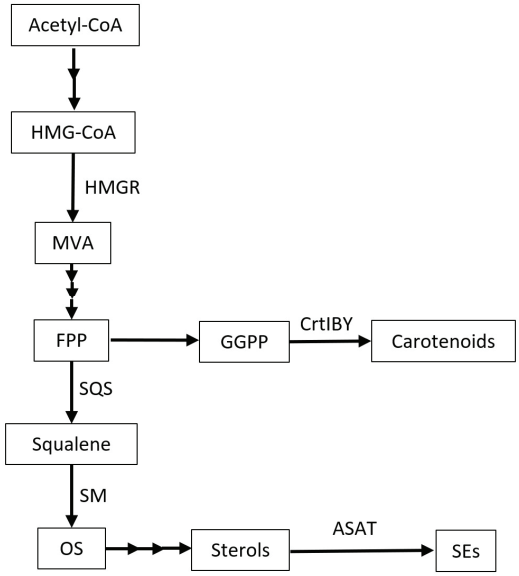

Figure 17. Tentative terpenoid synthesis pathway in thraustochytrids; MVA, mevalonate; FPP, farnesyl pyrophosphate; GGPP, geranylgeranyl pyrophosphate; SEs, sterol esters; OS, 2,3-oxidosqualene; HMG-CoA, β-Hydroxy β-methylglutaryl-CoA; HMGR, HMG-CoA reductase; SQS, squalene synthase; SM, squalene mono-oxygenase (or squalene epoxidase); CrtIBY, a trifunctional protein with phytoene desaturase (CrtI), geranylgeranyl phytoene synthase (CrtB) and lycopene cyclase (CrtY) activities. Multiple arrows between two compounds indicates that more than one enzymatic steps involved.

Only a few thraustochytrid species have had their free sterol content determined. These studies showed that cholesterol is dominant in most thraustochytrid, while some other major sterols include stigmasterol, Δ7-stigmasterol, lathosterol and 24-Methylenecholesterol (Lewis et al., 2001; Dellero et al., 2018). In SR21, the major sterols were cholesterol and lathosterol, the contents of which were ~62% and ~31%, respectively, in total sterols (Yoshida et al., 2020).

1.3.4.2 Regulation of squalene, sterol and steryl ester synthesis

The regulation of SE, squalene and sterol synthesis pathways have been elucidated in yeast and mammalian cells but it has not been studied in thraustochytrids, and might be different. In yeast and mammalian cells, HMG-CoA reductase (HMGR) and squalene mono-oxygenase (SM, also known as squalene epoxidase) are two rate-limiting flux-controlling enzymes in the sterol synthesis pathway (Figure 17 and 18). 24,25-dihydrolanosterol and 25-hydroxycholesterol, the intermediate in cholesterol synthesis and the derivative of cholesterol, respectively, stimulate ubiquitination and proteasomal degradation of HMGR in human cells (Lange et al., 2008). Cholesterol further accelerated the proteasomal degradation of SM and then caused the accumulation of squalene in human cells (Gill et al., 2011). In addition, unsaturated fatty acids, such as DHA, have been shown to stabilize SM by interfering with proteasomal degradation in human cells (Stevenson et al., 2014).

SE synthesis can affect squalene production. In yeast, disruption of SE synthesis by ASAT deletion (*are1are2* double-deletion) can increase the number of free sterols such as ergosterol (Zweytick et al., 2000; Sorger et al., 2004) and lanosterol (Foresti et al., 2013). Proteasomal degradation of the SM Erg1 is promoted by lanosterol (Foresti et al., 2013). The protein stability of the SM Erg1 was reduced, and the squalene level increased in the in yeast *are1are2* double-mutant, which lacks SEs (Figure 18) (Zweytick et al., 2000; Sorger et al., 2004).

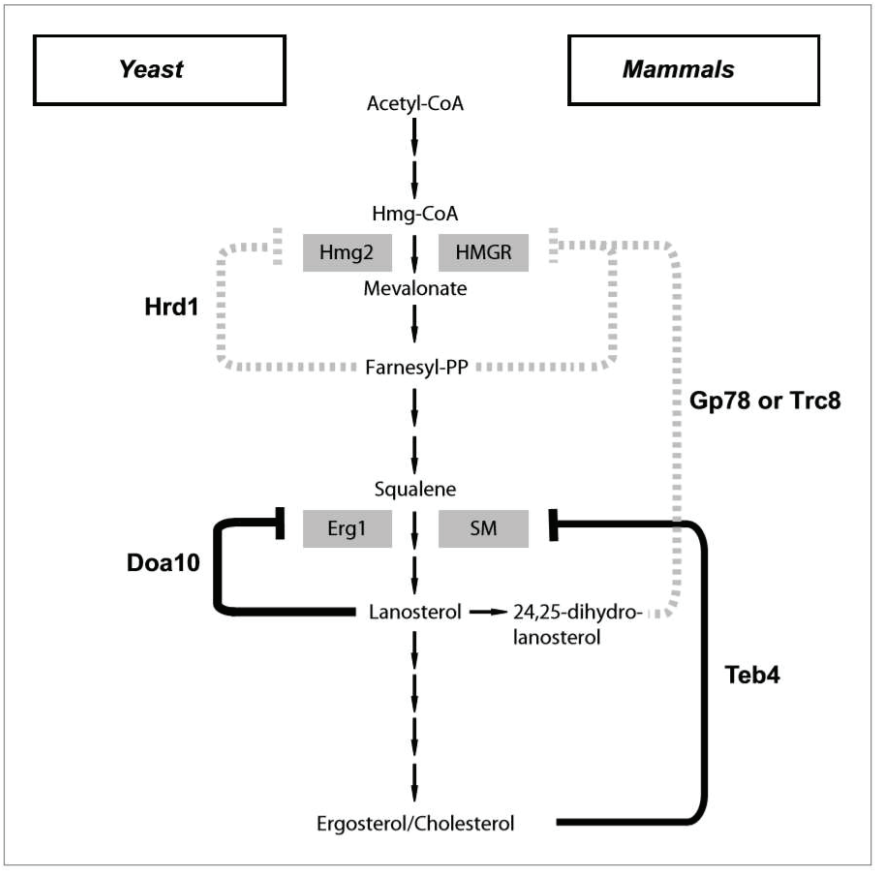

Figure 18. Schematic representation of the sterol-dependent, posttranslational feedback inhibition systems for sterol homeostasis in yeast (left) and mammals (right) targeting 3-Hydroxy-3-methylglutaryl-coenzyme A reductase (HMGR) (dotted lines) and squalene mono-oxygenase (SM) (solid lines). HMGR is also degraded in response to 25-hydroxycholesterol (not shown). Ubiquitin ligases leading to proteasomal degradation are in bold. Copied from Foresti et al. (2013).

2 Aims of the study

Thraustochytrids are considered promising sustainable sources of DHA, squalene and some MUFAs. This work aims to deepen our understanding of lipid metabolism and genetic engineering application in thraustochytrids through investigating two thraustochytrid strains, T66 and SR21. The knowledge is expected to be the foundation of improving the production of the above-mentioned valuable compounds from thraustochytrids. In order to reach the aims, several approaches were utilized:

1. The fatty acid and lipid accumulation in the two strains were compared, including how they were affected by chemicals that inhibit the FAS pathway.
2. The current development of thraustochytrid genetic engineering methodologies and the relevant experience in other organisms were reviewed.
3. Genes in T66 that were upregulated during lipid accumulation, and their homologs in SR21, including a putative desaturase and four putative DGATs, were functionally characterized after developing targeted knockin/knockout SR21mutant strains, followed by fatty acid and lipid characterization.

3 Summary of results and discussion

3.1 Paper I: Utilizing lipidomics and fatty acid synthase inhibitors to explore lipid accumulation in two *Aurantiochytrium* species

The aim was to look for potential metabolic engineering targets to enhance the production of DHA and DHA-rich lipid in thraustochytrids. Thus, the lipid accumulation of T66 and SR21 during N-starvation was characterized, focusing on how the lipid accumulation was affected by inhibiting FAS.

T66 and SR21 cultures reaching N-starvation in bioreactors were transferred to microbioreactors and then treated with three FAS inhibitors: cerulenin, taxifolin or isoniazid. Only the cerulenin-treated cell showed decreased FAS-derived FAs (FAS-FAs), while PKS-derived FAs (PKS-FAs) or DHA remained at a similar level in both T66 and SR21 (Figure 1, Paper 1). The effect of cerulenin on both strains was studied further. This time, the two strains cultivated in bioreactors were transferred to shake flasks when cells reached N-starvation, followed by cerulenin treatment and harvested in time series. For both strains, the cultures treated for three hours had lower total lipid than the untreated cultures (Figure 4, Paper 1). For SR21, and, but to a mild extent, T66, the cultures treated for three hours had a lower concentration of FAS-FA and glucose consumption rate, and a higher concentration of DHA-rich lipid species TG(22:6/22:6/22:6) and DG(22:6/22:6). Still, the concentration of PKS-FAs, DHA, and the FA yield on glucose remained at a similar level between the treated and untreated cells (Figure 2, 3, 5 and 6, Paper 1). This trend is similar to the result obtained from treating the cells with cerulenin at exponential growth phase (Chaung et al., 2012; Chen et al., 2016), when the

main lipid class produced is phospholipid (Dellero et al., 2018). The findings show that reducing the FAS pathway's consumption of common PKS and FAS precursors like acetyl-CoA, malonyl-CoA and NADPH did not improve DHA production in the PKS pathway. This indicates that precursor availability for the PKS pathway is less likely to be the bottleneck for DHA synthesis. However, presumably due to a higher proportion of DHA in total FA, more DHA was available for synthesizing DHA-rich lipid species.

The effect of cerulenin on the two strains was more significant after treating for 3 h than for 12 h. After 3 h, regardless of cerulenin concentration, the amount of FAS-FA and total lipid increased at a similar pace in SR21 (Figure 2 and 4, Paper 1). TG(22:6/22:6/22:6) and DG(22:6/22:6) decreased more in the treated cells, while other lipid species, mostly FAS-FA-rich TAGs, increased more in the treated cells (Figure 5 and Supplementary Figure S4, Paper 1). The results suggest that the effect of cerulenin does not last for a long time, possibly due to cerulenin inactivation.

The fatty acid and lipid profiles of the two strains during N-starvation were characterized without cerulenin treatment. The two strains cultivated in bioreactors were transferred to shake flasks when cells reached N-starvation, followed by being harvested in time series. The DAG DG(22:6/22:6) was disproportionally highly accumulated in both T66 and SR21 during N-starvation compared to the rest of the DAG species that can be the precursors for DHA-rich TAG (Figure 6, Paper 1). This suggests a rate-limiting step of DHA-rich TAG production in *Aurantiochytrium*, potentially mediated by enzymes such as DGAT or PDAT. In addition, the accumulation of some lipid species varied between the two strains, including TG(22:6/22:6/22:6), PC(22:6/22:6), DG(N/22:6), MG(22:6), DG(22:6/22:6) and LPC(22:6)

(Figure 5, 6 and Supplementary Figure S4, Paper 1). These results indicate the presence of flux difference of enzyme reactions that could relate to the amount of enzyme present and the enzyme properties.

3.2 Paper II: Method development progress in genetic engineering of thraustochytrids

Many thraustochytrid strains, including T66, have not yet been genetically manipulated. With the aim to serve as a starting point for protocol development on these strains, this Paper reviewed the genetic engineering methods applied for different thraustochytrid strains and the relevant experience in other organisms, covering the delivery and genomic integration of DNAs, followed by the elements that affect gene expression and transformant selection.

For *Aurantiochytrium*, electroporation is the most prevalent transformation approach. Still, biolistic transformation and *Agrobacterium*-mediated transformation have been applied in some strains belonging to other thraustochytrid genera (Figure 1, Paper II). Exponential decay is the most used pulse type in thraustochytrids, with the applied field strengths varying from 1.8 to 10 kV/cm, while the set pulse lengths range from 0.65 to 25 ms. One exponential decay pulse is usually considered to be sufficient, while the optimal pulse numbers can be narrow-ranged when applying square wave pulses. In addition, more complex pulse form, such as short, high voltage pulses, followed by a longer, lower voltage pulse has been applied (Faktorová et al., 2020). Disrupting cell walls by agitating with glass beads can facilitate electroporation (Adachi et al., 2017), while DTT treatment is the most used method for cell wall disruption, which can be used before applying cell wall degrading enzymes (Zhang et al., 2018). The non-ionic sorbitol, followed by sucrose, are the most used electroporation solutions. Still,

both ionic and non-ionic solution has been used to wash the cells (Figure 2, Paper II). The feasibility of approaches for optimizing electroporation conditions, such as transforming fluorescently labeled molecules and microfluidics, or other transformation techniques, like bacterial conjugation and cell-penetrating peptide application, remain to be evaluated.

In thraustochytrids, expression cassettes can be integrated into either random or specific genome position, or as extrachromosomal DNAs. Higher HR efficiency for site-specific integration could be achieved by transforming Linear DNA with a two-homology-arm design and assisted by the CRISPR-Cas9 system. Moreover, a yeast-derived self-replicating extrachromosomal DNA has been used in thraustochytrid (Sun et al., 2015), which potentially can be applied to express CRISPR-Cas9 so that the expression of Cas9 can be eliminated by removing the extrachromosomal DNA from the cell. On the other hand, an approach that could enhance HR by interfering with NHEJ-specific enzymes has not yet been utilized in thraustochytrid.

The *cis*-elements on the expression cassettes can affect gene expression. In thraustochytrids, the EF1α and the ccg1 promoters, which are not necessary to be endogenous, are likely to be more optimal options (Figure 3, Paper II). Other approaches that can be considered to identify stronger promoters include using transcriptomic analysis, transforming promoter-less marker genes or generating synthetic promoters by error-prone PCR or rational design. On the other hand, significantly fewer thraustochytrids were engineered with inducible promoters, but one of them has great potential for controlling the expression of toxic genes (Han et al., 2020).

The most frequently used antibiotics in thraustochytrids for transformant selection are G418, zeocin, and hygromycin (Table 1, Paper II). However, when establishing a protocol, it may be worthwhile to plate transformants on a variety of antibiotics concentrations to eliminate false negatives and the risk of exceeding the resistance level for transformed cells. Expanding the number of antibiotics available for transformant selection is critical for gene inactivation in diploid thraustochytrid strains. Potential antibiotics for thraustochytrids can be chosen from those used on other stramenopiles, such as phleomycin, nourseothricin, puromycin, and formaldehyde (Faktorová et al., 2020). Finally, the Cre/*lox*P method has been shown to remove the resistance gene from the genome (Sun et al., 2015), which can be used to reduce the number of different antibiotics required to generate a succession of genome integrations.

In thraustochytrids, cassettes containing a gene of interest and an antibiotic resistance gene are commonly expressed. Most of these cassettes had an individual pair of promoter and terminator flanking each gene, which differed for each gene on the cassette, while two same promoters could also be used on the same cassette (Liu et al., 2018). An alternative approach has been used is to connect multiple genes using 2A linker sequences that are driven by a single promoter and terminator pair. Up to three genes were shown to be able to express linked via 2A sequences (Ye et al., 2019). However, the efficiency of 2A cleavage may depend on the 2A peptide or the strain that is used. Moreover, another approach in which the antibiotic resistance gene and the genes of interest are placed on separate DNA molecules, followed by being transformed at the same time, has potentials to be used in thraustochytrids.

3.3 Paper III: A non-canonical Δ9-desaturase synthesizing palmitoleic acid identified in the thraustochytrid *Aurantiochytrium* sp. T66

The aim was to investigate how genes contribute to unsaturated fatty acid synthesis in thraustochytrids. The expression of *T66Des9*, a putative desaturase gene, was upregulated during lipid accumulation in T66 (Heggeset et al., 2019). The role of *T66Des9* in unsaturated fatty acid synthesis was studied in this paper utilizing a genetic engineering approach, based on the knowledge from Paper II

SR21 strain 26-1 was generated with an expression cassette containing a zeocin resistance gene (*ble*) linked to *T66des9* by a 2A peptide-encoding DNA fragment, and gene expression was controlled by the endogenous glyceraldehyde 3-phosphate dehydrogenase (GAPDH) promoter and terminator (Figure 4a, Paper III). The cassette was integrated at the β-carotene synthesis gene *crtIBY* via homologous recombination. In addition, a control strain 30-1 was generated with expression cassette same as described above, except for it only encoding *ble*. The targeted genomic integrations were verified by PCR reaction and the pale color of the transformant colonies (Figure 4b and c, Paper III). The presence of *T66des9* mRNA in 26-1 was detected by RT-PCR (Figure 4d, Paper III).

The growth and fatty acid profile of SR21 WT, 30-1 and 26-1 were then characterized. All three grew similarly with glucose as carbon sources in shake flask cultures (Figure 5, Paper III). Neither C16:1 n-7 nor C18:1 n-7 was detected in WT or strain 30-1, while C16:1 n-7 and C18:1 n-7 were detected in strain 26-1 (Table 1, Paper III). Since C16:1 n-7 is known to be synthesized from the desaturation of C16:0, indicating that T66Des9 is a Δ9-desaturase when C16:0 is the substrate (Figure 1, Paper III). On the other hand, C18:1 n-7 can be possibly

synthesized from either C18:0 or C16:1 n-7, with the latter be more likely when considering how desaturases bind their substrate, the absence of C16:1 n-5 and the presence of a C16-Δ9 elongase gene in strain 26-1 (Figure 1, Paper III). Since *Thraustochytrium* sp. ATCC 26185 encodes an C16-Δ9 elongase and a protein identical to T66Des9, the discovery of T66Des9's function seems to explain how *Thraustochytrium* sp. ATCC 26185 can produce C18:1 n-7, presumably one of the C18:1 isoform found in the strain (Weete et al., 1997). This implies that the function of T66Des9 could be prevalent among various thraustochytrid strains.

This work demonstrated that T66 presumably lacks a Δ12-desaturase activity because the gene previously annotated as a Δ12-desaturase gene encodes the Δ9-desaturase T66Des9. This could explain the absence of C18:2 in the strain. Since T66Des9 synthesizes C16:1 n-7, an FA that is not considered a DHA precursor, this supports the possibility that *Aurantiochytrium* sp. T66 does lack an intact FAS-DE pathway for DHA production, as suggested in previous reports (Figure 1, Paper III) (Jakobsen et al., 2008; Heggeset et al., 2019).

Sequence analysis showed that T66Des9 has higher degree of identity with proteins that are annotated as Δ12-desaturases, including those with verified functions in *Thraustochytrium aureum* and *Phaeodactylum tricornutum* (Domergue et al., 2003; Matsuda et al., 2012), than those proteins that are annotated as Δ9-desaturases (Figure 2, Paper III). T66Des9 contains three histidine boxes that are conserved in desaturases and necessary for catalysis. Still, the first histidine box does not have the consensus sequence prevalent among Δ9-desaturases (Figure 3, Paper III). A possible explanation could be that an ancestral Δ12-desaturase gene evolved into a Δ9-desaturase gene.

3.4 Paper IV: *Aurantiochytrium* species encode two acyl-CoA:diacylglycerol acyltransferase 2 like acyl-CoA:sterol acyltransferases whose overexpression facilitate squalene accumulation

The aim was to investigate the role of *DGAT* on TAG synthesis in thraustochytrids. The expression of two *DGAT2*-like genes in T66, *T66ASATa* and *T66ASATb,* were upregulated during lipid accumulation (Heggeset et al., 2019). Data in Paper I also imply that DGAT could be the bottleneck for TAG synthesis. Thus, the two genes, and their homologs in SR21, *AlASATa* and *AlASATb*, were characterized in this paper by genetic engineering.

By phylogenetic analysis, AlASATa, T66ASATa, AlASATb, T66ASATb were found in relatively individual lineages within the large cluster of DGAT2 (Figure 2, Paper IV). The C-terminal region of the four proteins contains some DGAT2-conserved motifs. Some of these motifs could be important to DGAT2 enzyme activity (Figure 3, Paper IV), and shares structural conservation with bacterial GPAT. On the other hand, their N-terminal parts were not found to be structurally similar to other proteins. Similar to DGAT1 and ASAT, their N-terminal parts are predicted to contain multiple TMDs (Figure 3, Paper IV).

SR21 strains with *AlASATa*, *AlASATb,* or both genes knocked-out, or with *AlASATa*, *AlASATb*, *T66ASATa* or *T66ASATb* knocked-in, were developed with genomic insertions verified by PCR. The reduced RNA expression of the former three strains was verified by RT-PCR, while the genomic insertions of the following four strains were verified further by the change of colonies' color (Figure 4 and 6, Paper IV). Cultures of the strains from late exponential phase (T1) and early stationary phase (T2) were analyzed. All the mutant strains had similar growth rates, FA

composition and total lipid content as the control strains (Figure 5, 7, Supplementary Figure S6 and 7, Paper IV).

The lipid classes and species of the double knockout strains were first analyzed. The disruption of *AlASATb* or both *AlASATa* and *AlASATb*, but not *AlASATa,* greatly decreased the amount of total SE, the SEs of C16:0, SE(16:0), and DHA, SE(22:6), at both time points, and slightly increased the amount of DAGs at T2. Moreover, the amount of the SE(22:6) in the double mutant was further decreased relatively to *AlASATb* mutant at T2 (Figure 5 and Supplementary Figure S8, Paper IV).

Lipid classes and species of the knockin strains were then determined. Expression of *AlASATb* or *T66ASATb* increased the total SE level, SE(16:0) and SE(22:6) at both time points, and slightly decreased the DG level at T2. The expression of *AlASATa* or *T66ASATa* increased the amount of SE(16:0) and SE(22:6) at at least one time point. The expression of *T66ASATa* also slightly decreased the DG level at T2 (Figure 7 and Supplementary Figure S8, Paper IV). The results show that the expression of all four genes contributes to SE accumulation but to different extents. The expression of *AlASATb* increased the total SE, SE(16:0) and SE(22:6) more than the expression of *AlASATa*. Similarly, expression of *T66ASATb* resulted in more total SE and SE(22:6) than did the expression of *T66ASATa.* Non-SE lipid species, including four TAG and three DAG species, were affected by the expression of *AlASATa, T66ASATa* and *T66ASATb* but only at one of the time points (Table 2 and 3, Paper IV).

Taken together, AlASATb, T66ASATb and, but to a lesser extent, AlASATa and T66ASATa are considered to have ASAT activity for synthesizing SE(16:0) and SE(22:6). These four proteins may have acquired or retained ASAT activity through an evolutionary process while losing

most of their original DGAT activity. The DG levels in mutants suggested that these proteins potentially have minor DGAT activity. Still, according to the data, it is not easy to hypothesize the substrate preference of the four enzymes.

Expression of *AlASATb* or *T66ASATb*, enhanced squalene production by up to 88%. The strain with both these genes knocked out displayed reduced squalene levels (Figure 8, Paper IV). The findings imply that the regulation of the SE synthesis pathway related to squalene in SR21 differs from that in yeast , where squalene levels increased when the ASAT genes was disrupted (Zweytick et al., 2000).

3.5 Discussion

Different strategies can be conducted to make biomanufacturing more competitive in commercial markets. Based on the content from chapter 3.1 to 3.4, the key findings in this work are illustrated in Figure 19. Paper I demonstrated that an inhibitor treatment increased DHA-rich TAG production in thraustochytrids. Paper II, III and IV uncovered a Δ9-desaturase gene encoded a protein that contributed to C16:1 n-7 production, and, indirectly, C18:1 n-7 production, and secondly, four *ASAT* genes encoded proteins that synthesized SEs, and two of them, indirectly, enhanced squalene production. Although the abundance of C16:1 n-7, C18:1 n-7 and squalene are significantly lower than DHA in thraustochytrids, they can potentially be developed as value-added products in co-production with DHA. This thesis provides knowledge for two major strategies that could pave the way for competitive DHA production.

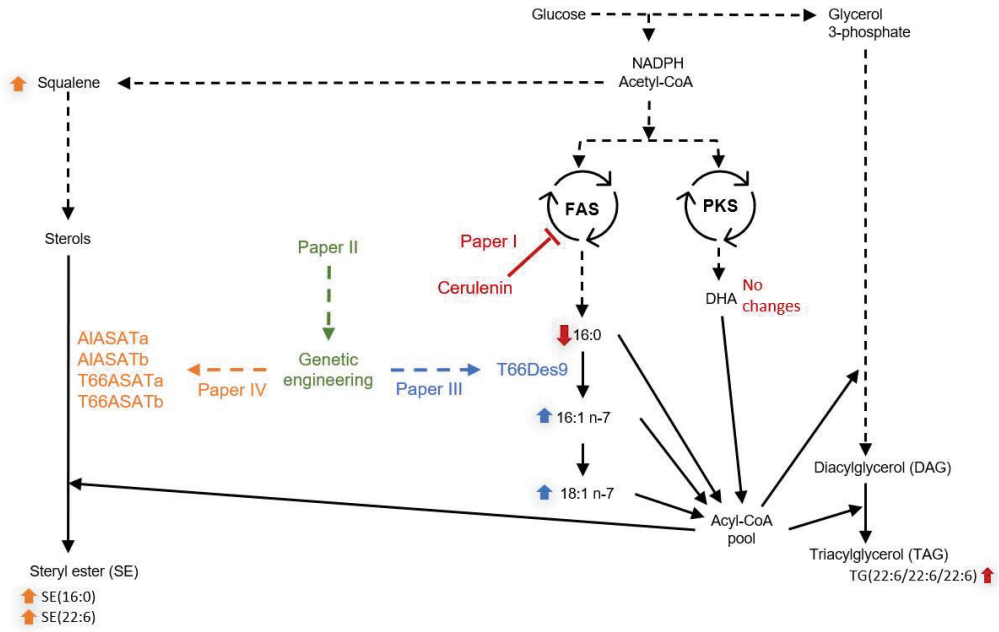

Figure 19. Major metabolic pathways related to this work with key results illustrated. Information in four different colors indicates the results from four papers. Red: Paper I, green: Paper II, blue: Paper III, orange: Paper IV. Solid black arrow: a single enzymatic reaction, dashed black arrow: multiple enzymatic reactions.

Despite the fact that omics analysis and metabolic modeling have been rapidly emerging, annotating genes with high accuracy remains one of the significant challenges. It is generally correct that homologous sequences have related functions. Still, exceptions could be found. The heavy reliance on homology-based annotation might also unintentionally discourage and limit the discovery of novel gene functions (Danchin et al., 2018). This work identified a Δ9-desaturase gene, previously was annotated as Δ12-desaturase gene based on homology in Paper III. Moreover, four *ASAT* genes were identified, encoding proteins that were annotated as DGAT2 based on homology in Paper IV. In other words, these enzymes do have catalytic activity

close to the previous annotation, but their substrate preferences were very different. The results of Paper III and IV provide a more accurate mapping of lipid and fatty acid pathways in thraustochytrids, which is critical to have an effective metabolic engineering strategy for biomanufacturing. Moreover, these results also highlight the challenge of constructing lipid and fatty acid pathways by homology-based functional annotation, suggesting that more detailed experimental validation or advanced functional prediction approaches should ought to be pursued.

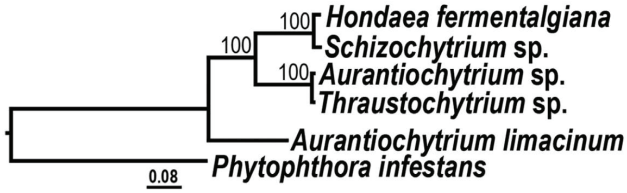

Figure 20. Phylogenomic analysis on 2389 homolog genes in the six genomes: *Hondaea fermentalgiana* strain CCAP 4062/3, *Schizochytrium* sp. CCTCC M209059, *Aurantiochytrium* sp. T66, *Thraustochytrium* sp. ATCC 26185, *Aurantiochytrium limacinum* SR21, The water mold *Phytophthora infestans* as outgroup. Bootstrap values are reported above the nodes. Copied from Dellero et al. (2018)

Thraustochytrid strains are highly diverse both genetically and phenotypically. T66 has been shown to not cluster closely to SR21 in a phylogenomic analysis (Figure 20) (Dellero et al., 2018). In Paper I, FAS was more significantly inhibited by cerulenin in SR21 than T66. Paper II showed that the genetic engineering methods have been established in SR21 but not in T66. In Paper III, *T66des9* was identified in T66, contributing to the production of C16:1 n-7, C18:1 n-7, while neither the gene nor the two FAs can be detected in SR21. In addition, several other differences not mentioned earlier were also observed during the investigation, including that T66 lumped more together, and more antibiotics resistant compared to SR21. Taken together,

these results suggest that the two strains are in relatively distant taxonomical positions, despite being assigned as the same genus. On the other hand, T66 is phenotypically clustered with three other thraustochytrid species of other genera (Figure 20). This also reflects that the taxonomy of thraustochytrids is not fully resolved. Further comparative studies between the two strains or their related strains can potentially expand the toolbox and flexibility for thraustochytrid metabolic engineering.

4 Conclusion and perspectives

In this thesis, two strains of thraustochytrids, a group of microbes with promising potentials in commercial productions, were characterized. Although utilizing inhibitors did not redistribute flux to increase DHA production, DHA could be enriched in lipids. Moreover, the production of TAG from DAG is presumably the bottleneck of DHA-rich TAGs production, mediated by enzymes like DGATs. These results could be further utilizing to facilitate DHA-rich lipid production in thraustochytrids by genetic engineering. There are many thraustochytrid strains, including T66 studied in this work, without established genetic methods. The method is influenced by various factors, such as how the expression cassettes are transformed and integrated into genomes. The elements on expression cassettes also affect gene expression and transformant selection. More systematic studies to narrow down the critical parameters are required to overcome fundamental barriers to protocol establishment. Nevertheless, by applying genetic engineering on SR21, this work demonstrated a Δ9-desaturase gene, previously annotated as Δ12-desaturase gene based on homology, encoded a protein that synthesizes C16:1 n-7 and indirectly enhanced C18:1 n-7 production. Moreover, four *ASAT* genes, encoding proteins that are homologous to DGAT2, synthesized SEs and two of them facilitated squalene production. The discoveries highlight the functional diversity of desaturases and acyl-CoA acyltransferases, which is important to consider when trying to deduce the potential a given organism has for producing unsaturated fatty acids and lipids based on its genome sequence alone. These genes could be explored further to increase the C16:1 n-7, C18:1 n-7 or squalene productivity of the strains used in biomanufacturing combined with bioprocess optimization in large-scale fermentation.

5 Appendix

5.1 Fatty acid profile analysis

In Paper I, III and IV, samples for determining the concentration (gram per liter of culture) of fatty acids were prepared as described:

> "Ten ml culture was frozen directly (−80 °C). Fatty acids were quantified by LC/MS/MS (QQQ) after hydrolysis of the lipids to free fatty acids: KOH (5 M, 400 µL) was added to culture sample (100 µl, well homogenized) to a final concentration 4 M and incubated at 80 °C for 120 min. The free fatty acids were extracted into dichloromethane (2 mL) after acidification with 500 µl of 4 M H_2SO_4. The sample was vortexed for 60 seconds before centrifugation (4000 g, 10 min). 200 µl of the organic phase were transferred to a sample vial and the solvent evaporated under nitrogen at 60 °C. The samples were reconstituted in absolute ethanol and the vials were flushed with nitrogen before capping." (Heggeset et al., 2019).

The prepared samples were then subjected to LC/MS/MS analysis as described:

> "For LC/MS/MS analysis 1 µl of sample was injected on an Agilent 1290 LC system coupled to an Agilent 6490 QQQ mass spectrometer. The LC system was set up with an Ascentis Express column (15 cm × 2,1 mm, 2.7 µm, Supelco). Mobile phase A was a 25 mM aqueous solution of ammonium formate and mobile phase B was pure acetonitrile. The LC separation was performed with a gradient elution. The starting condition was 75% B, which was held for 0.5 min. Then a linear gradient to 100% B at 8.5 min and held for 1 minute. The mobile phase flow was 0.5 ml /min. The Agilent 6490 was equipped with an Agilent Jet Stream (AJS) ion source and operated in negative mode. Ion source parameters were: Nebulizer: 45 psi, gas temp: 250 °C, drying gas flow: 12 l/min, Sheat gas temp: 400 °C, sheat gas flow: 11 L/min, Nozzle voltage: 1500 V and capillary voltage: 3000 V. The mass spectrometer was operated in single ion monitoring mode (SIM). External standards were used for confirmation and quantification of the fatty acids." (Heggeset et al., 2019).

5.2 Lipid profile analysis

Lipid extracted with procedures described in Paper I and IV were followed by lipid profile analysis using UHPSFC-MS described as follows:

> "A lipid profile analysis was performed using an UPC²® separation system coupled to a hybrid quadrupole orthogonal time-of-flight mass spectrometer SYNAPT G2-S HDMS (both Waters, Milford, MA, USA). The UPC²® system was equipped with a binary pump, a convergence manager, a column heater, an autosampler, and an auxiliary pump. The

separation system was coupled to the MS via a flow splitter kit that consisted of two T-pieces allowing control of the backpressure and infusion of a make-up liquid. The make-up liquid consisted of methanol:isopropanol:water (50:49:1, *v*/*v*/*v*) and its flow rate was set to 0.2 mL/min. Pressurized CO_2 was used as mobile phase A, methanol:water (99:1, *v*/*v*) with 30 mM ammonium acetate was used as mobile phase B. The gradient of mobile phase B followed the scheme: 0 min, 1%; 4.0 min, 30% (6); 4.4 min, 50% (2); 6.25 min 50% (1); 7.25 min, 50% (6); 7.35 min, 1% (6), 8.50 min, 1%. The column temperature was 50 °C, flow rate 1.9 mL/min and automated back-pressure regulator (ABPR) was set to 1800 psi. The mass spectrometer was equipped with an ESI source operated in positive mode. A data independent acquisition technique, MS^E, was applied for data acquisition and the collision energy ramped from 20 to 30 eV. The MS tuning parameters were set as follows: capillary voltages 3.0 kV, the source temperature 150 °C, the sampling cone 40 V, the source offset 60 V, the desolvation temperature 500 °C, the cone gas flow 50 L/h, the desolvation gas flow 850 L/h, and the nebulizer gas pressure 4 bar. Data were acquired over the mass range of 50–1200 Da and resolution of mass spectrometer was 20,000." (Bartosova et al., 2021a).

In Paper I, After data acquisition from UHPSFC-MS. The relative lipid concentration was determined. To consider the different ionization efficiency of different lipid class. The Progenesis QI-normalized abundance was RF-corrected by multiplying the RF of each lipid classes. RFs were determined in (Bartosova et al., 2021b) as follows: SE (CE): 1.7, TG: 0.29, DG: 0.35, MG: 1.25, CER: 0.32, PG: 41.77, PE: 3.59, PC: 1, LPC: 4.4 (Bartosova et al., 2021b). The RF-corrected abundance was then multiplied by the biomass per liter culture (g/l) to obtain the the relative lipid concentration, as each lipid sample were originated from a same biomass (five milligrams)

In Paper IV, the lipid concentration was determined by Single-point ISTD method (Bartosova et al., 2021b), described as follows:

> "Single-point ISTD method requires analysis of a sample containing analytes of unknown concentrations and known amount of ISTD. Amount of the unknown analyte is calculated using equation: $c = (c_{IS} \cdot A \cdot IRF)/A_{IS}$, where c is concentration, A is peak area, IRF is internal RF and IS stands for ISTD. Since we use set of ISTDs, one for each individual lipid class, IRF value was considered to be equal to 1, assuming that all lipid species in the same lipid class shows identical ionization efficiency." (Bartosova et al., 2021b).

ISTDs for each lipid classes: PC(13:0/13:0), LPC(22:0), CER(d18:1/17:0(OH)), MG(17:0), DG(15:0/15:0), PE(14:0/14:0), PG(14:0/14:0), CE(17:0) (for SE), TG(15:0/15:0/15:0) (Bartosova et al., 2021b).

5.3 Copyrights

Figure 1 is reprinted from Progress in Lipid Research, Vol 76, Christian Morabitoa, Caroline Bournauda, Cécile Maësa, Martin Schulera, Riccardo Aiese Ciglianob, Younès Delleroc, Eric Maréchala, Alberto Amatoa, Fabrice Rébeilléa, The lipid metabolism in thraustochytrids, 101007., Copyright (2019), with permission from Elsevier.

Figure 2, 5, 10, 11, 19 are used under the terms of the Creative Commons Attribution License (https://creativecommons.org/licenses/by/4.0/). Changes were made not in any way that suggests the licensor endorses me or my use.

Figure 3, 7 ,18 are used under the terms of the Creative Commons Attribution License (https://creativecommons.org/licenses/by/3.0/). Changes were made not in any way that suggests the licensor endorses me or my use.

Figure 9 is reprinted from Prostaglandins, Leukotrienes and Essential Fatty Acids, Vol 68, P. Sperling, P. Ternes, T.K. Zank, E. Heinz, The evolution of desaturases, 73-95., Copyright (2003), with permission from Elsevier.

Figure 13 is reprinted by permission from [Springer Nature Customer Service Centre GmbH]: [Springer] [Marine Biotechnology] [Docosahexaenoic Acid Production and Lipid-Body Formation in *Schizochytrium limacinum* SR21, Eiko Morita, Yasuyuki Kumon, Toro Nakahara, Satoshi Kagiwada, Tetsuko Noguchi], [2006]

Figure 16 is reprinted from Journal of Biotechnology, Vol 162, Jit Ern Chen, Alison G. Smith, A look at diacylglycerol acyltransferases (DGATs) in algae, 28-39., Copyright (2012), with permission from Elsevier.

Figure 20 is reprinted from Algal research, Vol 35, Younès Delleroa, Olivier Cagnacb, Suzanne Rosea, Khawla Seddikia, Mathilde Cussaca, Christian Morabitoa, Josselin Lupettea, Riccardo Aiese Ciglianoc, Walter Sanseverinoc, Marcel Kuntza, Juliette Jouheta, Eric Maréchala, Fabrice Rébeilléa, Alberto Amato, Proposal of a new thraustochytrid genus Hondaea gen. nov. and comparison of its lipid dynamics with the closely related pseudo-cryptic genus *Aurantiochytrium*, 125-141., Copyright (2018), with permission from Elsevier

Quotes from 'Heggeset et al., 2019' and 'Bartosova et al., 2021a' in the Appendix are used under the terms of the Creative Commons Attribution License (https://creativecommons.org/licenses/by/4.0/). Changes were made not in any way that suggests the licensor endorses me or my use.

Quotes from 'Bartosova et al., 2021a' in the Appendix are from Bartosova, Z., Gonzalez, S.V., Voigt, A., and Bruheim, P. (2021b). High throughput semiquantitative UHPSFC–MS/MS lipid profiling and lipid class determination. J. Chromatogr. Sci. 59, 670–680.

6 Reference

Aasen, I.M., Ertesvåg, H., Heggeset, T.M., Liu, B., Brautaset, T., Vadstein, O., and Ellingsen, T.E. (2016). Thraustochytrids as production organisms for docosahexaenoic acid (DHA), squalene, and carotenoids. *Appl. Microbiol. Biotechnol.* 100**,** 4309–4321.

Abe, E., Ikeda, K., Nutahara, E., Hayashi, M., Yamashita, A., Taguchi, R., Doi, K., Honda, D., Okino, N., and Ito, M. (2014). Novel lysophospholipid acyltransferase PLAT1 of *Aurantiochytrium limacinum* F26-b responsible for generation of palmitate-docosahexaenoate-phosphatidylcholine and phosphatidylethanolamine. *PLoS One* 9**,** e102377.

Adachi, T., Sahara, T., Okuyama, H., and Morita, N. (2017). Glass bead-based genetic transformation: an efficient method for transformation of thraustochytrid microorganisms. *J. Oleo. Sci.* 66**,** 791-795.

Aimola, I.A., Inuwa, H.M., Nok, A.J., Mamman, A.I., and Bieker, J.J. (2016). Cis-vaccenic acid induces differentiation and up-regulates gamma globin synthesis in K562, JK1 and transgenic mice erythroid progenitor stem cells. *Eur. J. Pharmacol.* 776**,** 9-18.

Alderman, D.J., Harrison, J.L., Bremer, G.B., and Jones, E.B.G. (1974). Taxonomic revisions in the marine biflagellate fungi: The ultrastructural evidence. *Mar. Biol.* 25**,** 345-357.

Alexa, O. (2020). Raising awareness about the impacts of squalene on the well-being of individuals, societies & the Environment! *J. Activist Sci. Tech. Edu.* 11**,** 9–13.

Aquafauna_Bio-Marine (2019). "AlgaMac-Enrich (https://www.aquafauna.com/algamac-enrich)".).

Athenstaedt, K., and Daum, G. (2006). The life cycle of neutral lipids: synthesis, storage and degradation. *Cellular and Molecular Life Sciences CMLS* 63**,** 1355-1369.

Bahnweg, G., and Sparrow Jr., F.K. (1974). Four new species of *Thraustochytrium* from antarctic regions, with notes on the distribution of zoosporic fungi in the antarctic marine ecosystems. *Am. J. Bot.* 61**,** 754-766.

Banaś, A., Carlsson, A.S., Huang, B., Lenman, M., Banaś, W., Lee, M., Noiriel, A., Benveniste, P., Schaller, H., Bouvier-Navé, P., and Stymne, S. (2005). Cellular sterol ester synthesis in plants is performed by an enzyme (phospholipid:sterol acyltransferase) different from the yeast and mammalian Acyl-CoA:sterol acyltransferases. *J. Biol. Chem.* 280**,** 34626-34634.

Bartosova, Z., Ertesvåg, H., Nyfløt, E.L., Kämpe, K., Aasen, I.M., and Bruheim, P. (2021a). Combined metabolome and lipidome analyses for in-depth characterization of lipid accumulation in the DHA producing *Aurantiochytrium* sp. T66. *Metabolites* 11**,** 135.

Bartosova, Z., Gonzalez, S.V., Voigt, A., and Bruheim, P. (2021b). High throughput semiquantitative UHPSFC–MS/MS lipid profiling and lipid class determination. *J. Chromatogr. Sci.* 59**,** 670–680.

Bazinet, R.P., and Layé, S. (2014). Polyunsaturated fatty acids and their metabolites in brain function and disease. *Nat. Rev. Neurosci.* 15**,** 771-785.

Bongiorni, L., Pusceddu, A., and Danovaro, R. (2005). Enzymatic activities of epiphytic and benthic thraustochytrids involved in organic matter degradation. *Aquat. Microb. Ecol.* 41**,** 299-305.

Calviello, G., Su, H.-M., Weylandt, K.H., Fasano, E., Serini, S., and Cittadini, A. (2013). Experimental evidence of ω-3 polyunsaturated fatty acid modulation of inflammatory cytokines and bioactive lipid mediators: Their potential role in inflammatory, neurodegenerative, and neoplastic diseases. *Biomed Res. Int.* 2013**,** 743171.
Cao, H. (2011). Structure-function analysis of diacylglycerol acyltransferase sequences from 70 organisms. *BMC Res. Notes* 4**,** 249.
Cardoso, C., Afonso, C., and Bandarra, N.M. (2016). Dietary DHA and health: cognitive function ageing. *Nutr. Res. Rev.* 29**,** 281-294.
Castro-González, M.I., and Méndez-Armenta, M. (2008). Heavy metals: Implications associated to fish consumption. *Environ. Toxicol. Pharmacol.* 26**,** 263-271.
Chan, P., Tomlinson, B., Lee, C.-B., and Lee, Y.-S. (1996). Effectiveness and safety of low-dose pravastatin and squalene, alone and in combination, in elderly patients with hypercholesterolemia. *J. Clin. Pharmacol.* 36**,** 422-427.
Chang, C.C.Y., Sun, J., and Chang, T.-Y. (2011). Membrane-bound O-acyltransferases (MBOATs). *Front. Biol.* 6**,** 177.
Chang, M., Zhang, T., Li, L., Lou, F., Ma, M., Liu, R., Jin, Q., and Wang, X. (2021). Choreography of multiple omics reveals the mechanism of lipid turnover in *Schizochytrium* sp. S31. *Algal Res.* 54**,** 102182.
Chang, T.-Y., Li, B.-L., Chang, C.C.Y., and Urano, Y. (2009). Acyl-coenzyme A:cholesterol acyltransferases. *Am. J. Physiol. Endocrinol. Metab.* 297**,** E1-E9.
Chaung, K.-C., Chu, C.-Y., Su, Y.-M., and Chen, Y.-M. (2012). Effect of culture conditions on growth, lipid content, and fatty acid composition of *Aurantiochytrium mangrovei* strain BL10. *AMB Express* 2**,** 42.
Chen, J.E., and Smith, A.G. (2012). A look at diacylglycerol acyltransferases (DGATs) in algae. *J. Biotechnol.* 162**,** 28-39.
Chen, Q., Steinhauer, L., Hammerlindl, J., Keller, W., and Zou, J. (2007). Biosynthesis of phytosterol esters: identification of a sterol O-acyltransferase in Arabidopsis. *Plant Physiol.* 145**,** 974-984.
Chen, W., Zhou, P.-P., Zhang, M., Zhu, Y.-M., Wang, X.-P., Luo, X.-A., Bao, Z.-D., and Yu, L.-J. (2016). Transcriptome analysis reveals that up-regulation of the fatty acid synthase gene promotes the accumulation of docosahexaenoic acid in *Schizochytrium* sp. S056 when glycerol is used. *Algal Res.* 15**,** 83-92.
Chodchoey, K., and Verduyn, C. (2012). Growth, fatty acid profile in major lipid classes and lipid fluidity of *Aurantiochytrium mangrovei* SK-02 As a function of growth temperature. *Braz J Microbiol* 43**,** 187-200.
Czabany, T., Athenstaedt, K., and Daum, G. (2007). Synthesis, storage and degradation of neutral lipids in yeast. *Biochim. Biophys. Acta Mol. Cell Biol. Lipids* 1771**,** 299-309.
Danchin, A., Ouzounis, C., Tokuyasu, T., and Zucker, J.-D. (2018). No wisdom in the crowd: genome annotation in the era of big data – current status and future prospects. *Microb. Biotechnol.* 11**,** 588-605.
De Stefani, E., and Ronco, A. (2013). Squalene: a multi-task link in the crossroads of cancer and aging. *Funct. Foods Health Dis.* 3**,** 462-476.
Dellero, Y., Cagnac, O., Rose, S., Seddiki, K., Cussac, M., Morabito, C., Lupette, J., Aiese Cigliano, R., Sanseverino, W., Kuntz, M., Jouhet, J., Maréchal, E., Rébeillé, F., and Amato, A. (2018). Proposal of a new thraustochytrid genus *Hondaea* gen. nov. and comparison of its lipid

dynamics with the closely related pseudo-cryptic genus *Aurantiochytrium*. *Algal Res.* 35**,** 125-141.
Dimopoulos, N., Watson, M., Sakamoto, K., and Hundal, Harinder s. (2006). Differential effects of palmitate and palmitoleate on insulin action and glucose utilization in rat L6 skeletal muscle cells. *Biochem. J.* 399**,** 473-481.
Dinicolantonio, J.J., and O'keefe, J.H. (2020). The importance of marine omega-3s for brain development and the prevention and treatment of behavior, mood, and other brain disorders. *Nutrients* 12**,** 2333.
Djoussé, L., Matsumoto, C., Hanson, N.Q., Weir, N.L., Tsai, M.Y., and Gaziano, J.M. (2014). Plasma cis-vaccenic acid and risk of heart failure with antecedent coronary heart disease in male physicians. *Clin. Nutr.* 33**,** 478-482.
Domergue, F., Spiekermann, P., Lerchl, J., Beckmann, C., Kilian, O., Kroth, P.G., Boland, W., Zähringer, U., and Heinz, E. (2003). New insight into *Phaeodactylum tricornutum* fatty acid metabolism. Cloning and functional characterization of plastidial and microsomal Δ12-fatty acid desaturases. *Plant Physiol.* 131**,** 1648-1660.
Dsm (2020). "DSM boosts maternal and infant nutrition portfolio with new plant-based high potency DHA oil (https://renewable-carbon.eu/news/dsm-boosts-maternal-and-infant-nutrition-portfolio-with-new-plant-based-high-potency-dha-oil/)".).
Faktorová, D., Nisbet, R.E.R., Fernández Robledo, J.A., Casacuberta, E., Sudek, L., Allen, A.E., Ares, M., Jr., Aresté, C., Balestreri, C., Barbrook, A.C., Beardslee, P., Bender, S., Booth, D.S., Bouget, F.Y., Bowler, C., Breglia, S.A., Brownlee, C., Burger, G., Cerutti, H., Cesaroni, R., Chiurillo, M.A., Clemente, T., Coles, D.B., Collier, J.L., Cooney, E.C., Coyne, K., Docampo, R., Dupont, C.L., Edgcomb, V., Einarsson, E., Elustondo, P.A., Federici, F., Freire-Beneitez, V., Freyria, N.J., Fukuda, K., Garcia, P.A., Girguis, P.R., Gomaa, F., Gornik, S.G., Guo, J., Hampl, V., Hanawa, Y., Haro-Contreras, E.R., Hehenberger, E., Highfield, A., Hirakawa, Y., Hopes, A., Howe, C.J., Hu, I., Ibañez, J., Irwin, N.a.T., Ishii, Y., Janowicz, N.E., Jones, A.C., Kachale, A., Fujimura-Kamada, K., Kaur, B., Kaye, J.Z., Kazana, E., Keeling, P.J., King, N., Klobutcher, L.A., Lander, N., Lassadi, I., Li, Z., Lin, S., Lozano, J.C., Luan, F., Maruyama, S., Matute, T., Miceli, C., Minagawa, J., Moosburner, M., Najle, S.R., Nanjappa, D., Nimmo, I.C., Noble, L., Novák Vanclová, A.M.G., Nowacki, M., Nuñez, I., Pain, A., Piersanti, A., Pucciarelli, S., Pyrih, J., Rest, J.S., Rius, M., Robertson, D., Ruaud, A., Ruiz-Trillo, I., Sigg, M.A., Silver, P.A., Slamovits, C.H., Smith, G.J., Sprecher, B.N., Stern, R., Swart, E.C., Tsaousis, A.D., Tsypin, L., Turkewitz, A., Turnšek, J., et al. (2020). Genetic tool development in marine protists: emerging model organisms for experimental cell biology. *Nat. Methods* 17**,** 481-494.
Fan, K.-W., Jiang, Y., Faan, Y.-W., and Chen, F. (2007). Lipid characterization of mangrove thraustochytrid – *Schizochytrium mangrovei*. *J. Agric. Food Chem.* 55**,** 2906-2910.
Fan, K.W., Aki, T., Chen, F., and Jiang, Y. (2010). Enhanced production of squalene in the thraustochytrid *Aurantiochytrium mangrovei* by medium optimization and treatment with terbinafine. *World J. Microbiol. Biotechnol.* 26**,** 1303-1309.
Fao (2010). "FAO Fats and fatty acids in human nutrition. Report of an expert consultation". (Rome: Food and Agriculture Organization of the United Nations).
Fao (2018). "The state of world fisheries and aquaculture 2018 - Meeting the sustainable development goals". (Rome).

Finco, A.M.D.O., Mamani, L.D.G., Carvalho, J.C.D., De Melo Pereira, G.V., Thomaz-Soccol, V., and Soccol, C.R. (2017). Technological trends and market perspectives for production of microbial oils rich in omega-3. *Crit. Rev. Biotechnol.* 37**,** 656-671.

Foresti, O., Ruggiano, A., Hannibal-Bach, H.K., Ejsing, C.S., and Carvalho, P. (2013). Sterol homeostasis requires regulated degradation of squalene monooxygenase by the ubiquitin ligase Doa10/Teb4. *eLife* 2**,** e00953.

Fox, C.B. (2009). Squalene emulsions for parenteral vaccine and drug delivery. *Molecules* 14**,** 3286-3312.

Freitas, U., and Leblanc, M. (2008). DHAid™ – The vegetarian source. *OCL* 15**,** 247-251.

Gao, M., Song, X., Feng, Y., Li, W., and Cui, Q. (2013). Isolation and characterization of *Aurantiochytrium* species: high docosahexaenoic acid (DHA) production by the newly isolated microalga, *Aurantiochytrium* sp. SD116. *J. Oleo. Sci.* 62**,** 143-151.

Gertsik, L., Poland, R.E., Bresee, C., and Rapaport, M.H. (2012). Omega-3 fatty acid augmentation of citalopram treatment for patients with major depressive disorder. *J. Clin. Psychopharmacol.* 32**,** 61-64.

Gill, S., Stevenson, J., Kristiana, I., and Brown, Andrew j. (2011). Cholesterol-dependent degradation of squalene monooxygenase, a control point in cholesterol synthesis beyond HMG-CoA Reductase. *Cell Metab.* 13**,** 260-273.

Giudice, G.D., Fragapane, E., Bugarini, R., Hora, M., Henriksson, T., Palla, E., O'hagan, D., Donnelly, J., Rappuoli, R., and Podda, A. (2006). Vaccines with the MF59 adjuvant do not stimulate antibody responses against squalene. *Clin. Vaccine Immunol.* 13**,** 1010-1013.

Gohil, N., Bhattacharjee, G., Khambhati, K., Braddick, D., and Singh, V. (2019). Engineering strategies in microorganisms for the enhanced production of squalene: advances, challenges and opportunities. *Front. Bioeng. Biotechnol.* 7**,** 50.

Güneş, F. (2013). Medical use of squalene as a natural antioxidant. *J. Marmara U. Inst. Health Sci.* 3**,** 221-229.

Hamre, K., Kolås, K., Sandnes, K., Julshamn, K., and Kiessling, A. (2001). Feed intake and absorption of lipid oxidation products in Atlantic salmon (*Salmo salar*) fed diets coated with oxidised fish oil. *Fish Physiol. Biochem.* 25**,** 209-219.

Han, X., Zhao, Z., Wen, Y., and Chen, Z. (2020). Enhancement of docosahexaenoic acid production by overexpression of ATP-citrate lyase and acetyl-CoA carboxylase in *Schizochytrium* sp. *Biotechnol. Biofuels* 13**,** 131.

Hauvermale, A., Kuner, J., Rosenzweig, B., Guerra, D., Diltz, S., and Metz, J.G. (2006). Fatty acid production in *Schizochytrium* sp.: Involvement of a polyunsaturated fatty acid synthase and a type I fatty acid synthase. *Lipids* 41**,** 739-747.

Heggeset, T.M.B., Ertesvåg, H., Liu, B., Ellingsen, T.E., Vadstein, O., and Aasen, I.M. (2019). Lipid and DHA-production in *Aurantiochytrium* sp. - Responses to nitrogen starvation and oxygen limitation revealed by analyses of production kinetics and global transcriptomes. *Sci. Rep.* 9**,** 19470.

Hernández, M.L., Whitehead, L., He, Z., Gazda, V., Gilday, A., Kozhevnikova, E., Vaistij, F.E., Larson, T.R., and Graham, I.A. (2012). A cytosolic acyltransferase contributes to triacylglycerol synthesis in sucrose-rescued Arabidopsis seed oil catabolism mutants. *Plant Physiol.* 160**,** 215-225.

Honda, D., Yokochi, T., Nakahara, T., Erata, M., and Higashihara, T. (1998). *Schizochytrium limacinum* sp. nov., a new thraustochytrid from a mangrove area in the west Pacific Ocean. *Mycol. Res.* 102**,** 439-448.

Huang, J., Aki, T., Yokochi, T., Nakahara, T., Honda, D., Kawamoto, S., Shigeta, S., Ono, K., and Suzuki, O. (2003). Grouping newly isolated docosahexaenoic acid-producing thraustochytrids based on their polyunsaturated fatty acid profiles and comparative analysis of 18S rRNA genes. *Mar. Biotechnol.* 5**,** 450-457.

Jacome-Sosa, M.M., Borthwick, F., Mangat, R., Uwiera, R., Reaney, M.J., Shen, J., Quiroga, A.D., Jacobs, R.L., Lehner, R., and Proctor, S.D. (2014). Diets enriched in *trans*-11 vaccenic acid alleviate ectopic lipid accumulation in a rat model of NAFLD and metabolic syndrome. *J. Nutr. Biochem.* 25**,** 692-701.

Jakobsen, A.N., Aasen, I.M., Josefsen, K.D., and Strøm, A.R. (2008). Accumulation of docosahexaenoic acid-rich lipid in thraustochytrid *Aurantiochytrium* sp. strain T66: effects of N and P starvation and O_2 limitation. *Appl. Microbiol. Biotechnol.* 80**,** 297–306.

Jakobsen, A.N., Aasen, I.M., and Strom, A.R. (2007). Endogenously synthesized (-)-*proto*-quercitol and glycine betaine are principal compatible solutes of *Schizochytrium* sp. strain S8 (ATCC 20889) and three new isolates of phylogenetically related thraustochytrids. *Appl. Environ. Microbiol.* 73**,** 5848-5856.

Janthanomsuk, P., Verduyn, C., and Chauvatcharin, S. (2015). Improved docosahexaenoic acid production in *Aurantiochytrium* by glucose limited pH-auxostat fed-batch cultivation. *Bioresour. Technol.* 196**,** 592-599.

Jiang, Y., Fan, K.-W., Tsz-Yeung Wong, R., and Chen, F. (2004). Fatty acid composition and squalene content of the marine microalga *Schizochytrium mangrovei*. *J. Agric. Food Chem.* 52**,** 1196-1200.

Jonas, A. (2000). Lecithin cholesterol acyltransferase. *Biochim. Biophys. Acta Mol. Cell Biol. Lipids* 1529**,** 245-256.

Jovanovic, S., Dietrich, D., Becker, J., Kohlstedt, M., and Wittmann, C. (2021). Microbial production of polyunsaturated fatty acids — high-value ingredients for aquafeed, superfoods, and pharmaceuticals. *Curr. Opin. Biotechnol.* 69**,** 199-211.

Kang, D.H., Anbu, P., Jeong, Y.S., Chaulagain, B.P., Seo, J.W., and Hur, B.-K. (2010). Identification and characterization of a novel enzyme related to the synthesis of PUFAs derived from *Thraustochytrium aureum* ATCC 34304. *Biotechnol. Bioprocess Eng.* 15**,** 261-272.

Knothe, G. (2010). Biodiesel derived from a model oil enriched in palmitoleic acid, macadamia nut oil. *Energy Fuels* 24**,** 2098-2103.

Koba, K., and Yanagita, T. (2014). Health benefits of conjugated linoleic acid (CLA). *Obes. Res. Clin. Pract.* 8**,** e525-e532.

Kobayashi, T., Sakaguchi, K., Matsuda, T., Abe, E., Hama, Y., Hayashi, M., Honda, D., Okita, Y., Sugimoto, S., Okino, N., and Ito, M. (2011). Increase of eicosapentaenoic acid in thraustochytrids through thraustochytrid ubiquitin promoter-driven expression of a fatty acid Δ5 desaturase gene. *Appl. Environ. Microbiol.* 77**,** 3870-3876.

Korber, M., Klein, I., and Daum, G. (2017). Steryl ester synthesis, storage and hydrolysis: A contribution to sterol homeostasis. *Biochim. Biophys. Acta Mol. Cell Biol. Lipids* 1862**,** 1534-1545.

Lange, Y., Ory, D.S., Ye, J., Lanier, M.H., Hsu, F.-F., and Steck, T.L. (2008). Effectors of rapid homeostatic responses of endoplasmic reticulum cholesterol and 3-hydroxy-3-methylglutaryl-CoA reductase. *J. Biol. Chem.* 283**,** 1445-1455.

Lee, J.W., Na, D., Park, J.M., Lee, J., Choi, S., and Lee, S.Y. (2012). Systems metabolic engineering of microorganisms for natural and non-natural chemicals. *Nat. Chem. Biol.* 8**,** 536-546.

Lewis, T.E., Nichols, P.D., and Mcmeekin, T.A. (2001). Sterol and squalene content of a docosahexaenoic-acid-producing thraustochytrid: influence of culture age, temperature, and dissolved oxygen. *Mar. Biotechnol.* 3**,** 439-447.

Li, J., Liu, R., Chang, G., Li, X., Chang, M., Liu, Y., Jin, Q., and Wang, X. (2015). A strategy for the highly efficient production of docosahexaenoic acid by *Aurantiochytrium limacinum* SR21 using glucose and glycerol as the mixed carbon sources. *Bioresour. Technol.* 177**,** 51-57.

Li, Z., Chen, X., Li, J., Meng, T., Wang, L., Chen, Z., Shi, Y., Ling, X., Luo, W., Liang, D., Lu, Y., Li, Q., and He, N. (2018a). Functions of PKS genes in lipid synthesis of *Schizochytrium* sp. by gene disruption and metabolomics analysis. *Mar. Biotechnol.* 20**,** 792-802.

Li, Z., Meng, T., Ling, X., Li, J., Zheng, C., Shi, Y., Chen, Z., Li, Z., Li, Q., Lu, Y., and He, N. (2018b). Overexpression of malonyl-CoA: ACP transacylase in *Schizochytrium* sp. to improve polyunsaturated fatty acid production. *J. Agric. Food Chem.* 66**,** 5382-5391.

Liang, L., Zheng, X., Fan, W., Chen, D., Huang, Z., Peng, J., Zhu, J., Tang, W., Chen, Y., and Xue, T. (2020). Genome and transcriptome analyses provide insight into the omega-3 long-chain polyunsaturated fatty acids biosynthesis of *Schizochytrium limacinum* SR21. *Front. Microbiol.* 11**,** 687.

Liang, Y., Liu, Y., Tang, J., Ma, J., Cheng, J.J., and Daroch, M. (2018). Transcriptomic profiling and gene disruption revealed that two genes related to PUFAs/DHA biosynthesis may be essential for cell growth of *Aurantiochytrium* sp. *Mar. Drugs* 16**,** 310.

Ling, X., Zhou, H., Yang, Q., Yu, S., Li, J., Li, Z., He, N., Chen, C., and Lu, Y. (2020). Functions of enyolreductase (ER) domains of PKS cluster in lipid synthesis and enhancement of PUFAs accumulation in *Schizochytrium limacinum* SR21 using triclosan as a regulator of ER. *Microorganisms* 8**,** 300.

Lippmeier, J.C., Crawford, K.S., Owen, C.B., Rivas, A.A., Metz, J.G., and Apt, K.E. (2009). Characterization of both polyunsaturated fatty acid biosynthetic pathways in *Schizochytrium* sp. *Lipids* 44**,** 621-630.

Liu, Q., Siloto, R.M.P., Lehner, R., Stone, S.J., and Weselake, R.J. (2012). Acyl-CoA:diacylglycerol acyltransferase: Molecular biology, biochemistry and biotechnology. *Prog. Lipid Res.* 51**,** 350-377.

Liu, Q., Siloto, R.M.P., Snyder, C.L., and Weselake, R.J. (2011). Functional and topological analysis of yeast acyl-CoA:diacylglycerol acyltransferase 2, an endoplasmic reticulum enzyme essential for triacylglycerol biosynthesis. *J. Biol. Chem.* 286**,** 13115-13126.

Liu, Q., Siloto, R.M.P., and Weselake, R.J. (2010). Role of cysteine residues in thiol modification of acyl-CoA:diacylglycerol acyltransferase 2 from yeast. *Biochemistry* 49**,** 3237-3245.

Liu, Y., Tang, J., Li, J., Daroch, M., and Cheng, J.J. (2014). Efficient production of triacylglycerols rich in docosahexaenoic acid (DHA) by osmo-heterotrophic marine protists. *Appl. Microbiol. Biotechnol.* 98**,** 9643-9652.

Liu, Z., Zang, X., Cao, X., Wang, Z., Liu, C., Sun, D., Guo, Y., Zhang, F., Yang, Q., Hou, P., and Pang, C. (2018). Cloning of the *pks3* gene of *Aurantiochytrium limacinum* and functional study of

the 3-ketoacyl-ACP reductase and dehydratase enzyme domains. *PLoS One* 13**,** e0208853.
Lordan, R., Tsoupras, A., and Zabetakis, I. (2017). Phospholipids of Animal and Marine Origin: Structure, Function, and Anti-Inflammatory Properties. *Molecules* 22**,** 1964.
Ma, Z., Tan, Y., Cui, G., Feng, Y., Cui, Q., and Song, X. (2015). Transcriptome and gene expression analysis of DHA producer *Aurantiochytrium* under low temperature conditions. *Sci. Rep.* 5**,** 14446-14446.
Ma, Z., Tian, M., Tan, Y., Cui, G., Feng, Y., Cui, Q., and Song, X. (2017). Response mechanism of the docosahexaenoic acid producer *Aurantiochytrium* under cold stress. *Algal Res.* 25**,** 191-199.
Macdonald, C., and Soll, J. (2020). Shark conservation risks associated with the use of shark liver oil in SARS-CoV-2 vaccine development. *bioRxiv***,** 2020.2010.2014.338053.
Maedler, K., Oberholzer, J., Bucher, P., Spinas, G.A., and Donath, M.Y. (2003). Monounsaturated fatty acids prevent the deleterious effects of palmitate and high glucose on human pancreatic β-cell turnover and function. *Diabetes* 52**,** 726-733.
Marchan, L.F., Chang, K.J.L., Nichols, P.D., Mitchell, W.J., Polglase, J.L., and Gutierrez, T. (2018). Taxonomy, ecology and biotechnological applications of thraustochytrids: a review. *Biotechnol. Adv.* 36**,** 26-46.
Matsuda, T., Sakaguchi, K., Hamaguchi, R., Kobayashi, T., Abe, E., Hama, Y., Hayashi, M., Honda, D., Okita, Y., Sugimoto, S., Okino, N., and Ito, M. (2012). Analysis of Δ12-fatty acid desaturase function revealed that two distinct pathways are active for the synthesis of PUFAs in *T. aureum* ATCC 34304. *J. Lipid Res.* 53**,** 1210-1222.
Mazereeuw, G., Lanctôt, K.L., Chau, S.A., Swardfager, W., and Herrmann, N. (2012). Effects of omega-3 fatty acids on cognitive performance: a meta-analysis. *Neurobiol. Aging* 33**,** 1482.e1417-1482.e1429.
Mcfie, P.J., Stone, S.L., Banman, S.L., and Stone, S.J. (2010). Topological orientation of acyl-CoA:diacylglycerol acyltransferase-1 (DGAT1) and identification of a putative active site histidine and the role of the N terminus in dimer/tetramer formation. *J. Biol. Chem.* 285**,** 37377-37387.
Meesapyodsuk, D., and Qiu, X. (2016). Biosynthetic mechanism of very long chain polyunsaturated fatty acids in *Thraustochytrium* sp. 26185. *J. Lipid Res.* 57**,** 1854-1864.
Meng, Y., Shao, X., Wang, Y., Li, Y., Zheng, X., Wei, G., Kim, S.-W., and Wang, C. (2020). Extension of cell membrane boosting squalene production in the engineered *Escherichia coli*. *Biotechnol. Bioeng.* 117**,** 3499-3507.
Metz, J.G., Roessler, P., Facciotti, D., Levering, C., Dittrich, F., Lassner, M., Valentine, R., Lardizabal, K., Domergue, F., Yamada, A., Yazawa, K., Knauf, V., and Browse, J. (2001). Production of polyunsaturated fatty acids by polyketide synthases in both prokaryotes and eukaryotes. *Science* 293**,** 290-293.
Mocking, R.J.T., Harmsen, I., Assies, J., Koeter, M.W.J., Ruhé, H.G., and Schene, A.H. (2016). Meta-analysis and meta-regression of omega-3 polyunsaturated fatty acid supplementation for major depressive disorder. *Transl. Psychiatry* 6**,** e756-e756.
Mohankumar, S.K., Hanke, D., Siemens, L., Cattini, A., Enns, J., Shen, J., Reaney, M., Zahradka, P., and Taylor, C.G. (2013). Dietary supplementation of *trans*-11-vaccenic acid reduces adipocyte size but neither aggravates nor attenuates obesity-mediated metabolic abnormalities in *fa/fa* Zucker rats. *Br. J. Nutr.* 109**,** 1628-1636.

Moore, K., Hughes, C.F., Ward, M., Hoey, L., and Mcnulty, H. (2018). Diet, nutrition and the ageing brain: current evidence and new directions. *Proc. Nutr. Soc.* 77**,** 152-163.
Morabito, C., Bournaud, C., Maës, C., Schuler, M., Aiese Cigliano, R., Dellero, Y., Maréchal, E., Amato, A., and Rébeillé, F. (2019). The lipid metabolism in thraustochytrids. *Prog. Lipid Res.* 76**,** 101007.
Morita, E., Kumon, Y., Nakahara, T., Kagiwada, S., and Noguchi, T. (2006). Docosahexaenoic acid production and lipid-body formation in *Schizochytrium limacinum* SR21. *Mar. Biotechnol.* 8**,** 319-327.
Mozaffarian, D., and Wu, J.H.Y. (2011). Omega-3 fatty acids and cardiovascular disease: effects on risk factors, molecular pathways, and clinical events. *J. Am. Coll. Cardiol.* 58**,** 2047-2067.
Nachtschatt, M., Okada, S., and Speight, R. (2020). Integral membrane fatty acid desaturases: a review of biochemical, structural, and biotechnological advances. *Eur. J. Lipid Sci. Technol.* 122**,** 2000181.
Nagao, K., Murakami, A., and Umeda, M. (2019). Structure and function of Δ9-fatty acid desaturase. *Chem. Pharm. Bull.* 67**,** 327-332.
Nakahara, T., Yokochi, T., Higashihara, T., Tanaka, S., Yaguchi, T., and Honda, D. (1996). Production of docosahexaenoic and docosapentaenoic acids by *Schizochytrium* sp. isolated from Yap Islands. *J. Am. Oil Chem.' Soc.* 73**,** 1421-1426.
Nguyen, H.T., Mishra, G., Whittle, E., Pidkowich, M.S., Bevan, S.A., Merlo, A.O., Walsh, T.A., and Shanklin, J. (2010). Metabolic engineering of seeds can achieve levels of ω-7 fatty acids comparable with the highest levels found in natural plant sources. *Plant Physiol.* 154**,** 1897-1904.
Nguyen, H.T., Park, H., Koster, K.L., Cahoon, R.E., Nguyen, H.T.M., Shanklin, J., Clemente, T.E., and Cahoon, E.B. (2015). Redirection of metabolic flux for high levels of omega-7 monounsaturated fatty acid accumulation in camelina seeds. *Plant Biotechnol. J.* 13**,** 38-50.
Nutahara, E., Abe, E., Uno, S., Ishibashi, Y., Watanabe, T., Hayashi, M., Okino, N., and Ito, M. (2019). The glycerol-3-phosphate acyltransferase PLAT2 functions in the generation of DHA-rich glycerolipids in *Aurantiochytrium limacinum* F26-b. *PLoS One* 14**,** e0211164.
Okino, N., Wakisaka, H., Ishibashi, Y., and Ito, M. (2018). Visualization of endoplasmic reticulum and mitochondria in *Aurantiochytrium limacinum* by the expression of EGFP with cell organelle-specific targeting/retaining signals. *Mar. Biotechnol.***,** 182-192.
Patel, A., Karageorgou, D., Katapodis, P., Sharma, A., Rova, U., Christakopoulos, P., and Matsakas, L. (2021). Bioprospecting of thraustochytrids for omega-3 fatty acids: A sustainable approach to reduce dependency on animal sources. *Trends Food Sci. Technol.* 115**,** 433-444.
Patel, A., Liefeldt, S., Rova, U., Christakopoulos, P., and Matsakas, L. (2020). Co-production of DHA and squalene by thraustochytrid from forest biomass. *Sci. Rep.* 10**,** 1992.
Patel, A., Rova, U., Christakopoulos, P., and Matsakas, L. (2019). Simultaneous production of DHA and squalene from *Aurantiochytrium* sp. grown on forest biomass hydrolysates. *Biotechnol. Biofuels* 12**,** 255.
Raghukumar, S. (2002). Ecology of the marine protists, the Labyrinthulomycetes (Thraustochytrids and Labyrinthulids). *European Journal of Protistology* 38**,** 127-145.

Raghukumar, S., and Damare, V.S. (2011). Increasing evidence for the important role of Labyrinthulomycetes in marine ecosystems. *Botanica Marina* 54**,** 3-11.
Raghukumar, S., Sharma, S., Raghukumar, C., Sathe-Pathak, V., and Chandramohan, D. (1994). Thraustochytrid and fungal component of marine detritus. IV. Laboratory studies on decomposition of leaves of the mangrove *Rhizophora apiculata* Blume. *J. Exp. Mar. Biol. Ecol.* 183**,** 113-131.
Ramaiah, N., Raghukumar, S., Mangesh, G., and Madhupratap, M. (2005). Seasonal variations in carbon biomass of bacteria, thraustochytrids and microzooplankton in the Northern Arabian Sea. *Deep Sea Res. Part II Top. Stud. Oceanogr.* 52**,** 1910-1921.
Ratledge, C. (2004). Fatty acid biosynthesis in microorganisms being used for single cell oil production. *Biochimie* 86**,** 807-815.
Ravi Kumar, S., Yamauchi, I., Narayan, B., Katsuki, A., Hosokawa, M., and Miyashita, K. (2016). Squalene modulates fatty acid metabolism: Enhanced EPA/DHA in obese/diabetic mice (*KK-A^{y}*) model. *Eur. J. Lipid Sci. Technol.* 118**,** 1935-1941.
Ren, L.-J., Chen, S.-L., Geng, L.-J., Ji, X.-J., Xu, X., Song, P., Gao, S., and Huang, H. (2018). Exploring the function of acyltransferase and domain replacement in order to change the polyunsaturated fatty acid profile of *Schizochytrium* sp. *Algal Res.* 29**,** 193-201.
Ren, L.-J., Ji, X.-J., Huang, H., Qu, L., Feng, Y., Tong, Q.-Q., and Ouyang, P.-K. (2010). Development of a stepwise aeration control strategy for efficient docosahexaenoic acid production by *Schizochytrium* sp. *Appl. Microbiol. Biotechnol.* 87**,** 1649-1656.
Ren, L.-J., Sun, G.-N., Ji, X.-J., Hu, X.-C., and Huang, H. (2014). Compositional shift in lipid fractions during lipid accumulation and turnover in *Schizochytrium* sp. *Bioresour. Technol.* 157**,** 107-113.
Ren, L.J., Zhuang, X.Y., Chen, S.L., Ji, X.J., and Huang, H. (2015). Introduction of omega-3 desaturase obviously changed the fatty acid profile and sterol content of *Schizochytrium* sp. *J. Agric. Food Chem.* 63**,** 9770-9776.
Reynolds, C.M., Loscher, C.E., Moloney, A.P., and Roche, H.M. (2008). *Cis*-9, *trans*-11-conjugated linoleic acid but not its precursor *trans*-vaccenic acid attenuate inflammatory markers in the human colonic epithelial cell line Caco-2. *Br. J. Nutr.* 100**,** 13-17.
Riley, L.A., and Guss, A.M. (2021). Approaches to genetic tool development for rapid domestication of non-model microorganisms. *Biotechnol. Biofuels* 14**,** 30.
Rimm, E.B., Appel, L.J., Chiuve, S.E., Djoussé, L., Engler, M.B., Kris-Etherton, P.M., Mozaffarian, D., Siscovick, D.S., and Lichtenstein, A.H. (2018). Seafood long-chain n-3 polyunsaturated fatty acids and cardiovascular disease: a science advisory from the American Heart Association. *Circulation* 138**,** e35-e47.
Rosa, S.M., Galvagno, M.A., and Vélez, C.G. (2011). Adjusting culture conditions to isolate thraustochytrids from temperate and cold environments in southern Argentina. *Mycoscience* 52**,** 242-252.
Rosa, S.M., Soria, M.A., Vélez, C.G., and Galvagno, M.A. (2010). Improvement of a two-stage fermentation process for docosahexaenoic acid production by *Aurantiochytrium limacinum* SR21 applying statistical experimental designs and data analysis. *Bioresour. Technol.* 101**,** 2367-2374.
Ruth, L., and Javier, A.M. (2006). Pharmacological inhibitors of fatty acid synthase (FASN)-catalyzed endogenous fatty acid biogenesis: A new family of anti-cancer agents? *Curr. Pharm. Biotechnol.* 7**,** 483-494.

Rybak, A., Fokou, P.A., and Meier, M.a.R. (2008). Metathesis as a versatile tool in oleochemistry. *Eur. J. Lipid Sci. Technol.* 110**,** 797-804.
Sakaguchi, K., Matsuda, T., Kobayashi, T., Ohara, J., Hamaguchi, R., Abe, E., Nagano, N., Hayashi, M., Ueda, M., Honda, D., Okita, Y., Taoka, Y., Sugimoto, S., Okino, N., and Ito, M. (2012). Versatile transformation system that is applicable to both multiple transgene expression and gene targeting for thraustochytrids. *Appl. Environ. Microbiol.* 78**,** 3193-3202.
Sakthivel, G. (2016). Prediction of CI engine performance, emission and combustion characteristics using fish oil as a biodiesel at different injection timing using fuzzy logic. *Fuel* 183**,** 214-229.
Salem, N.J., and Eggersdorfer, M. (2015). Is the world supply of omega-3 fatty acids adequate for optimal human nutrition? *Curr. Opin. Clin. Nutr. Metab. Care* 18**,** 147-154.
Sandager, L., Dahlqvist, A., Banaś, A., Ståhl, U., Lenman, M., Gustavsson, M., and Stymne, S. (2000). An acyl-CoA:cholesterol acyltransferase (ACAT)-related gene is involved in the accumulation of triacylglycerols in *Sacchoromyces cerevisiae*. *Biochem. Soc. Trans.* 28**,** 700-702.
Sasso, S., Pohnert, G., Lohr, M., Mittag, M., and Hertweck, C. (2012). Microalgae in the postgenomic era: a blooming reservoir for new natural products. *FEMS Microbiol. Rev.* 36**,** 761-785.
Shi, Y., Chen, Z., Li, Y., Cao, X., Yang, L., Xu, Y., Li, Z., and He, N. (2021). Function of ORFC of the polyketide synthase gene cluster on fatty acid accumulation in *Schizochytrium limacinum* SR21. *Biotechnol. Biofuels* 14**,** 163.
Silva, A.R., Moraes, B.P.T., and Gonçalves-De-Albuquerque, C.F. (2020). Mediterranean Diet: Lipids, Inflammation, and Malaria Infection. *Int. J. Mol. Sci.* 21**,** 4489.
Sinn, N., Milte, C.M., Street, S.J., Buckley, J.D., Coates, A.M., Petkov, J., and Howe, P.R.C. (2012). Effects of n-3 fatty acids, EPA v. DHA, on depressive symptoms, quality of life, memory and executive function in older adults with mild cognitive impairment: a 6-month randomised controlled trial. *Br. J. Nutr.* 107**,** 1682-1693.
Song, Z., Stajich, J.E., Xie, Y., Liu, X., He, Y., Chen, J., Hicks, G.R., and Wang, G. (2018). Comparative analysis reveals unexpected genome features of newly isolated Thraustochytrids strains: on ecological function and PUFAs biosynthesis. *BMC Genom.* 19**,** 541.
Sorger, D., Athenstaedt, K., Hrastnik, C., and Daum, G. (2004). A yeast strain lacking lipid particles bears a defect in ergosterol formation. *J. Biol. Chem.* 279**,** 31190-31196.
Sperling, P., Ternes, P., Zank, T.K., and Heinz, E. (2003). The evolution of desaturases. *Prostaglandins, Leukotrienes & Essential Fatty Acids* 68**,** 73-95.
Stefan, N., Kantartzis, K., Celebi, N., Staiger, H., Machann, J., Schick, F., Cegan, A., Elcnerova, M., Schleicher, E., Fritsche, A., and Häring, H.-U. (2010). Circulating palmitoleate strongly and independently predicts insulin sensitivity in humans. *Diabetes Care* 33**,** 405-407.
Stevenson, J., Luu, W., Kristiana, I., and Brown, Andrew j. (2014). Squalene mono-oxygenase, a key enzyme in cholesterol synthesis, is stabilized by unsaturated fatty acids. *Biochem. J.* 461**,** 435-442.
Stone, S.J., Levin, M.C., and Farese, R.V. (2006). Membrane topology and identification of key functional amino acid residues of murine acyl-CoA:diacylglycerol acyltransferase-2. *J. Biol. Chem.* 281**,** 40273-40282.
Stone, S.J., Levin, M.C., Zhou, P., Han, J., Walther, T.C., and Farese, R.V. (2009). The endoplasmic reticulum enzyme DGAT2 is found in mitochondria-associated membranes and has a

mitochondrial targeting signal that promotes its association with mitochondria. *J. Biol. Chem.* 284**,** 5352-5361.
Sun, H., Chen, H., Zang, X., Hou, P., Zhou, B., Liu, Y., Wu, F., Cao, X., and Zhang, X. (2015). Application of the Cre/*lox*P site-specific recombination system for gene transformation in *Aurantiochytrium limacinum*. *Molecules* 20**,** 10110-10121.
Sun, X.M., Xu, Y.S., and Huang, H. (2020). Thraustochytrid cell factories for producing lipid compounds. *Trends Biotechnol.* 39**,** 648-650.
Tocher, D.R. (2015). Omega-3 long-chain polyunsaturated fatty acids and aquaculture in perspective. *Aquaculture* 449**,** 94-107.
Tocher, D.R., Betancor, M.B., Sprague, M., Olsen, R.E., and Napier, J.A. (2019). Omega-3 long-chain polyunsaturated fatty acids, EPA and DHA: bridging the gap between supply and demand. *Nutrients* 11**,** 89.
Turchetto-Zolet, A.C., Maraschin, F.S., De Morais, G.L., Cagliari, A., Andrade, C.M.B., Margis-Pinheiro, M., and Margis, R. (2011). Evolutionary view of acyl-CoA diacylglycerol acyltransferase (DGAT), a key enzyme in neutral lipid biosynthesis. *BMC Evol. Biol.* 11**,** 263.
Van Der Veen, J.N., Kennelly, J.P., Wan, S., Vance, J.E., Vance, D.E., and Jacobs, R.L. (2017). The critical role of phosphatidylcholine and phosphatidylethanolamine metabolism in health and disease. *Biochim. Biophys. Acta Biomembr.* 1859**,** 1558-1572.
Van Der Voort, M., Spruijt, J., Potters, J., De Wolf, P., and Elissen, H. (2017). "Socio-economic assessment of Algae-based PUFA production, public output report of the PUFA chain project". (Göttingen).
Vanhercke, T., Shrestha, P., Green, A.G., and Singh, S.P. (2011). Mechanistic and structural insights into the regioselectivity of an acyl-CoA fatty acid desaturase via directed molecular evolution. *J. Biol. Chem.* 286**,** 12860-12869.
Wang, S., Lan, C., Wang, Z., Wan, W., Cui, Q., and Song, X. (2020). PUFA-synthase-specific PPTase enhanced the polyunsaturated fatty acid biosynthesis via the polyketide synthase pathway in *Aurantiochytrium*. *Biotechnol. Biofuels* 13**,** 152-152.
Wang, Y., Lu, J., Ruth, M.R., Goruk, S.D., Reaney, M.J., Glimm, D.R., Vine, D.F., Field, C.J., and Proctor, S.D. (2008). *Trans*-11 Vaccenic Acid Dietary Supplementation Induces Hypolipidemic Effects in JCR:LA-*cp* Rats. *J. Nutr.* 138**,** 2117-2122.
Watanabe, K., Perez, C.M.T., Kitahori, T., Hata, K., Aoi, M., Takahashi, H., Sakuma, T., Okamura, Y., Nakashimada, Y., Yamamoto, T., Matsuyama, K., Mayuzumi, S., and Aki, T. (2020). Improvement of fatty acid productivity of thraustochytrid, *Aurantiochytrium* sp. by genome editing. *J. Biosci. Bioeng.***,** 373-380.
Weete, J.D., Kim, H., Gandhi, S.R., Wang, Y., and Dute, R. (1997). Lipids and ultrastructure of *Thraustochytrium* sp. ATCC 26185. *Lipids* 32**,** 839-845.
Wilding, M., Nachtschatt, M., Speight, R., and Scott, C. (2017). An improved and general streamlined phylogenetic protocol applied to the fatty acid desaturase family. *Mol. Phylogenet. Evol.* 115**,** 50-57.
Won-Kyung, H., Sun-Yeon, H., Hye-Mi, P., Chul Ho, K., Jung-Hoon, S., and Akihiko, K. (2013). Characterization of a squalene synthase from the thraustochytrid microalga *Aurantiochytrium* sp. KRS101. *J. Microbiol. Biotechnol.* 23**,** 759-765.
Xu, W., Ma, X., and Wang, Y. (2016). Production of squalene by microbes: an update. *World J. Microbiol. Biotechnol.* 32**,** 195.

Xu, X., Qu, R., Wu, W., Jiang, C., Shao, D., and Shi, J. (2021a). Applications of microbial co-cultures in polyketides production. *J. Appl. Microbiol.* 130**,** 1023-1034.
Xu, Y., Pan, X., Lu, J., Wang, J., Shan, Q., Stout, J., and Chen, G. (2021b). Evolutionary and biochemical characterization of a *Chromochloris zofingiensis* MBOAT with wax synthase and diacylglycerol acyltransferase activity. *J. Exp. Bot.* 72**,** 5584-5598.
Ye, J., Liu, M., He, M., Ye, Y., and Huang, J. (2019). Illustrating and enhancing the biosynthesis of astaxanthin and docosahexaenoic acid in *Aurantiochytrium* sp. SK4. *Mar. Drugs* 17**,** 45.
Yokochi, T., Honda, D., Higashihara, T., and Nakahara, T. (1998). Optimization of docosahexaenoic acid production by *Schizochytrium limacinum* SR21. *Appl. Microbiol. Biotechnol.* 49**,** 72-76.
Yokoyama, R., and Honda, D. (2007). Taxonomic rearrangement of the genus *Schizochytrium* sensu lato based on morphology, chemotaxonomic characteristics, and 18S rRNA gene phylogeny (Thraustochytriaceae, Labyrinthulomycetes): emendation for *Schizochytrium* and erection of *Aurantiochytrium* and *Oblongichytrium* gen. nov. *Mycoscience* 48**,** 199-211.
Yoshida, K., Hashimoto, M., Hori, R., Adachi, T., Okuyama, H., Orikasa, Y., Nagamine, T., Shimizu, S., Ueno, A., and Morita, N. (2016). Bacterial long-chain polyunsaturated fatty acids: their biosynthetic genes, functions, and practical use. *Mar. Drugs* 14**,** 94.
Yoshida, M., Ioki, M., Matsuura, H., Hashimoto, A., Kaya, K., Nakajima, N., and Watanabe, M.M. (2020). Diverse steroidogenic pathways in the marine alga *Aurantiochytrium*. *J. Appl. Phycol.* 32**,** 1631-1642.
Yu, C., Kennedy, N.J., Chang, C.C.Y., and Rothblatt, J.A. (1996). Molecular cloning and characterization of two isoforms of *Saccharomyces cerevisiae* acyl-CoA:sterol acyltransferase. *J. Biol. Chem.* 271**,** 24157-24163.
Yue, X.-H., Chen, W.-C., Wang, Z.-M., Liu, P.-Y., Li, X.-Y., Lin, C.-B., Lu, S.-H., Huang, F.-H., and Wan, X. (2019). Lipid distribution pattern and transcriptomic insights revealed the potential mechanism of docosahexaenoic acid traffics in *Schizochytrium* sp. A-2. *J. Agric. Food Chem.* 67**,** 9683-9693.
Zhang, S., He, Y., Sen, B., Chen, X., Xie, Y., Keasling, J.D., and Wang, G. (2018). Alleviation of reactive oxygen species enhances PUFA accumulation in *Schizochytrium* sp. through regulating genes involved in lipid metabolism. *Metab. Eng. Commun.* 6**,** 39-48.
Zhao, X., and Qiu, X. (2018). Analysis of the biosynthetic process of fatty acids in *Thraustochytrium*. *Biochimie* 144**,** 108-114.
Zhou, X.R., Horne, I., Damcevski, K., Haritos, V., Green, A., and Singh, S. (2008). Isolation and functional characterization of two independently-evolved fatty acid Δ12-desaturase genes from insects. *Insect Mol. Biol.* 17**,** 667-676.
Zhou, Y.J., Buijs, N.A., Siewers, V., and Nielsen, J. (2014). Fatty acid-derived biofuels and chemicals production in *Saccharomyces cerevisiae*. *Front. Bioeng. Biotechnol.* 2.
Zweytick, D., Leitner, E., Kohlwein, S.D., Yu, C., Rothblatt, J., and Daum, G. (2000). Contribution of Are1p and Are2p to steryl ester synthesis in the yeast *Saccharomyces cerevisiae*. *Eur. J. Biochem.* 267**,** 1075-1082.

7 Papers

Paper I

Utilizing lipidomics and fatty acid synthase inhibitors to explore lipid accumulation in two *Aurantiochytrium* species

Authors

E-Ming Rau[1], Inga Marie Aasen[2], Zdenka Bartosova[1], Per Bruheim[1], Helga Ertesvåg[1*]

[1]Department of Biotechnology and Food Science, NTNU Norwegian University of Science and Technology, Trondheim, Norway

[2]Department of Biotechnology and Nanomedicine, SINTEF Industry, Trondheim, Norway

* Correspondence to: helga.ertesvag@ntnu.no

Paper II

marine drugs

MDPI

Review

Method Development Progress in Genetic Engineering of Thraustochytrids

E-Ming Rau and Helga Ertesvåg *

Department of Biotechnology and Food Science, NTNU Norwegian University of Science and Technology, N7491 Trondheim, Norway; e.m.rau@ntnu.no
* Correspondence: helga.ertesvag@ntnu.no; Tel.: +47-7359-8678

Abstract: Thraustochytrids are unicellular, heterotrophic marine eukaryotes. Some species are known to store surplus carbon as intracellular lipids, and these also contain the long-chain polyunsaturated fatty acid docosahexaenoic acid (DHA). Most vertebrates are unable to synthesize sufficient amounts of DHA, and this fatty acid is essential for, e.g., marine fish, domesticated animals, and humans. Thraustochytrids may also produce other commercially valuable fatty acids and isoprenoids. Due to the great potential of thraustochytrids as producers of DHA and other lipid-related molecules, a need for more knowledge on this group of organisms is needed. This necessitates the ability to do genetic manipulation of the different strains. Thus far, this has been obtained for a few strains, while it has failed for other strains. Here, we systematically review the genetic transformation methods used for different thraustochytrid strains, with the aim of aiding studies on strains not yet successfully transformed. The designs of transformation cassettes are also described and compared. Moreover, the potential problems when trying to establish transformation protocols in new thraustochytrid species/strains are discussed, along with suggestions utilized in other organisms to overcome similar challenges. The approaches discussed in this review could be a starting point when designing protocols for other non-model organisms.

Keywords: thraustochytrids; *Aurantiochytrium*; *Schizochytrium*; transformation; electroporation

Citation: Rau, E.-M.; Ertesvåg, H. Method Development Progress in Genetic Engineering of Thraustochytrids. *Mar. Drugs* **2021**, *19*, 515. https://doi.org/10.3390/md19090515

Academic Editors: Alberto Amato and Bill J. Baker

Received: 30 June 2021
Accepted: 9 September 2021
Published: 11 September 2021

1. Introduction

Thraustochytrids are heterotrophic marine microorganisms divided into ten genera [1]. They belong to stramenopiles, one of the most diverse eukaryotic phyla, known for groups such as diatoms, oomycetes and brown algae [1,2]. Thraustochytrids commonly inhabit oceans and sediments, especially in nutrient-rich areas, such as mangrove forests, where they grow on decomposing biological debris, and they play critical ecological roles for carbon recycling. Detailed biological features and classification have recently been extensively reviewed by others [3].

Thraustochytrids are well-known for storing up to 70% lipids (triacylglycerols) containing high amounts of ω3-polyunsaturated fatty acids (ω3-PUFAs), especially docosahexaenoic acid (DHA), produced by a dedicated polyketide synthase-like (PKS) enzyme complex [4–6]. DHA and other ω3-PUFAs, such as eicosapentaenoic acid (EPA), have substantial benefits for human health, including reducing the risks of cardiovascular, depressional, and neurodegenerative diseases [7–9]. As humans and most other vertebrates hardly synthesize DHA, it must be obtained by the diet. Currently, fish oil is the most used source for human and domesticated animals, including fish. Due to the limited fish stock available, alternative sustainable sources of DHA are needed, and thraustochytrids have been developed as commercial DHA-rich oils producers [10–12]. However, DHA from thraustochytrids is currently considered to be less competitive in low-cost markets [13]. On the other hand, some thraustochytrids produce other substances, such as squalene [10,14], carotenoids [15], extracellular enzymes [16], and extracellular polysaccharides [17], that potentially could be valuable biproducts.

Genetic engineering tools have become increasingly important in understanding specific metabolic pathways that could eventually be the prerequisite to create strains producing valuable materials in higher rates and titers [11,18,19]. Due to the advance and reduced cost of sequencing techniques, it is relatively easy to acquire genome sequences and identify gene targets for engineering. However, genetic method development of marine protists across taxa showed that no protocol could be universally applied [20]. Additionally, as will become apparent later, the established protocols for thraustochytrids all seem to be restrained to one or only a few strains. This is a general challenge for anyone working on non-model organisms; the transformation protocol needs to be designed for that particular strain.

When a new strain is to be transformed, the challenge is how to find the first true transformant when one does not know which antibiotic resistance markers can be used, which promoters and terminators will work, how to transfer the DNA, or the efficiency of recombination in that particular strain. The multiple possible combinations of parameters make the method development on new strains complicated without proper feasibility clues based on previous experiences in the same genus. Still, experiences from related species may help. This review aims to compile and discuss the current transformation protocols and choice of DNA elements for thraustochytrids. Knowledge of what has been achieved for other microorganisms is included. Additionally, while this review focuses on thraustochytrids, it may also be read as an example of the different approaches that can be used to achieve gene knock-outs and gene knock-ins in other microorganisms.

2. Transforming DNA into the Cells: Methods and Considerations

Electroporation, biolistic transformation, and *Agrobacterium*-mediated transformation (AMT) are used for many microbial cells, and all three methods have been successfully applied in thraustochytrids (Figure 1).

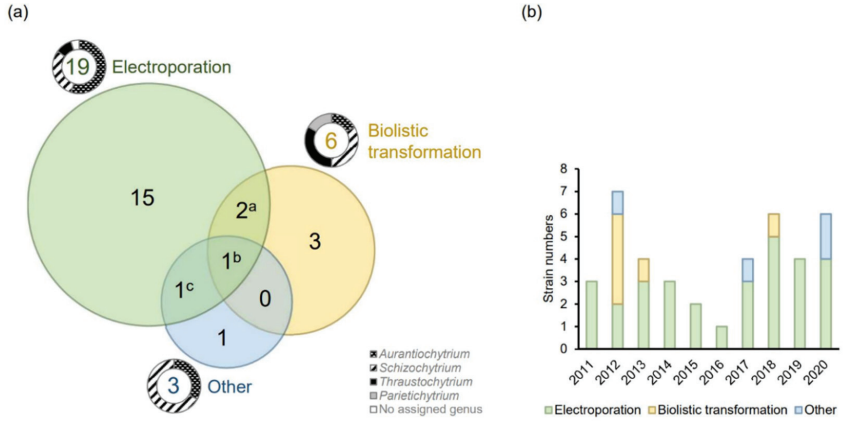

Figure 1. (**a**) The number of successfully engineered thraustochytrid strains by one or more methods (electroporation [20–52], biolistic transformation [5,27,53–55], and others [56–59]) (Tables S1 and S2). The doughnut pie charts indicate the proportion of different genera. Four strains have been transformed by more than one method: [a] *A. limacinum* mh018 and *T. aureum* ATCC 34304; [b] *Schizochytrium* sp. S31; [c] *Schizochytrium* sp. TIO1101; (**b**) The number of successfully transformed thraustochytrid strains and the methods applied in recent years. Any strain–method combinations are counted only once, even if they are used in several publications.

During electroporation, electric pulses are applied to the cells, and pores may be generated in both the cell membrane and the nuclear membrane. Depending on the conditions, the pores can be reversible and non-lethal for the cell. When such pore-generation is used to facilitate the uptake of exogenous DNA, the process is called electrotransforma-

tion [60]. Biolistic transformation, or particle bombardment mediated transformation, uses high-pressure helium to inject DNA-coated non-reactive metal (tungsten or gold) particles into host cells. This has been applied to a wide variety of species [61]. The procedure is relatively simple, and it is the most widely used technique for genetic engineering in diatoms [62]. Still, the method has a relatively high cost. Its frequency of multiple copy random insertions is higher, and it causes more cell damage [61,63]. *Agrobacterium tumefaciens* is a plant pathogen that is widely used in generating transgenic plants, fungi, and microalgae. When *A. tumefaciens* infects a cell, part of its Ti plasmid, or binary vector, is integrated into the genome of the cell. AMT is relatively inexpensive. The DNA being transferred can be large (up to 150 kb) and with a single copy genome integration [64,65], which makes it possible to introduce an entire metabolic pathway.

It is important to note that there is a marked difference as to which thraustochytrid genera can be transformed by which method. Sakaguchi et al. [27] showed that electroporation is far more efficient than biolistic transformation in *Aurantiochytrium limacinum* mh0186, while biolistic transformation is more efficient than electroporation in *Thraustochytrium aureum* ATCC 34304. The electroporation protocol did not succeed at all in *Parietichytrium* sp. TA04Bb and *Schizochytrium* sp. SEK 579, both of which could be transformed by a particle gun. These results indicate that the fundamental biological features determining the success of any transformation method can be quite different between genera. As ectoplasmic nets, the unique 'rhizoid-like' cell membrane structures that extend from sub-cellular organelles are more apparent in *Parietichytrium* and *Schizochytrium* than *Aurantiochytrium* [3], the cellular structural features may affect the effectiveness of different transformation methods. This further suggests that one should test another of these principally different methods if the first one tested does not yield any results in a new microorganism.

2.1. Transformation by Electroporation

In thraustochytrids, electroporation is the most common method for delivering DNA into cells (Figure 1). In the methods developed for thraustochytrid strains, both the treatment of cells prior to electroporation and the electroporation conditions themselves have been varied, as described in Figure 2. Exponential decay pulses and square wave pulses are the two most widely used pulse types for electrotransformation [66]. An exponential decay pulse is generated by exponentially reducing the initial voltage. Exponential decay pulse is described by two components: (1) electric field strength (kV/cm) is the electric potential difference (voltage) per unit distance between two electrodes; and (2) pulse length or time constant (ms), is equal to resistance multiplied by capacity [67]. The ionic strength and the volume of electroporation solutions affect the resistance of the samples so that the time constants are also affected. High ionic solutions with large volumes tend to have lower resistance, resulting in greater current and a higher probability of arcing and cell lethality. These parameters are further described below.

2.1.1. Pulse Types, Numbers, and the Parameters

The known optimal values of pulse length and field strength vary among different species. For most microbes, pulse lengths lie within a range from 1 to 30 ms, and field strength from 1 to 20 kV/cm [60]. Exponential decay is the most used pulse type in thraustochytrids, with the applied field strengths vary from 1.8 to 10 kV/cm, while the set pulse lengths range from 0.65 to 25 ms (Figure 2). A square wave pulse is generated by quickly turning on and off a voltage, which is maintained at a stable level (constant field strength) in a short period of time (pulse length) [68]. Square wave pulses have been used to transform two thraustochytrid species (Figure 2, Table S1).

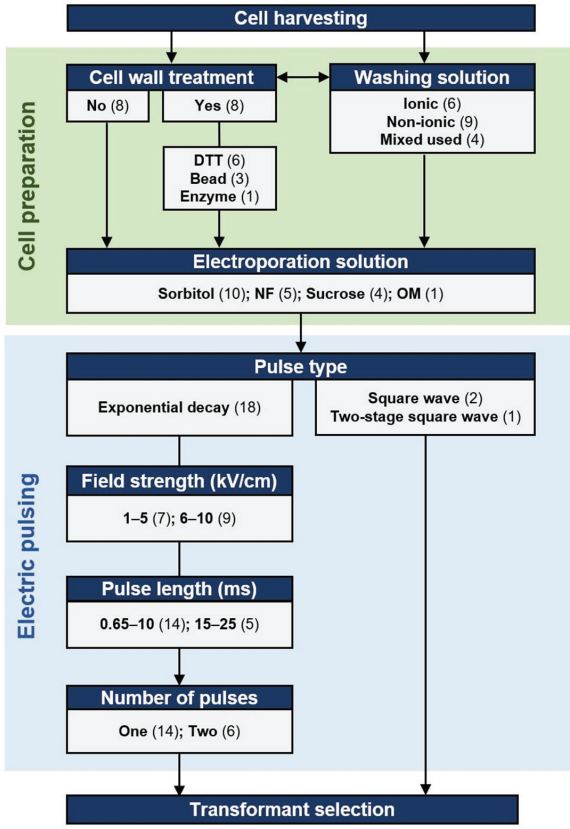

Figure 2. The parameters prevalence and the procedure scheme of transformation by electroporation in thraustochytrid strains. Numbers in parentheses, the number of strains that have used the parameter in at least one publication (Table S1); NF, Nucleofector™ solution L; OM, OPTI-MEM™ I; Ionic buffers include BSS, artificial sea water and phosphate buffer; Non-ionic, buffers include 50 mM Sucrose, 1 M Sorbitol, water, PEG 8000; Enzyme, 20 g/L pectinase and 20 g/L snailase in 7 M KCl.

A series of pulse parameters can be tested to find the optimal values. For *Aurantiochytrium* sp. SD116, the number of transformants decreased as the pulse length in the tested range increased [40]. Previous studies also show that a series of voltages should be tested to find the optimal field strength values during the new protocol [40,51]. For bacteria, optimal transformation results were often obtained by applying high field strengths with shorter time constants, or low field strengths with high time constants [67,69]. However, we found no similar correlations in the published protocols for thraustochytrids.

Most thraustochytrid protocols applied one exponential decay pulse per electroporation, while some applied two exponential pulses (Figure 2). In the microalgae *Chlamydomonas reinhardtii*, two pulses were required to introduce DNA into the cell, but only one pulse was needed to deliver DNA into the cell-wall-deficient mutant [70]. However, at least four thraustochytrid strains were engineered successfully with only one pulse without cell wall disruption (see Section 2.1.2), indicating that introducing DNA into thraustochytrid cells with intact cell walls does not require two exponential decay pulses. In addition, the transformation efficiency in *Aurantiochytrium* sp. SD116 increased about five times when the square wave pulse number increased from 30 to 50, followed by a five-times reduction when the number increased from 50 to 60 [40], suggesting that optimal pulse numbers can be narrow-ranged when applying electroporation with square wave pulses.

The initial voltage of an exponential decay pulse is high, to enhance cell permeabilization by pore generation, while the subsequential decayed low voltage part of the pulse contributes to electrophoretic transferring molecules into the cells [66]. As the voltages of the initial and later stage of an exponential decay pulse are related to one another, and cannot be adjusted independently, methods were developed with combinations of a first rapid high-voltage pulse followed by a longer low-voltage pulse in mammalian cells [71,72]. The low-voltage pulse was shown to contribute to the transfection efficiency when the plasmid concentration is low [73]. For thraustochytrids, *A. limacinum* SR21 has been transformed by two short, high voltage square pulses for poring cells, followed by one longer, lower voltage square pulse for molecule transferring using the NEPA21 electroporator [20]. This instrument can measure the resistance, allowing it to be adjusted to a specific range by altering cell volumes before pulsing (see Section 2.1.3), an informative function for further parameter optimization.

High-throughput approaches can be performed to optimize pulse parameters. Through transforming the cells with fluorescently labeled DNA or cell-impermeable fluorescent molecules, the efficiency of delivering molecules to the cells can be measured by the number of fluorescent cells detected under different pulse conditions. This approach separates the process of transforming DNA from recombination and transcription of the inserted DNA. For example, the transformation of YOYO-1 labeled plasmid DNA was used to determine the permeability of yeast cells [74]. Similar approaches have been applied in microalgae, *Caecitelus* sp., *Nannochloropsis oceanica*, and *C. reinhardtii* through FITC-Dextran transformation [20,75]. However, fluorescently labeled DNA or cell-impermeable fluorescent chemicals can also accumulate in permeable but non-viable cells. In order to distinguish the permeable viable cells from permeable non-viable cells, Muñoz et al. [76] utilized two cell-impermeable dyes with different florescent emission wavelengths, Sytox Green and propidium iodide; these were mixed with the cells before the pulses and after the recovery from pulses, respectively, to measure transient cell permeability and viability independently. This method was successfully applied to find optimized pulse conditions in four microalgae species. A similar approach on thraustochytrids has not been reported to date.

A more specific challenge for thraustochytrids is that their cells can co-exist in various growth stages, including medium vegetative cells, large multinucleated or sporangium cells, and small zoospores [1]. There are not only ambiguities between a single multinucleated cell, a single sporangium, and a cluster of multiple zoospores; the cleavages formed on the sporangium cells also decrease the roundness of cells to different extents. These various cell sizes and shapes make it difficult to distinguish individual cells by fluorescence microscopy or flow cytometry. They probably also are electrotransformed at different frequencies.

2.1.2. Cell Wall Disruption or Removal

Cell walls are complex structures that generally contain various polysaccharides, lipids, and proteins. Disruption of cell walls has been shown to facilitate the uptake of molecules of the cells. For instance, the cell wall-less mutants of the microalgae *C. reinhardtii* could take up larger-sized molecules such as polysaccharides and proteins more efficiently [75,77]. In general, the electrotransformation efficiency of marine protists is relatively low without cell wall removal [20]. One example was the transformation efficiency in *C. reinhardtii*, shown to be up to ten times higher for the cell wall-less mutant than for the wild type [78].

Chemical treatments have been used to disrupt or remove cell walls. Dithiothreitol (DTT) contains two sulfhydryl groups, which can reduce the disulfide bridges of cell wall proteins to destabilize cell wall structures or even generate protoplasts. In yeast, cell wall porosity increased when the number of disulfide bridges of cell wall proteins decreased [79]. DTT-treatment resulted in the release of various proteins, glycoproteins, and polysaccharides from the outer cell wall layers of the yeast *Candida albicans* [80]. DTT

has been applied to the transformation of multiple species, such as *Saccharomyces cerevisiae* and other fungi [81]. In thraustochytrids, DTT treatment is the most used method to disrupt or remove cell walls before electric pulses (Figure 2). Cell wall degrading enzymes, including pectinase and snailase (a mixture of many enzymes including cellulase, beta-glucuronidase, polygalacturonase, hemicellulase, protease, and pectinase), can also be used to prepare microalgae protoplast [82,83]. In *Schizochytrium* sp. PKU#Mn4, the two enzymes were applied to weaken the cell wall further after DTT treatment [46]. As thraustochytrid cell walls are generally composed of galactose-rich polysaccharides without cellulose [3], one would expect pectinase and polygalacturonase, but not the cellulase and hemicellulase, to play the major role in decomposing the cell walls in the protocol. However, using only these enzymes for disrupting cell walls remains to be tested in preparing thraustochytrid cells for electroporation.

Cell walls can also be physically weakened by vigorously agitating the cells in the presence of glass beads, as demonstrated for yeast, the microalgae *Chlamydomonas* and thraustochytrids [32,84,85]. In thraustochytrid strain 12B and *A. limacinum* SR21, the transformation efficiency was improved by agitating with glass beads from nearly no transformants to 1.5–15 transformants/μg and 3–150 transformants/μg, respectively [32]. Hence, when establishing a thraustochytrid electroporation protocol, cell wall disruption is a parameter to consider.

2.1.3. Effect of the Solutions Used to Prepare the Electrocompetent Cells

Typical electroporation solutions used on microbial cells are non-ionic osmotic stabilizers such as sorbitol and sucrose, to increase the cell survival rate [86]. In yeast, the transformation was more efficient with sorbitol as an electroporation solution than with sucrose [87]. Similarly, sorbitol is the most used electroporation solution for thraustochytrids, followed by sucrose (Figure 2), indicating that sorbitol can be a prioritized option in establishing the protocols. Although the absence of ions during electric pulse increases the cell viability, washing cells without ions could decrease the cell viability [88], which further complicates the selection of solutions. Even if the solutions used are non-ionic, the cells' environment will not be entirely non-ionic due to incomplete washing. In thraustochytrids, both ionic (e.g., artificial seawater, BSS [51], and phosphate buffer) and non-ionic solution (H_2O, sorbitol, and sucrose) has been used to wash cells (Figure 2).

2.2. Transforming DNA into Thraustochytrid Cells by Non-Electroporation Methods

In thraustochytrids, biolistic transformation is the second most used approach (Figure 1a), but apparently is less used for thraustochytrids now (Figure 1b). However, it might just be that more groups have the equipment for studying the electrotransformable strains, and hence they are studied more. As mentioned earlier, some strains are only transformed by the biolistic method. Moreover, AMT has been used to engineer two *Schizochytrium* species (Table S2). Recently, a commercial kit originally developed for yeast transformation was successfully applied on *Aurantiochytrium* sp. YLH70 [56]. The protocol is significantly simpler than the methods mentioned previously. Although the detailed principle of the kit is not described, it seems to be related to the lithium cation-based chemical transformation that is commonly applied in yeast [81]. This implies that establishing protocols based on other existing protocols with more straightforward procedures might still be possible.

2.3. Other Strategies for Transferring DNA into Cells

Tremendous efforts have been dedicated from different research groups to broaden our skillsets in the genetic manipulation of thraustochytrids. However, several concerns could hinder generating systematic strategies based on the existing protocols. For instance, it would be beneficial if details on unsuccessful protocols and optimization strategies had been revealed, as demonstrated amiably by few studies [27,32,40,51], to reduce the unnecessary trials under limited times and resources. Moreover, it is unfortunately common

to have transformation protocols reported without necessary details. This could affect the reproducibility and make it more challenging to interpret the optimal factors by protocol comparisons. Nevertheless, there are still genetic engineering strategies that could be tested on thraustochytrids, especially those that have been used on other stramenopiles and microalgae, or technologies developed recently.

Escherichia coli can transfer plasmids or episomes based on conjugative plasmids through conjugative bridges between the donor *E. coli* and the recipient cells, a process similar to AMT. Two plasmids are often used, including a cargo plasmid that contains the expression cassette and a helper plasmid (without the origin of transfer, *oriT*) that includes all genes required for transferring an *oriT*-containing plasmid. Conjugation does not require expensive equipment such as electroporators, and efficient conjugation-based genetic methods have been established for some diatom and green algae species [20,62,89]. For instance, the transformation efficiency of conjugation is higher than biolistic and electroporation in the diatom *Phaeodactylum tricornutum* [90,91], and a vector with 49 kb cargo DNA were introduced and maintained in *P. tricornutum* after conjugation [91].

Electroporation can also be developed in combination with digital microfluidics systems. Traditional 'bulk' electroporation usually applies voltage from hundreds to thousands of volts, which can cause water electrolysis in the part of solutions near the electrodes, resulting in local pH changes that reduce cell viability. In digital microfluidics systems, cells and DNA cassettes are encapsulated in tiny oily droplets before electric pulses with electrodes placed near the surfaces of the droplets so that the applied voltages can be largely reduced to 1 V–2 V though still being able to give an electric field strength in a range similar to bulk electroporation [92,93]. In addition, due to the relatively sizeable area-to-volume ratio of the droplets, the heat generated by the pulses can be more rapidly dissipated [94]. The droplet electroporation on microfluidic chips was found to have up to a thousand times higher transformation efficiency for the microalgae *C. reinhardtii* than the bulk electroporation using cuvettes [78,95], and can therefore be a promising system to test on transforming thraustochytrids and other microbes.

Cell-penetrating peptides (CPPs) are small peptides usually with less than 30 amino acids that show a remarkable ability to cross cell membranes and can transport biological materials intracellularly through non-covalent binding [96]. The TAT peptide (GRKKRRQRRRPQ) was the first CPP to be discovered. It is naturally part of the transactivator of transcription (TAT) protein of human immunodeficiency viruses. The TAT peptide has been used to facilitate the translocation of the dsDNA T-DNA into the microalgae *Chlorella vulgaris*, resulting in genomic integration of a DNA cassette. The peptide pVEC (LLIILRRRIRKQAHAHSK) derived from the murine vascular endothelial cadherin protein, has been used to transport Cas9-gRNA RNPs (see Section 3.3 and 3.4) into the microalgae *C. reinhardtii* for gene disruption. One advantage of both methods is the simplicity of the procedure, which only requires cells being treated with detergent or protease before or after mixing with the corresponding CPP-cargo [97,98]. Further investigation is required to determine the potential application of CPPs on the transformation of other species.

3. The Properties of the DNA Affect the Outcome of the Transformation

After the DNA has been transformed into the cell, it can be integrated in the genome at a specific location by homologous recombination (HR), utilizing the sequence homology-based DNA repair mechanism of the cells. Alternatively, DNA can be integrated in the genome at the location of random double-strand breaks (DSBs) by the non-homologous end joining repair (NHEJ) pathway. In most microalgae, random integration is significantly more efficient than HR, and widely applied to the genome engineering [62,99,100]. However, the site of the genomic integrations can affect the expression levels, and with random integration, one cannot utilize previous knowledge on the integration site. Moreover, non-target genes can be disrupted by random integration, resulting in misinterpretation of phenotypes unless the integration site is mapped [101]. Therefore, approaches such as introducing dedicated nucleases or interfering with NHEJ-specific enzymes have been proposed

to enhance HR efficiency [102]. Exogenous genes without homology arms have been randomly integrated and expressed in at least nine thraustochytrid strains (Table S3). For four of these strains, random integration was shown to be more efficient than HR-based genome integration [27]. Episomes and plasmids, which can autonomously replicate extrachromosomally and carry expression cassettes, would also reduce the potential side effects from random genomic integration. Additionally, it is possible to eliminate extrachromosomal DNAs from the cell simply by removing the selection pressure from the culture.

3.1. The Presence and the Design of Homology Arms Affect Genome Integration

HR has been used for genome editing in prokaryotes and eukaryotes for decades, and it has, e.g., been exploited to express exogenous genes or disrupt existing genes in at least 20 thraustochytrid strains (Table S3). The most common design is to flank the cassettes with two homology arms, that is DNA with sequence homologous to a specific genome location, which can then integrate the cassette into genomes by HR. The efficiency of HR in cells could be enhanced when the length of the homology arms was increased [103,104]. A plasmid design for more straightforward construction work is to place only one homology arm next to the expression cassettes. The plasmid is then linearized by restriction enzymes cutting a site in the middle of the homology arm before transformation, and thus designed to integrate into the genome through a single crossover. This approach has been used in *T. aureum* ATCC 34304 and *A. limacinum* SR21 [20,27]. However, the HR efficiency of the one-homology-arm design is two times lower than the two-homology-arm design in *T. aureum* ATCC 34304 [27].

Endogenous promoter and terminator regions can be used directly as homology arms flanking the exogenous gene [39,55], the shorter cassettes could potentially increase DNA delivery efficiency. However, this would result in the replacement of the endogenous gene.

3.2. The Structure and Quantity of DNA Affect Transformation Frequencies

The efficiency of HR also depends on whether DNA is linear or circular. Both linear and circular DNA molecules have been used to transform thraustochytrids (Tables S1 and S2). In *Schizochytrium* sp. CB15-5, there were no significant differences in the electrotransformation efficiency between introducing circular and linear DNA [51]. However, for the biolistic transformation of *T. aureum* ATCC 34304, only the linear, and not the circular, DNA molecule successfully generated transformants [27]. As DNA molecules are attached to beads, and then penetrate the cell by a pressurized gun in biolistic transformation, DNA structures are not expected to affect the ability of DNA to enter the cells. Moreover, Zhang et al., 2018 [46] performed electrotransformations in *Schizochytrium* sp. PKU#Mn4 with linearized DNA for genome integration by HR, but used a circular DNA vector for random genome insertion. This indicates that linear DNA could be more advantageous in performing HR in thraustochytrid cells. However, the paper does not quantitatively compare the two approaches.

In addition, adding more DNA could generate more transformants [60,87], which can be expected due to the increased possibility of DNA to contact with chromosomal DNA, resulting in higher genome integration rate. The amount of DNA added per electroporation ranges widely from 1 to 20 μg in thraustochytrids protocols. In *A. limacinum* SR21, adding one μg of DNA resulted in the highest electroporation efficiency, but the number of transformants increased from 44 to 68 when the DNA rose from 1 to 10 μg [20]. As DNA is not a costly material, and the goal of most studies is to obtain a high number of transformants, starting with a high amount of linear DNA seems the best strategy when a new strain is to be transformed.

3.3. Strategies That Facilite Homologous Recombination

Inducing DSBs at specific sequences by sequence-specific nucleases can increase the efficiency of HR. Clustered, regularly interspaced short palindromic repeats (CRISPR)-associated protein (Cas) is a genome-editing technique widely used across species, with principles and features reviewed extensively by others [102]. With the assistance of site-

specific guide RNA, DNA DSBs can be introduced by Cas9 or similar endonucleases. The DSBs can be repaired explicitly by homology-directed repair (HDR), resulting in predetermined deletions, insertions, or nucleotide changes determined by the added DNA where flanking arms are homologous to each side of the cut(s). Cas9 or Cas12 nuclease-induced DNA DSBs were shown to increase the efficiency of HR in the microalgae *C. reinhardtii* and diatom *Thalassiosira pseudonana* [105–107]. Recently, zeocin resistance cassettes were shown to be more efficiently integrated into the genome of *Aurantiochytrium* sp. RH-7A and *A. limacinum* SR21 with assistance from the CRISPR-Cas9 system using HDR [36]

Another approach to enhance HR might be to interfere with NHEJ-specific enzymes. For instance, does DNA ligase type IV ligate the nonhomologous DNA ends at the last step of NHEJ, and knockdown of this enzyme increased the rate of homologous recombination in *P. tricornutum* [103]. It is possible that HR efficiency in thraustochytrids can be increased by attenuating the expression of DNA ligase IV. However, thraustochytrid proteins are usually evolutionarily distant from those of model species, and a BLAST search in GenBank shows that most putative DNA ligase IV homologs encoded in the thraustochytrid genomes have less than 30% identity to those of *S. cerevisiae*, *Arabidopsis thaliana*, or *P. tricornutum* (unpublished). Hence, the function of putative proteins in the HR and NHEJ pathways in thraustochytrids needs to be experimentally verified, but the experimental data show them to be functional for genome engineering.

3.4. Application of Extrachromosomal DNAs

Extrachromosomal DNAs contain elements that function as centromere and origin of replication (or autonomously replicating sequences, ARS), and yeast-derived centromere and ARS and have been used to construct a replicating plasmid for *A. limacinum* OUC88, which was used to deliver the Cre-recombinase [30]. It is also possible to isolate elements that function as centromere or ARS from host genomes to support the autonomous replication of extrachromosomal DNAs [108].

In the recently established CRISPR-Cas9 method in thraustochytrids, the Cas9-gRNA Ribonucleoprotein (RNP) complex was directly electroporated into the cell to execute its function [36]. As Cas9-gRNA RNP is assembled in vitro by relatively costly gRNA and Cas9 proteins, an alternative strategy is to express both gRNA and the endonuclease after their genes are integrated into the genome, as already established in the diatoms *T. pseudonana* and *P. tricornutum* [109,110]. However, constitutive expression of Cas9 can cause re-editing (correction) of mutants, have a higher probability of off-target editing, and may be toxic to cells, which has been shown in microalgae such as *C. reinhardtii* [111]. To avoid this, Cas9 and gRNA can be expressed on an autonomously replicating episome so that the expression of Cas9 can be eliminated by removing the episome from the cell. This approach has been demonstrated in the diatom *P. tricornutum* [90], and is a promising approach to optimize the application of CRISPR-Cas9 genome editing in thraustochytrids.

4. The Properties of the DNA Related to Gene Expression in Thraustochytrids

The gene expression level from an expression cassette will be affected by the choice of promoter and terminators, originated either endogenously, from other closely related species, or from other species. Constitutive promoters are commonly used to express heterologous genes with different strengths, while inducible promoters are advantageous at controlling the expression of toxic genes. Once transformation has been achieved, several strategies have been used to discover or design promoters that could be used to enhance transformation efficiency or control gene expression. Antibiotics selection is widely used to identify transformants expressing the corresponding antibiotic resistance gene. When the goal is gene-inactivation, one only needs to express a selectable marker gene if the organism is haploid, while diploid organisms would necessitate two marker genes for complete inactivation. Expanding the number of antibiotics applicable for transformant selection can boost the genetic engineering capability, as multiple genes of an organism

can be disrupted by different antibiotic-resistance cassettes through HR. On the other hand, in most cases one would want to express one or more additional genes. Then, each gene would need their own promoter and terminator, resulting in long DNA cassettes for transformation. Approaches such as utilizing self-cleaving peptides (Section 4.3) or co-transforming separate single gene-containing DNA molecules can reduce DNA size when co-expressing antibiotic-resistance gene with gene of interests (GOIs), which potentially enhance DNA delivery.

4.1. Promoters and Terminators Used for Controlling Cassette Expression Level

In yeast, the elongation factor 1-alpha (EF1α) promoter is one of the strongest constitutive promoters used [112,113], and the cytochrome c1 (CYC1) terminator is among the three most used terminators [114]. In thraustochytrids, the EF1α promoter and terminator are one of the most frequently used endogenous promoters and terminators, while *S. cerevisiae*'s EF1α (TEF1) promoter and CYC1 terminator are the most frequently used non-endogenous promoter and terminator (Figure 3 and Table S4). In *Schizochytrium* sp. CB15-5, transformants were more efficiently generated by expressing the zeocin resistance cassette with the endogenous EF1α promoter-terminator than with the endogenous actin promoter-terminator, followed by the endogenous glyceraldehyde 3-phosphate dehydrogenase (GAP) promoter-terminator. The number of transformants with the endogenous EF1α promoter-terminator was up to 15 times higher than that with the endogenous GAP promoter-terminator [51]. Recently, a promoter activity assay was established in *Schizochytrium* sp. S31 and the tested promoters, here listed by descending promoter strength, were glucose-repressible gene (ccg1) of *Neurospora*, TEF1, endogenous EF1α, and endogenous ubiquitin [48]. Hence, the EF1α and the ccg1 promoters are presumably more secure options for establishing protocols on new strains. There are also no indications that endogenous promoters are preferable in thraustochytrids. However, these comparisons of promoter strength were all performed in the *Schizochytrium* genus. Whether the trends are similar in *Aurantiochytrium* and other genera is unknown.

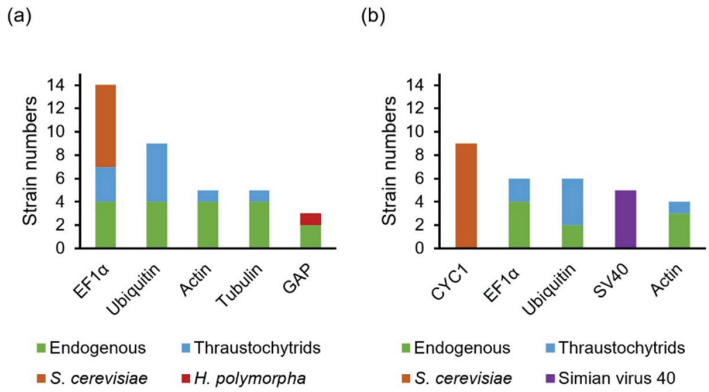

Figure 3. The prevalence of constitutive promoters (**a**) and terminators (**b**) used in thraustochytrids genetic engineering. Strain numbers: the number of strains that have used the promoter/terminator in at least one publication (Tables S3 and S4).

Strong promoters have been determined based on a transcriptomic analysis in the diatom *P. tricornutum* [115]. One approach has also been to transform promoter-less marker genes to subsequently identify the marker genes' upstream sequence with strong expression in the transformants of the microalgae *C. reinhardtii* [116]. However, this approach only applies to those strains with established transformation protocols. There are also limited choices of marker genes that are able to generate easy-to-screen phenotypes when they are expressed. Finally, it is possible to generate synthetic promoters by error-prone PCR or

rational design, which has been reviewed in detail [94,95]. Similarly, stronger terminators can also be identified by screening fluorescent reporter proteins with a combination of thousands of terminators [117].

Compared to constitutive promoters, significantly fewer thraustochytrids were engineered with inducible promoters, including the galactose-inducible galactokinase (GAL1) promoter of *S. cerevisiae* [30], the ethanol-inducible alcohol dehydrogenase I (AlcA) promoter of *Aspergillus nidulans* [57,58], and the methanol-inducible alcohol oxidase I (AOX1) promoter of *Pichia pastoris* [48] (Table S3). Although the strength of the induced AOX1 promoter was discovered to be weaker than TEF1, the AOX1 promoter had no detectable promoter activity in the absence of methanol [48], indicating its great potential for controlling the expression of a toxic gene in thraustochytrids.

4.2. Antibiotics Resistance Genes for Transformant Selection in Thraustochytrids

G418, zeocin, and hygromycin are the most frequently used antibiotics in thraustochytrids. However, the concentrations needed vary largely between different strains (Table 1). For example, the zeocin concentration applied for selecting transformants in *Thraustochytrium* sp. ONC-T18 is more than 100 times higher than that used for *Schizochytrium* sp. HX-308 [55]. The antibiotic concentration used in different protocols for the same strain also varies (Table 1). One possibility is that one tends to choose a concentration somewhat higher than the minimum inhibitory concentration (MIC). Additionally, as the transformation process may result in different cell fragility levels, cells can have different levels of antibiotic tolerance. Furthermore, the density of cells growing on the selective agar media can alter the resistance. For the yeast *P. pastoris*, it has been shown that dead cells can absorb zeocin and reduce the perceived concentration, allowing untransformed cells to grow as false-positive colonies [118]. A similar phenomenon also existed when we attempted to select *Aurantiochytrium* sp. T66 transformants by zeocin (unpublished), potentially aggravated by the cells' clustering-prone phenotype. Overall, although G418, zeocin, and hygromycin can be prioritized for new protocol establishments, it is difficult to estimate the concentration for a new strain based on previous research on other strains. The MIC must always be determined using cell concentrations similar to those that will be utilized when plating out transformed cells. When establishing a protocol, it may be worthwhile to plate transformants on a couple of different antibiotics concentrations to avoid both false negatives and the risk of exceeding the resistance level for transformed cells.

Table 1. Antibiotics used for selecting transformants of thraustochytrids.

Strain	Zeocin	Hygromycin	G418	Blasticidin	Other	Reference
A. limacinum F26-b		2000	500			[21–23]
A. limacinum mh0186	500 *	1000; 2000 *	500	1200	500 (neomycin)	[24–28]
A. limacinum OUC168	5				100 (chloramphenicol)	[29]
A. limacinum OUC88	5				100 (chloramphenicol)	[30]
A. limacinum SR21	30; 50; 100	200	500			[20,31–36,52]
Aurantiochytrium sp. KRS101					30 (cycloheximide)	[37]
Aurantiochytrium sp. MP4	50					[38]
Aurantiochytrium sp. PKU#SW7		500	500			[39]
Aurantiochytrium sp. RH-7A	100					[36]
Aurantiochytrium sp. SD116	30; 50; 100	500 *	50 *; 50		100 *(anhydrotetracycline)	[40–42]
Aurantiochytrium sp. SK4	50					[38,43]
Aurantiochytrium sp. YLH70	15					[56]
Parietichytrium sp. TA04Bb		2000	500	800		[27]
Schizochytrium sp. S31	40; 50		100		50 (bleomycin); 250 (cefotaxime); 50 (paromomycin)	[5,47,48,53,57,58]

Table 1. *Cont.*

Strain	Zeocin	Hygromycin	G418	Blasticidin	Other	Reference
Schizochytrium sp. HX-308	1.5; 20					[44,45]
Schizochytrium sp. PKU#Mn4			800			[46]
Schizochytrium sp. TIO01	100					[49]
Schizochytrium sp. TIO1101			300			[50,59]
Schizochytrium sp. SEK 579		2000	500			[27]
Schizochytrium sp. CB15-5	20					[51]
Thraustochytrid strain 12B			500			[32]
T. aureum ATCC 34304		2000	1000; 2000	200–400		[27,54]
Thraustochytrium sp. ONC-T18	250	400				[55]

Each number represents the minimal concentration (μg/mL) used on agar for transformant selection in the reference; * MIC identified in the reference that was not used in transformant selection. The references of each used concentration are shown in Table S5.

Expanding the number of antibiotics applicable for transformant selection is especially critical for gene inactivation in diploid thraustochytrid strains such as *T. aureum* ATCC 34304, as each allele must be disrupted separately to inactivate the gene function completely [27,54]. Potentially applicable antibiotics for thraustochytrids can be selected from those applied on other stramenopiles, including phleomycin, nourseothricin, puromycin, and formaldehyde [20]. As both zeocin and phleomycin belong to the bleomycin family with the same corresponding resistance gene, phleomycin can be tested on those strains that fail to be selected by zeocin without changing the resistance cassette. However, as antibiotic resistance of thraustochytrids is among the highest compared to other marine protists, expanding the number of applicable antibiotics is expected to be challenging [20].

Finally, removal of the resistance gene from the genome by Cre/*lox*P system was demonstrated in *A. limacinum* OUC88 [30]. This method can reduce the number of different antibiotics needed to generate a series of genome integrations and, therefore, it would be worthwhile to explore its application on more thraustochytrid strains.

4.3. Expression of Multiple Genes

Cassettes containing a GOI and antibiotic resistance gene have been expressed in at least 18 thraustochytrid strains (Table S3). In most of these cassettes, each gene was flanked with an individual pair of promoter and terminator. These were different for each gene on the cassette, potentially intended to avoid intramolecular HR that can truncate the plasmids [119]. One exception is that two copies of the same phosphoglycerate kinase (PGK) promoter were used on the same cassette without negative consequences mentioned in *A. limacinum* OUC168 [29].

As multiple promoters and terminators on the same cassette significantly increase the cassette size, it potentially reduces DNA delivery efficiency and limits the number of genes expressed on a single cassette. An alternative approach is to connect multiple genes with 2A linker sequences as a single multicistronic transcription unit, driven by a single pair of promoter and terminator. 2A linker sequences are 18–22 amino acids viral origin peptides that introduce cleavage of polypeptides during translation in eukaryotic cells [120]. Picornavirus 2A (P2A) peptides have been used in *Aurantiochytrium* sp. SK4 [43], *Thraustochytrium* sp. ONC-T18 [55], and *A. limacinum* SR21 [52], while foot-and-mouth disease virus 2A (F2A) peptides have been used in *Aurantiochytrium* sp. SD116 [41]. In *Aurantiochytrium* sp. SK4, three genes were linked via P2A sequences [43], demonstrating the possibility for co-expressing several genes of interest. The efficiency of 2A cleavage may depend on the 2A peptide or the strain that is used. In *Aurantiochytrium* sp. SD116, the proteins that contain F2A peptides were nearly 100% cleaved [41]. However, in *Thraustochytrium* sp. ONC-T18, the proteins that comprise P2A peptides were only partially cleaved [55].

Another approach that could reduce the cassette sizes for transformation would be to put the antibiotics resistance gene and the genes of interest on separate DNA molecules

and transform them simultaneously. Although it is apparent that not all antibiotic-resistant transformants can be expected to express the gene from the other DNA molecule, this approach has been applied in the diatom *P. tricornutum* combined with biolistic transformation and around 60–70% of the transformants expressed genes originated from both plasmid [121]. Studies using this approach on thraustochytrids have not yet been published.

5. Conclusions

Most eukaryotic microorganisms have not been identified to date, and among those known to have biotechnologically interesting properties, only a small fraction have been transformed. This review compiles the current knowledge that is either used or have the potential to be used in one group of marine microorganisms that, evolutionarily, is quite different from other organisms as recently shown [122]. However, the approaches and elements used are similar to those used in other species, such as yeast, green microalgae, and diatoms, and hence will be relevant to consider for eukaryotic microorganisms in general.

Thraustochytrids are becoming increasingly interesting for sustainable biomanufacturing. Thus far, only some thraustochytrids have been successfully engineered by protocols tailored to the species and strains of interest. Still, developing genetic tools in new thraustochytrid strains presents significant challenges. Although methods such as biolistic transformation and AMT have been used, electroporation is the most widely used method for delivering DNA into thraustochytrids cells, with experimental setup of electric pulses, cell wall treatment, and the solutions as most common factors to be considered. Moreover, the properties of expression cassettes, including promoters, terminators, homology arms, antibiotics resistance genes, self-replicating sequences, linkers, and vector structure and quantity, play important roles in heterologous expression experiments. Further systematic studies to narrow down the critical parameters involved in thraustochytrid genetic engineering methods are needed to effectively overcome fundamental barriers of protocol establishment. Emerging tools such as CRISPR-Cas, conjugation, microfluidics, and CPPs may open up new solutions to simplify the engineering process establishment in thraustochytrids, as well as other microorganisms.

Supplementary Materials: The following are available online at https://www.mdpi.com/article/10.3390/md19090515/s1, Table S1: Electroporation conditions used in thraustochytrid transformation, Table S2: Non-electroporation transformation methods used in thraustochytrids, Table S3: Promoters and terminators used for thraustochytrids genetic engineering as well as the insertion type and the expressions of GOIs in thraustochytrids genetic engineering, Table S4: The prevalence of constitutive promoters and terminators used in thraustochytrids genetic engineering, and Table S5: Antibiotics used for selecting transformants of thraustochytrids with detailed information regarding to the reference of each concentration.

Author Contributions: Conceptualization, E.-M.R. and H.E.; writing—original draft preparation, E.-M.R.; writing—review and editing, E.-M.R. and H.E. Both authors have read and agreed to the published version of the manuscript.

Funding: This research was funded by Research Council of Norway, grant number 269432. The APC was funded by NTNU.

Institutional Review Board Statement: Not applicable.

Data Availability Statement: Not applicable.

Conflicts of Interest: The authors declare no conflict of interest.

References

1. Morabito, C.; Bournaud, C.; Maës, C.; Schuler, M.; Aiese Cigliano, R.; Dellero, Y.; Maréchal, E.; Amato, A.; Rébeillé, F. The lipid metabolism in thraustochytrids. *Prog. Lipid Res.* **2019**, *76*, 101007. [CrossRef]
2. Yoon, H.S.; Andersen, R.A.; Boo, S.M.; Bhattacharya, D. Stramenopiles. In *Encyclopedia of Microbiology*, 3rd ed.; Schaechter, M., Ed.; Academic Press: Oxford, UK, 2009; pp. 721–731. [CrossRef]

3. Marchan, L.F.; Chang, K.J.L.; Nichols, P.D.; Mitchell, W.J.; Polglase, J.L.; Gutierrez, T. Taxonomy, ecology and biotechnological applications of thraustochytrids: A review. *Biotechnol. Adv.* **2018**, *36*, 26–46. [CrossRef] [PubMed]
4. Hauvermale, A.; Kuner, J.; Rosenzweig, B.; Guerra, D.; Diltz, S.; Metz, J.G. Fatty acid production in *Schizochytrium* sp.: Involvement of a polyunsaturated fatty acid synthase and a type I fatty acid synthase. *Lipids* **2006**, *41*, 739–747. [CrossRef] [PubMed]
5. Lippmeier, J.C.; Crawford, K.S.; Owen, C.B.; Rivas, A.A.; Metz, J.G.; Apt, K.E. Characterization of both polyunsaturated fatty acid biosynthetic pathways in *Schizochytrium* sp. *Lipids* **2009**, *44*, 621–630. [CrossRef]
6. Du, F.; Wang, Y.-Z.; Xu, Y.-S.; Shi, T.-Q.; Liu, W.-Z.; Sun, X.-M.; Huang, H. Biotechnological production of lipid and terpenoid from thraustochytrids. *Biotechnol. Adv.* **2021**, *48*, 107725. [CrossRef]
7. Bentsen, H. Dietary polyunsaturated fatty acids, brain function and mental health. *Microb. Ecol. Health Dis.* **2017**, *28*, 1281916. [CrossRef]
8. Elagizi, A.; Lavie, C.J.; O'Keefe, E.; Marshall, K.; O'Keefe, J.H.; Milani, R.V. An update on omega-3 polyunsaturated fatty acids and cardiovascular health. *Nutrients* **2021**, *13*, 204. [CrossRef]
9. Yamagata, K. Dietary docosahexaenoic acid inhibits neurodegeneration and prevents stroke. *J. Neurosci. Res.* **2021**, *99*, 561–572. [CrossRef]
10. Aasen, I.M.; Ertesvåg, H.; Heggeset, T.M.; Liu, B.; Brautaset, T.; Vadstein, O.; Ellingsen, T.E. Thraustochytrids as production organisms for docosahexaenoic acid (DHA), squalene, and carotenoids. *Appl. Microbiol. Biotechnol.* **2016**, *100*, 4309–4321. [CrossRef] [PubMed]
11. Jovanovic, S.; Dietrich, D.; Becker, J.; Kohlstedt, M.; Wittmann, C. Microbial production of polyunsaturated fatty acids—High-value ingredients for aquafeed, superfoods, and pharmaceuticals. *Curr. Opin. Biotechnol.* **2021**, *69*, 199–211. [CrossRef]
12. Tocher, D.R.; Betancor, M.B.; Sprague, M.; Olsen, R.E.; Napier, J.A. Omega-3 long-chain polyunsaturated fatty acids, EPA and DHA: Bridging the gap between supply and demand. *Nutrients* **2019**, *11*, 89. [CrossRef] [PubMed]
13. Xu, X.; Huang, C.; Xu, Z.; Xu, H.; Wang, Z.; Yu, X. The strategies to reduce cost and improve productivity in DHA production by *Aurantiochytrium* sp.: From biochemical to genetic respects. *Appl. Microbiol. Biotechnol.* **2020**, *104*, 9433–9447. [CrossRef] [PubMed]
14. Patel, A.; Rova, U.; Christakopoulos, P.; Matsakas, L. Mining of squalene as a value-added byproduct from DHA producing marine thraustochytrid cultivated on food waste hydrolysate. *Sci. Total Environ.* **2020**, *736*, 139691. [CrossRef] [PubMed]
15. Park, H.; Kwak, M.; Seo, J.; Ju, J.; Heo, S.; Park, S.; Hong, W. Enhanced production of carotenoids using a Thraustochytrid microalgal strain containing high levels of docosahexaenoic acid-rich oil. *Bioprocess Biosyst. Eng.* **2018**, *41*, 1355–1370. [CrossRef]
16. Taoka, Y.; Nagano, N.; Okita, Y.; Izumida, H.; Sugimoto, S.; Hayashi, M. Extracellular enzymes produced by marine eukaryotes, thraustochytrids. *Biosci. Biotechnol. Biochem.* **2009**, *73*, 180–182. [CrossRef]
17. Nham Tran, T.L.; Miranda, A.F.; Gupta, A.; Puri, M.; Ball, A.S.; Adhikari, B.; Mouradov, A. The nutritional and pharmacological potential of new Australian thraustochytrids isolated from mangrove sediments. *Mar. Drugs* **2020**, *18*, 151. [CrossRef]
18. Nivetha, K.; Rao, A.S.; Nair, A. Microbial production of omega-3 fatty acids: An overview. *J. Appl. Microbiol.* **2021**. [CrossRef]
19. Riley, L.A.; Guss, A.M. Approaches to genetic tool development for rapid domestication of non-model microorganisms. *Biotechnol. Biofuels* **2021**, *14*, 30. [CrossRef]
20. Faktorová, D.; Nisbet, R.E.R.; Fernández Robledo, J.A.; Casacuberta, E.; Sudek, L.; Allen, A.E.; Ares, M., Jr.; Aresté, C.; Balestreri, C.; Barbrook, A.C.; et al. Genetic tool development in marine protists: Emerging model organisms for experimental cell biology. *Nat. Methods* **2020**, *17*, 481–494. [CrossRef] [PubMed]
21. Watanabe, T.; Sakiyama, R.; Iimi, Y.; Sekine, S.; Abe, E.; Nomura, K.H.; Nomura, K.; Ishibashi, Y.; Okino, N.; Hayashi, M.; et al. Regulation of TG accumulation and lipid droplet morphology by the novel TLDP1 in *Aurantiochytrium limacinum* F26-b. *J. Lipid Res.* **2017**, *58*, 2334–2347. [CrossRef] [PubMed]
22. Nutahara, E.; Abe, E.; Uno, S.; Ishibashi, Y.; Watanabe, T.; Hayashi, M.; Okino, N.; Ito, M. The glycerol-3-phosphate acyltransferase PLAT2 functions in the generation of DHA-rich glycerolipids in *Aurantiochytrium limacinum* F26-b. *PLoS ONE* **2019**, *14*, e0211164. [CrossRef]
23. Abe, E.; Ikeda, K.; Nutahara, E.; Hayashi, M.; Yamashita, A.; Taguchi, R.; Doi, K.; Honda, D.; Okino, N.; Ito, M. Novel lysophospholipid acyltransferase PLAT1 of *Aurantiochytrium limacinum* F26-b responsible for generation of palmitate-docosahexaenoate-phosphatidylcholine and phosphatidylethanolamine. *PLoS ONE* **2014**, *9*, e102377. [CrossRef]
24. Kobayashi, T.; Sakaguchi, K.; Matsuda, T.; Abe, E.; Hama, Y.; Hayashi, M.; Honda, D.; Okita, Y.; Sugimoto, S.; Okino, N.; et al. Increase of eicosapentaenoic acid in thraustochytrids through thraustochytrid ubiquitin promoter-driven expression of a fatty acid Δ5 desaturase gene. *Appl. Environ. Microbiol.* **2011**, *77*, 3870–3876. [CrossRef]
25. Ishibashi, Y.; Aoki, K.; Okino, N.; Hayashi, M.; Ito, M. A thraustochytrid-specific lipase/phospholipase with unique positional specificity contributes to microbial competition and fatty acid acquisition from the environment. *Sci. Rep.* **2019**, *9*, 16357. [CrossRef]
26. Ohara, J.; Sakaguchi, K.; Okita, Y.; Okino, N.; Ito, M. Two fatty acid elongases possessing C18-Δ6/C18-Δ9/C20-Δ5 or C16-Δ9 elongase activity in *Thraustochytrium* sp. ATCC 26185. *Mar. Biotechnol.* **2013**, *15*, 476–486. [CrossRef]
27. Sakaguchi, K.; Matsuda, T.; Kobayashi, T.; Ohara, J.; Hamaguchi, R.; Abe, E.; Nagano, N.; Hayashi, M.; Ueda, M.; Honda, D.; et al. Versatile transformation system that is applicable to both multiple transgene expression and gene targeting for thraustochytrids. *Appl. Environ. Microbiol.* **2012**, *78*, 3193–3202. [CrossRef]

28. Matsuda, T.; Sakaguchi, K.; Kobayashi, T.; Abe, E.; Kurano, N.; Sato, A.; Okita, Y.; Sugimoto, S.; Hama, Y.; Hayashi, M.; et al. Molecular cloning of a *Pinguiochrysis pyriformis* oleate-specific microsomal Δ12-fatty acid desaturase and functional analysis in yeasts and thraustochytrids. *J. Biochem.* **2011**, *150*, 375–383. [CrossRef]
29. Liu, Z.; Zang, X.; Cao, X.; Wang, Z.; Liu, C.; Sun, D.; Guo, Y.; Zhang, F.; Yang, Q.; Hou, P.; et al. Cloning of the *pks3* gene of *Aurantiochytrium limacinum* and functional study of the 3-ketoacyl-ACP reductase and dehydratase enzyme domains. *PLoS ONE* **2018**, *13*, e0208853. [CrossRef] [PubMed]
30. Sun, H.; Chen, H.; Zang, X.; Hou, P.; Zhou, B.; Liu, Y.; Wu, F.; Cao, X.; Zhang, X. Application of the Cre/*lox*P site-specific recombination system for gene transformation in *Aurantiochytrium limacinum*. *Molecules* **2015**, *20*, 10110–10121. [CrossRef] [PubMed]
31. Okino, N.; Wakisaka, H.; Ishibashi, Y.; Ito, M. Visualization of endoplasmic reticulum and mitochondria in *Aurantiochytrium limacinum* by the expression of EGFP with cell organelle-specific targeting/retaining signals. *Mar. Biotechnol.* **2018**, *20*, 182–192. [CrossRef] [PubMed]
32. Adachi, T.; Sahara, T.; Okuyama, H.; Morita, N. Glass bead-based genetic transformation: An efficient method for transformation of thraustochytrid microorganisms. *J. Oleo. Sci.* **2017**, *66*, 791–795. [CrossRef]
33. Li, Z.; Meng, T.; Ling, X.; Li, J.; Zheng, C.; Shi, Y.; Chen, Z.; Li, Z.; Li, Q.; Lu, Y.; et al. Overexpression of malonyl-CoA: ACP transacylase in *Schizochytrium* sp. to improve polyunsaturated fatty acid production. *J. Agric. Food Chem.* **2018**, *66*, 5382–5391. [CrossRef]
34. Li, Z.; Chen, X.; Li, J.; Meng, T.; Wang, L.; Chen, Z.; Shi, Y.; Ling, X.; Luo, W.; Liang, D.; et al. Functions of PKS genes in lipid synthesis of *Schizochytrium* sp. by gene disruption and metabolomics analysis. *Mar. Biotechnol.* **2018**, *20*, 792–802. [CrossRef]
35. Ling, X.; Zhou, H.; Yang, Q.; Yu, S.; Li, J.; Li, Z.; He, N.; Chen, C.; Lu, Y. Functions of enyolreductase (ER) domains of PKS cluster in lipid synthesis and enhancement of PUFAs accumulation in *Schizochytrium limacinum* SR21 using triclosan as a regulator of ER. *Microorganisms* **2020**, *8*, 300. [CrossRef] [PubMed]
36. Watanabe, K.; Perez, C.M.T.; Kitahori, T.; Hata, K.; Aoi, M.; Takahashi, H.; Sakuma, T.; Okamura, Y.; Nakashimada, Y.; Yamamoto, T.; et al. Improvement of fatty acid productivity of thraustochytrid, *Aurantiochytrium* sp. by genome editing. *J. Biosci. Bioeng.* **2020**, *131*, 373–380. [CrossRef] [PubMed]
37. Hong, W.-K.; Heo, S.-Y.; Oh, B.-R.; Kim, C.H.; Sohn, J.-H.; Yang, J.-W.; Kondo, A.; Seo, J.-W. A transgene expression system for the marine microalgae *Aurantiochytrium* sp. KRS101 using a mutant allele of the gene encoding ribosomal protein L44 as a selectable transformation marker for cycloheximide resistance. *Bioprocess Biosyst. Eng.* **2013**, *36*, 1191–1197. [CrossRef]
38. Suen, Y.L.; Tang, H.; Huang, J.; Chen, F. Enhanced production of fatty acids and astaxanthin in *Aurantiochytrium* sp. by the expression of *Vitreoscilla* hemoglobin. *J. Agric. Food Chem.* **2014**, *62*, 12392–12398. [CrossRef]
39. Liang, Y.; Liu, Y.; Tang, J.; Ma, J.; Cheng, J.J.; Daroch, M. Transcriptomic profiling and gene disruption revealed that two genes related to PUFAs/DHA biosynthesis may be essential for cell growth of *Aurantiochytrium* sp. *Mar. Drugs* **2018**, *16*, 310. [CrossRef] [PubMed]
40. Cui, G.-Z.; Ma, Z.; Liu, Y.-J.; Feng, Y.; Sun, Z.; Cheng, Y.; Song, X.; Cui, Q. Overexpression of glucose-6-phosphate dehydrogenase enhanced the polyunsaturated fatty acid composition of *Aurantiochytrium* sp. SD116. *Algal Res.* **2016**, *19*, 138–145. [CrossRef]
41. Wang, S.; Lan, C.; Wang, Z.; Wan, W.; Zhang, H.; Cui, Q.; Song, X. Optimizing eicosapentaenoic acid production by grafting a heterologous polyketide synthase pathway in the thraustochytrid *Aurantiochytrium*. *J. Agric. Food Chem.* **2020**, *68*, 11253–11260. [CrossRef] [PubMed]
42. Wang, S.; Lan, C.; Wang, Z.; Wan, W.; Cui, Q.; Song, X. PUFA-synthase-specific PPTase enhanced the polyunsaturated fatty acid biosynthesis via the polyketide synthase pathway in *Aurantiochytrium*. *Biotechnol. Biofuels* **2020**, *13*, 152. [CrossRef] [PubMed]
43. Ye, J.; Liu, M.; He, M.; Ye, Y.; Huang, J. Illustrating and enhancing the biosynthesis of astaxanthin and docosahexaenoic acid in *Aurantiochytrium* sp. SK4. *Mar. Drugs* **2019**, *17*, 45. [CrossRef] [PubMed]
44. Ren, L.-j.; Chen, S.-l.; Geng, L.-j.; Ji, X.-j.; Xu, X.; Song, P.; Gao, S.; Huang, H. Exploring the function of acyltransferase and domain replacement in order to change the polyunsaturated fatty acid profile of *Schizochytrium* sp. *Algal Res.* **2018**, *29*, 193–201. [CrossRef]
45. Ren, L.J.; Zhuang, X.Y.; Chen, S.L.; Ji, X.J.; Huang, H. Introduction of omega-3 desaturase obviously changed the fatty acid profile and sterol content of *Schizochytrium* sp. *J. Agric. Food Chem.* **2015**, *63*, 9770–9776. [CrossRef]
46. Zhang, S.; He, Y.; Sen, B.; Chen, X.; Xie, Y.; Keasling, J.D.; Wang, G. Alleviation of reactive oxygen species enhances PUFA accumulation in *Schizochytrium* sp. through regulating genes involved in lipid metabolism. *Metab. Eng. Commun.* **2018**, *6*, 39–48. [CrossRef]
47. Wang, F.; Bi, Y.; Diao, J.; Lv, M.; Cui, J.; Chen, L.; Zhang, W. Metabolic engineering to enhance biosynthesis of both docosahexaenoic acid and odd-chain fatty acids in *Schizochytrium* sp. S31. *Biotechnol. Biofuels* **2019**, *12*, 141. [CrossRef] [PubMed]
48. Han, X.; Zhao, Z.; Wen, Y.; Chen, Z. Enhancement of docosahexaenoic acid production by overexpression of ATP-citrate lyase and acetyl-CoA carboxylase in *Schizochytrium* sp. *Biotechnol. Biofuels* **2020**, *13*, 131. [CrossRef] [PubMed]
49. Cheng, R.-B.; Lin, X.-Z.; Wang, Z.-K.; Yang, S.-J.; Rong, H.; Ma, Y. Establishment of a transgene expression system for the marine microalga *Schizochytrium* by 18S rDNA-targeted homologous recombination. *World J. Microbiol. Biotechnol.* **2011**, *27*, 737–741. [CrossRef]
50. Yan, J.; Cheng, R.; Lin, X.; You, S.; Li, K.; Rong, H.; Ma, Y. Overexpression of acetyl-CoA synthetase increased the biomass and fatty acid proportion in microalga *Schizochytrium*. *Appl. Environ. Microbiol.* **2013**, *97*, 1933–1939. [CrossRef]
51. Ono, K.; Aki, T.; Kawamoto, S. Method for Introducing a Gene into Labyrinthulomycota. U.S. Patent 7888123B2, 15 February 2011.

52. Rau, E.M.; Aasen, I.M.; Ertesvåg, H. A non-canonical Δ9-desaturase synthesizing palmitoleic acid identified in the thraustochytrid *Aurantiochytrium* sp. T66. *Appl. Microbiol. Biotechnol.* **2021**, *105*, 5931–5941. [CrossRef]
53. Bayne, A.C.; Boltz, D.; Owen, C.; Betz, Y.; Maia, G.; Azadi, P.; Archer-Hartmann, S.; Zirkle, R.; Lippmeier, J.C. Vaccination against influenza with recombinant hemagglutinin expressed by *Schizochytrium* sp. confers protective immunity. *PLoS ONE* **2013**, *8*, e61790. [CrossRef]
54. Matsuda, T.; Sakaguchi, K.; Hamaguchi, R.; Kobayashi, T.; Abe, E.; Hama, Y.; Hayashi, M.; Honda, D.; Okita, Y.; Sugimoto, S.; et al. Analysis of Δ12-fatty acid desaturase function revealed that two distinct pathways are active for the synthesis of PUFAs in *T. aureum* ATCC 34304. *J. Lipid Res.* **2012**, *53*, 1210–1222. [CrossRef]
55. Merkx-Jacques, A.; Rasmussen, H.; Muise, D.M.; Benjamin, J.J.R.; Kottwitz, H.; Tanner, K.; Milway, M.T.; Purdue, L.M.; Scaife, M.A.; Armenta, R.E.; et al. Engineering xylose metabolism in thraustochytrid T18. *Biotechnol. Biofuels* **2018**, *11*, 248. [CrossRef] [PubMed]
56. Yu, X.J.; Wang, Z.P.; Liang, M.J.; Wang, Z.; Liu, X.Y.; Hu, L.; Xia, J. One-step utilization of inulin for docosahexaenoic acid (DHA) production by recombinant *Aurantiochytrium* sp. carrying *Kluyveromyces marxianus* inulinase. *Bioprocess Biosyst. Eng.* **2020**, *43*, 1801–1811. [CrossRef]
57. Hernández-Ramírez, J.; Wong-Arce, A.; González-Ortega, O.; Rosales-Mendoza, S. Expression in algae of a chimeric protein carrying several epitopes from tumor associated antigens. *Int. J. Biol. Macromol.* **2020**, *147*, 46–52. [CrossRef]
58. Bañuelos-Hernández, B.; Monreal-Escalante, E.; González-Ortega, O.; Angulo, C.; Rosales-Mendoza, S. Algevir: An expression system for microalgae based on viral vectors. *Front. Microbiol.* **2017**, *8*, 1100. [CrossRef]
59. Cheng, R.; Ma, R.; Li, K.; Rong, H.; Lin, X.; Wang, Z.; Yang, S.; Ma, Y. *Agrobacterium tumefaciens* mediated transformation of marine microalgae *Schizochytrium*. *Microbiol. Res.* **2012**, *167*, 179–186. [CrossRef]
60. Kotnik, T.; Frey, W.; Sack, M.; Haberl Meglič, S.; Peterka, M.; Miklavčič, D. Electroporation-based applications in biotechnology. *Trends Biotechnol.* **2015**, *33*, 480–488. [CrossRef]
61. Finer, J.J.; Finer, K.R.; Ponappa, T. Particle bombardment mediated transformation. In *Plant Biotechnology: New Products and Applications*; Hammond, J., McGarvey, P., Yusibov, V., Eds.; Springer: Berlin/Heidelberg, Germany, 2000; pp. 59–80. [CrossRef]
62. Huang, W.; Daboussi, F. Genetic and metabolic engineering in diatoms. *Phil. Trans. R. Soc. B* **2017**, *372*, 20160411. [CrossRef] [PubMed]
63. Kikkert, J.; Vidal, J.; Reisch, B. Stable transformation of plant cells by particle bombardment/biolistics. In *Transgenic Plants: Methods and Protocols. Methods in Molecular Biology™*; Peña, L., Ed.; Humana Press: Totowa, NJ, USA, 2005; Volume 286, pp. 61–78. [CrossRef]
64. Michielse, C.B.; Hooykaas, P.J.; van den Hondel, C.A.; Ram, A.F. *Agrobacterium*-mediated transformation as a tool for functional genomics in fungi. *Curr. Genet.* **2005**, *48*, 1–17. [CrossRef] [PubMed]
65. Ortiz-Matamoros, M.F.; Villanueva, M.A.; Islas-Flores, T. Genetic transformation of cell-walled plant and algae cells: Delivering DNA through the cell wall. *Brief. Funct. Genom.* **2017**, *17*, 26–33. [CrossRef] [PubMed]
66. Reberšek, M.; Miklavčič, D. Advantages and disadvantages of different concepts of electroporation pulse generation. *Automatika* **2011**, *52*, 12–19. [CrossRef]
67. Dower, W.J.; Miller, J.F.; Ragsdale, C.W. High efficiency transformation of *E. coli* by high voltage electroporation. *Nucleic Acids Res.* **1988**, *16*, 6127–6145. [CrossRef]
68. Kumar, P.; Nagarajan, A.; Uchil, P.D. Electroporation. *Cold Spring Harb. Protoc.* **2019**, 096271. [CrossRef]
69. Hattermann, D.R.; Stacey, G. Efficient DNA transformation of *Bradyrhizobium japonicum* by electroporation. *Appl. Environ. Microbiol.* **1990**, *56*, 833–836. [CrossRef]
70. Brown, L.E.; Sprecher, S.L.; Keller, L.R. Introduction of exogenous DNA into *Chlamydomonas reinhardtii* by electroporation. *Mol. Cell Biol.* **1991**, *11*, 2328–2332. [CrossRef]
71. Demiryurek, Y.; Nickaeen, M.; Zheng, M.; Yu, M.; Zahn, J.D.; Shreiber, D.I.; Lin, H.; Shan, J.W. Transport, resealing, and re-poration dynamics of two-pulse electroporation-mediated molecular delivery. *Biochim. Biophys. Acta Biomembr.* **2015**, *1848*, 1706–1714. [CrossRef]
72. Satkauskas, S.; Bureau, M.F.; Puc, M.; Mahfoudi, A.; Scherman, D.; Miklavcic, D.; Mir, L.M. Mechanisms of in vivo DNA electrotransfer: Respective contributions of cell electropermeabilization and DNA electrophoresis. *Mol. Ther.* **2002**, *5*, 133–140. [CrossRef]
73. Kandušer, M.; Miklavčič, D.; Pavlin, M. Mechanisms involved in gene electrotransfer using high- and low-voltage pulses—An in vitro study. *Bioelectrochemistry* **2009**, *74*, 265–271. [CrossRef]
74. Zheng, H.-Z.; Liu, H.-H.; Chen, S.-X.; Lu, Z.-X.; Zhang, Z.-L.; Pang, D.-W.; Xie, Z.-X.; Shen, P. Yeast transformation process studied by fluorescence labeling technique. *Bioconjug. Chem.* **2005**, *16*, 250–254. [CrossRef] [PubMed]
75. Jeon, K.; Suresh, A.; Kim, Y.-C. Highly efficient molecular delivery into *Chlamydomonas reinhardtii* by electroporation. *Korean J. Chem. Eng.* **2013**, *30*, 1626–1630. [CrossRef]
76. Muñoz, C.F.; de Jaeger, L.; Sturme, M.H.J.; Lip, K.Y.F.; Olijslager, J.W.J.; Springer, J.; Wolbert, E.J.H.; Martens, D.E.; Eggink, G.; Weusthuis, R.A.; et al. Improved DNA/protein delivery in microalgae—A simple and reliable method for the prediction of optimal electroporation settings. *Algal Res.* **2018**, *33*, 448–455. [CrossRef]
77. Azencott, H.R.; Peter, G.F.; Prausnitz, M.R. Influence of the cell wall on intracellular delivery to algal cells by electroporation and sonication. *Ultrasound Med. Biol.* **2007**, *33*, 1805–1817. [CrossRef] [PubMed]

78. Qu, B.; Eu, Y.-J.; Jeong, W.-J.; Kim, D.-P. Droplet electroporation in microfluidics for efficient cell transformation with or without cell wall removal. *Lab Chip* **2012**, *12*, 4483–4488. [CrossRef]
79. De Nobel, J.G.; Dijkers, C.; Hooijberg, E.; Klis, F.M. Increased cell wall porosity in *Saccharomyces cerevisiae* after treatment with dithiothreitol or EDTA. *J. Gen. Microbiol.* **1989**, *135*, 2077–2084. [CrossRef]
80. Ponton, J.; Jones, J.M. Analysis of cell wall extracts of *Candida albicans* by sodium dodecyl sulfate-polyacrylamide gel electrophoresis and Western blot techniques. *Infect. Immun.* **1986**, *53*, 565–572. [CrossRef] [PubMed]
81. Kawai, S.; Hashimoto, W.; Murata, K. Transformation of *Saccharomyces cerevisiae* and other fungi. *Bioeng. Bugs* **2010**, *1*, 395–403. [CrossRef]
82. Lu, Y.; Kong, R.; Hu, L. Preparation of protoplasts from *Chlorella protothecoides*. *World J. Microbiol. Biotechnol.* **2012**, *28*, 1827–1830. [CrossRef]
83. Braun, E.; Aach, H.G. Enzymatic degradation of the cell wall of *Chlorella*. *Planta* **1975**, *126*, 181–185. [CrossRef]
84. Costanzo, M.C.; Fox, T.D. Transformation of yeast by agitation with glass beads. *Genetics* **1988**, *120*, 667–670. [CrossRef]
85. Kindle, K.L. High-frequency nuclear transformation of *Chlamydomonas reinhardtii*. *Proc. Natl. Acad. Sci. USA* **1990**, *87*, 1228–1232. [CrossRef]
86. Prasanna, G.L.; Panda, T. Electroporation: Basic principles, practical considerations and applications in molecular biology. *Bioprocess Eng.* **1997**, *16*, 261–264. [CrossRef]
87. Benatuil, L.; Perez, J.M.; Belk, J.; Hsieh, C.-M. An improved yeast transformation method for the generation of very large human antibody libraries. *Protein Eng. Des. Sel.* **2010**, *23*, 155–159. [CrossRef]
88. Harris, J.R.; Lundgren, B.R.; Grzeskowiak, B.R.; Mizuno, K.; Nomura, C.T. A rapid and efficient electroporation method for transformation of *Halomonas* sp. O-1. *J. Microbiol. Methods* **2016**, *129*, 127–132. [CrossRef] [PubMed]
89. Muñoz, C.F.; Sturme, M.H.J.; D'Adamo, S.; Weusthuis, R.A.; Wijffels, R.H. Stable transformation of the green algae *Acutodesmus obliquus* and *Neochloris oleoabundans* based on *E. coli* conjugation. *Algal Res.* **2019**, *39*, 101453. [CrossRef]
90. Sharma, A.K.; Nymark, M.; Sparstad, T.; Bones, A.M.; Winge, P. Transgene-free genome editing in marine algae by bacterial conjugation—Comparison with biolistic CRISPR/Cas9 transformation. *Sci. Rep.* **2018**, *8*, 14401. [CrossRef] [PubMed]
91. Karas, B.J.; Diner, R.E.; Lefebvre, S.C.; McQuaid, J.; Phillips, A.P.R.; Noddings, C.M.; Brunson, J.K.; Valas, R.E.; Deerinck, T.J.; Jablanovic, J.; et al. Designer diatom episomes delivered by bacterial conjugation. *Nat. Commun.* **2015**, *6*, 6925. [CrossRef]
92. Wang, S.; Lee, L.J. Micro-/nanofluidics based cell electroporation. *Biomicrofluidics* **2013**, *7*, 011301. [CrossRef] [PubMed]
93. Shih, S.C.C.; Goyal, G.; Kim, P.W.; Koutsoubelis, N.; Keasling, J.D.; Adams, P.D.; Hillson, N.J.; Singh, A.K. A versatile microfluidic device for automating synthetic biology. *ACS Synth. Biol.* **2015**, *4*, 1151–1164. [CrossRef] [PubMed]
94. Fox, M.B.; Esveld, D.C.; Valero, A.; Luttge, R.; Mastwijk, H.C.; Bartels, P.V.; van den Berg, A.; Boom, R.M. Electroporation of cells in microfluidic devices: A review. *Anal. Bioanal. Chem.* **2006**, *385*, 474. [CrossRef]
95. Im, D.J.; Jeong, S.-N.; Yoo, B.S.; Kim, B.; Kim, D.-P.; Jeong, W.-J.; Kang, I.S. Digital microfluidic approach for efficient electroporation with high productivity: Transgene expression of microalgae without cell wall removal. *Anal. Chem.* **2015**, *87*, 6592–6599. [CrossRef]
96. Kim, G.C.; Cheon, D.H.; Lee, Y. Challenge to overcome current limitations of cell-penetrating peptides. *Biochim. Biophys. Acta Proteins Proteom.* **2021**, *1869*, 140604. [CrossRef] [PubMed]
97. Gadamchetty, P.; Mullapudi, P.L.V.; Sanagala, R.; Markandan, M.; Polumetla, A.K. Genetic transformation of *Chlorella vulgaris* mediated by HIV-TAT peptide. *3 Biotech* **2019**, *9*, 139. [CrossRef] [PubMed]
98. Kang, S.; Jeon, S.; Kim, S.; Chang, Y.K.; Kim, Y.-C. Development of a pVEC peptide-based ribonucleoprotein (RNP) delivery system for genome editing using CRISPR/Cas9 in *Chlamydomonas reinhardtii*. *Sci. Rep.* **2020**, *10*, 22158. [CrossRef]
99. Zorin, B.; Lu, Y.; Sizova, I.; Hegemann, P. Nuclear gene targeting in *Chlamydomonas* as exemplified by disruption of the *PHOT* gene. *Gene* **2009**, *432*, 91–96. [CrossRef] [PubMed]
100. Zhang, Y.-T.; Jiang, J.-Y.; Shi, T.-Q.; Sun, X.-M.; Zhao, Q.-Y.; Huang, H.; Ren, L.-J. Application of the CRISPR/Cas system for genome editing in microalgae. *Appl. Microbiol. Biotechnol.* **2019**, *103*, 3239–3248. [CrossRef] [PubMed]
101. Diner, R.E.; Bielinski, V.A.; Dupont, C.L.; Allen, A.E.; Weyman, P.D. Refinement of the diatom episome maintenance sequence and improvement of conjugation-based DNA delivery methods. *Front. Bioeng. Biotechnol.* **2016**, *4*, 65. [CrossRef]
102. Anzalone, A.V.; Koblan, L.W.; Liu, D.R. Genome editing with CRISPR–Cas nucleases, base editors, transposases and prime editors. *Nat. Biotechnol.* **2020**, *38*, 824–844. [CrossRef]
103. Angstenberger, M.; Krischer, J.; Aktaş, O.; Büchel, C. Knock-down of a *ligIV* homologue enables DNA integration via homologous recombination in the marine diatom *Phaeodactylum tricornutum*. *ACS Synth. Biol.* **2019**, *8*, 57–69. [CrossRef]
104. Plecenikova, A.; Mages, W.; Andrésson, Ó.S.; Hrossova, D.; Valuchova, S.; Vlcek, D.; Slaninova, M. Studies on recombination processes in two *Chlamydomonas reinhardtii* endogenous genes, *NIT1* and *ARG7*. *Protist* **2013**, *164*, 570–582. [CrossRef]
105. Jiang, W.Z.; Weeks, D.P. A gene-within-a-gene Cas9/sgRNA hybrid construct enables gene editing and gene replacement strategies in *Chlamydomonas reinhardtii*. *Algal Res.* **2017**, *26*, 474–480. [CrossRef]
106. Ferenczi, A.; Pyott, D.E.; Xipnitou, A.; Molnar, A. Efficient targeted DNA editing and replacement in *Chlamydomonas reinhardtii* using Cpf1 ribonucleoproteins and single-stranded DNA. *Proc. Natl. Acad. Sci. USA* **2017**, *114*, 13567–13572. [CrossRef]
107. Belshaw, N.; Grouneva, I.; Aram, L.; Gal, A.; Hopes, A.; Mock, T. Efficient CRISPR/Cas-mediated homologous recombination in the model diatom *Thalassiosira pseudonana*. *bioRxiv* **2017**, 215582. [CrossRef]
108. Cao, M.; Gao, M.; Lopez-Garcia, C.L.; Wu, Y.; Seetharam, A.S.; Severin, A.J.; Shao, Z. Centromeric DNA facilitates nonconventional yeast genetic engineering. *ACS Synth. Biol.* **2017**, *6*, 1545–1553. [CrossRef]

109. Nymark, M.; Sharma, A.K.; Sparstad, T.; Bones, A.M.; Winge, P. A CRISPR/Cas9 system adapted for gene editing in marine algae. *Sci. Rep.* **2016**, *6*, 24951. [CrossRef] [PubMed]
110. Hopes, A.; Nekrasov, V.; Kamoun, S.; Mock, T. Editing of the urease gene by CRISPR-Cas in the diatom *Thalassiosira pseudonana*. *Plant Methods* **2016**, *12*, 49. [CrossRef]
111. Jiang, W.; Brueggeman, A.J.; Horken, K.M.; Plucinak, T.M.; Weeks, D.P. Successful transient expression of Cas9 and single guide RNA genes in *Chlamydomonas reinhardtii*. *Eukaryot. Cell* **2014**, *13*, 1465–1469. [CrossRef] [PubMed]
112. Partow, S.; Siewers, V.; Bjørn, S.; Nielsen, J.; Maury, J. Characterization of different promoters for designing a new expression vector in *Saccharomyces cerevisiae*. *Yeast* **2010**, *27*, 955–964. [CrossRef] [PubMed]
113. Sun, J.; Shao, Z.; Zhao, H.; Nair, N.; Wen, F.; Xu, J.H.; Zhao, H. Cloning and characterization of a panel of constitutive promoters for applications in pathway engineering in *Saccharomyces cerevisiae*. *Biotechnol. Bioeng.* **2012**, *109*, 2082–2092. [CrossRef] [PubMed]
114. Redden, H.; Morse, N.; Alper, H.S. The synthetic biology toolbox for tuning gene expression in yeast. *FEMS Yeast Res.* **2015**, *15*, 1–10. [CrossRef]
115. Zou, L.-G.; Chen, J.-W.; Zheng, D.-L.; Balamurugan, S.; Li, D.-W.; Yang, W.-D.; Liu, J.-S.; Li, H.-Y. High-efficiency promoter-driven coordinated regulation of multiple metabolic nodes elevates lipid accumulation in the model microalga *Phaeodactylum tricornutum*. *Microb. Cell Fact.* **2018**, *17*, 54. [CrossRef] [PubMed]
116. Vila, M.; Díaz-Santos, E.; De la Vega, M.; Rodríguez, H.; Vargas, Á.; León, R. Promoter trapping in microalgae using the antibiotic paromomycin as selective agent. *Mar. Drugs* **2012**, *10*, 2749–2765. [CrossRef] [PubMed]
117. Yamanishi, M.; Ito, Y.; Kintaka, R.; Imamura, C.; Katahira, S.; Ikeuchi, A.; Moriya, H.; Matsuyama, T. A genome-wide activity assessment of terminator regions in *Saccharomyces cerevisiae* provides a "terminatome" toolbox. *ACS Synth. Biol.* **2013**, *2*, 337–347. [CrossRef] [PubMed]
118. Higgins, D.R.; Busser, K.; Comiskey, J.; Whittier, P.S.; Purcell, T.J.; Hoeffler, J.P. Small vectors for expression based on dominant drug resistance with direct multicopy selection. In *Pichia Protocols. Methods in Molecular Biology*™; Higgins, D.R., Cregg, J.M., Eds.; Humana Press: Totowa, NJ, USA, 1998; Volume 103, pp. 41–53. [CrossRef]
119. Napierala, M.; Parniewski, P.; Pluciennik, A.; Wells, R.D. Long CTG.CAG repeat sequences markedly stimulate intramolecular recombination. *J. Biol. Chem.* **2002**, *277*, 34087–34100. [CrossRef] [PubMed]
120. Liu, Z.; Chen, O.; Wall, J.B.J.; Zheng, M.; Zhou, Y.; Wang, L.; Ruth Vaseghi, H.; Qian, L.; Liu, J. Systematic comparison of 2A peptides for cloning multi-genes in a polycistronic vector. *Sci. Rep.* **2017**, *7*, 2193. [CrossRef]
121. Falciatore, A.; Casotti, R.; Leblanc, C.; Abrescia, C.; Bowler, C. Transformation of nonselectable reporter genes in marine diatoms. *Mar. Biotechnol.* **1999**, *1*, 239–251. [CrossRef] [PubMed]
122. Tan, M.H.; Loke, S.; Croft, L.J.; Gleason, F.H.; Lange, L.; Pilgaard, B.; Trevathan-Tackett, S.M. First genome of *Labyrinthula* sp., an opportunistic seagrass pathogen, reveals novel Insight into marine protist phylogeny, ecology and CAZyme cell-wall degradation. *Microb. Ecol.* **2021**, *82*, 498–511. [CrossRef]

Table S1. Electroporation conditions used in thraustochytrid transformation.

Strain	Washing solution	Cell wall treatment	Electroporation solution	DNA structure	Pulse length, ms (mF × Ω)	Field strength (kv/cm)	Pulse numbers	Efficiency	Notes	Reference
Aurantiochytrium limacinum F26-b	ASW	No	OPTI-MEM™ I	L	5	8.5	2	n/a		[21]
	water	No	NF	L	2.5; 10	7.5	2	n/a		[22]
	water	No	NF	C	2.5	7.5	2	n/a		[23]
Aurantiochytrium limacinum mh0186	n/a	n/a	NF	L	2.5	7.5	2	n/a		[24]
	ASW	No	NF	L	5	7.5	2	n/a		[25]
	ASW	No	NF	L	2.5	6	2	n/a		[26]
	ASW	No	NF	L	2.5	7.5	2	160	Highest efficiency reported	[27]
	n/a	n/a	n/a	n/a	n/a	n/a	n/a	n/a		[28]
Aurantiochytrium limacinum OUC168	n/a	n/a	n/a	L	10	1.8	1	n/a		[29]
Aurantiochytrium limacinum OUC88	Water; Sorbitol	No	Sorbitol	C	10	1.8	1	n/a		[30]
Aurantiochytrium limacinum SR21	BSS, Sucrose	No	Sucrose	L	25	2.25	2	44	This efficiency was the best among the tested conditions, including protocols done by two-staged square wave pulses (NEPA21)	[20]
	BSS, Sucrose	No	Sucrose	L	n/r	n/r	3	n/a	Two-staged square wave pulses (NEPA21)	[52]

	ASW	No	NF	L	2.5	7.5	2	n/a		[31]
	50% ASW; Sucrose	Beads	Sucrose	L	5	5	1	30-150	The efficiency was nearly zero without treating beads	[32]
	Water; 0.1 M PB pH 6.5	DTT	Sorbitol	L	n/a	n/a	n/a	n/a	Square wave pulses	[33]
	n/a	n/a	n/a	n/a	n/a	n/a	n/a	n/a	Square wave pulses by custom-built electroporator	[34]
	Water	DTT	Sorbitol	L	6	10	1	n/a		[35]
	ASW	No	NF	n/r	2.5	7.5	1	n/a	Electroporation of Cas9-gRNA RNP complex	[36]
Aurantiochytrium sp. KRS101	Water	DTT	Sorbitol	L	25	10	1	7-55	The efficiency varied according to the antibiotics (Cycloheximide) selection concentration	[37]
Aurantiochytrium sp. MP4	n/a	n/a	n/a	L	15	n/a	1	n/a	50–100 colonies/plate by unknown amounts of DNA	[38]
Aurantiochytrium sp. PKU#SW7	n/a	n/a	Sorbitol	C	2.5	3	2	n/a		[39]
Aurantiochytrium sp. RH-7A	ASW	No	NF	n/r	2.5	7.5	1	n/a	Electroporation of Cas9-gRNA RNP complex	[36]
Aurantiochytrium sp. SD116	Sorbitol	DTT (buffer A)	Sorbitol (buffer B)	L	0.1	6	50	30-80	Square wave pulses by custom-built electroporator Multiple parameters were screened	[40]
	Sorbitol	DTT (buffer A)	Sorbitol (buffer B)	L	0.1	6	50	n/a	Square wave pulses by custom-built electroporator	[41, 42]
Aurantiochytrium sp. SK4	n/a	n/a	n/a	L	15	n/a	1	n/a	50–100 colonies/plate by unknown amounts of DNA	[38, 43]
Schizochytrium sp. HX-308	Water; Sorbitol	No	Sorbitol	L	10	3.75	1	n/a		[44]

Schizochytrium sp. PKU#Mn4	Water; Sorbitol	DTT; Enzymes	Sorbitol	L/C	25	10	1	n/a	The cassettes with 18S homology arms were linearized	[45]
Schizochytrium sp. S31	5.0% PEG 8000; 114% ASW; Sucrose	Beads	Sucrose	n/a	10	10	1	n/a		[46]
	Water; Sorbitol	No	Sorbitol	L	10	7.5	2	n/a		[47]
Schizochytrium sp. TIO01	Water; Sorbitol	DTT	Sorbitol	L	10	9	1	>100		[49]
Schizochytrium sp. TIO1101	20 mM PB	DTT	Sorbitol	L	4.5	n/a	1	n/a		[50]
Schizochytrium sp. CB15-5	BSS; Sucrose	n/a	Sucrose	L	0.65	2.5	1	0.5-7, 1.2-50, 0.5-3	Different efficiencies by using Actin, ef1α, GAP promoter, respectively	[51]
Thraustochytrid strain 12B	50% ASW; Sucrose	Beads	Sucrose	L	5	5	1	1.5-15	The efficiency was zero without treating beads	[32]
Thraustochytrium aureum ATCC 34304	ASW	No	NF	L	2.5	7.5	2	n/a	The efficiency was described as extremely low	[27]

The waveform was exponential decay if not specially mentioned; Efficiency, number of transformants per ug of cassette DNA; ASW, artificial sea water (1.75% (weight/volume) sea salt); n/a, not available; NF, Nucleofector™ solution L; Sorbitol, 1 M sorbitol; BSS, 10 mM KCl, 10 mM NaCl, and 3 mM CaCl2; Sucrose, 50 mM sucrose; PB, phosphate buffer; n/r, not relevant; Buffer A, 0.6 M sorbitol, 0.1 M LiAc, 10 mM DTT, pH 7.0; Buffer B, 10 mM K2HPO4, 5 mM MgCl2, 1 M sorbitol, pH 7.4; Enzymes, 20 g/L pectinase and 20 g/L snailase in 7 M KCl; L, linear; C, circular.

Table S2. Non-electroporation transformation methods used in thraustochytrids.

Strain	Transformation method	DNA structure	Efficiency	Reference
Aurantiochytrium sp. YLH70	Frozen-EZ Yeast Transformation II	L	n/a	[56]
A. limacinum mh0186	Biolistic	L	Extremely rare	[27]
Parietichytrium sp. TA04Bb	Biolistic	L	50	[27]
Schizochytrium sp. S31	AMT	n/r	n/r	[57]
	AMT	n/r	n/r	[58]
	Biolistic	C	>2	[53]
	Biolistic	C	125-12.5	[5]
Schizochytrium sp. TIO1101	AMT	n/r	n/r	[59]
Schizochytrium sp. SEK 579	Biolistic	L	46	[27]
T. aureum ATCC 34304	Biolistic	L	190	[27]
	Biolistic	L	n/a	[54]
Thraustochytrium sp. ONC-T18	Biolistic	L	n/a	[55]

Efficiency, number of transformants per ug of cassette DNA; n/a, not available; AMT, *Agrobacterium tumefaciens*-mediated transformation; n/r, not relevant; L, linear; C, circular.

Table S3. Promoters and terminators used for thraustochytrids genetic engineering as well as the insertion type and the expressions of GOIs in thraustochytrids genetic engineering.

Strain	Promoter	Terminator	Insertion type
A. limacinum F26-b[a]	EF1α (n/a) [21, 22]; Ubiquitin (*T. aureum*) [21-23]	EF1α (n/a) [22]; Ubiquitin (n/a) [21]; SV40 [21-23]	HR [21-23]; Random [21, 22]
A. limacinum mh0186[a]	EF1α (*T. aureum*) [24-28]; Ubiquitin (*T. aureum*) [24-28]	EF1α (*T. aureum*) [24-28]; Ubiquitin (*T. aureum*) [24-28]	HR [25]; Random [24-28]
A. limacinum OUC168[a]	PGK (*Sc*) [29]	CYC1 [29]	HR [29]
A. limacinum OUC88[a]	EF1α (*Sc*) [30]; PGK (*Sc*) [30]; GAL1(*Sc*) [30]	CYC1 [30]	HR [30]
A. limacinum SR21[a]	EF1α (*Sc*) [33-35]; GAP [20, 52]; Ubiquitin (*T. aureum*) [31]; EF1α (*T. aureum*) [31]; EF1α (12B) [32]; Actin (RH-7A) [36]	CYC1 [33-35]; GAP [20, 52]; Ubiquitin (*T. aureu*m) [31]; EF1α (*T. aureum*) [31]; EF1α (12B) [32]; Actin (RH-7A) [36]	HR [20, 32-35, 52]; Random [31]
Aurantiochytrium sp. KRS101[a]	GAP (*Hp*) [37]	AOX (*Hp*) [37]	HR [37]
Aurantiochytrium sp. MP4[a]	Tubulin (SK4) [38]	SV40 [38]	HR [38]
Aurantiochytrium sp. PKU#SW7	PH [39]; DH [39]	PH [39]; DH [39]	HR [39]
Aurantiochytrium sp. RH-7A	Actin [36]	Actin [36]	n.r.
Aurantiochytrium sp. SD116[a]	EF1α [40]; Actin [40]; EF1α (*Sc*) [41, 42]; Tubulin [42]	EF1α [40]; Actin [40, 42]; CYC1 [40-42]	HR [40-42]
Aurantiochytrium sp. SK4[a]	Tubulin [38, 43]	SV40 [38, 43]	HR [38, 43]
Aurantiochytrium sp. YLH70[a]	Actin [56]; ubiquitin [56]	orfC [56]	HR [56]
Parietichytrium sp. TA04Bb	Ubiquitin (*T. aureum*) [27]	Ubiquitin (*T. aureum*) [27]	Random [27]
Schizochytrium sp. S31[a]	35S (CMV) [47, 57, 58]; Tubulin [5, 47]; AlcA (*An*, inducible) [57, 58]; EF1α [48, 53]; EF1α (*Sc*) [48]; ccg1 (Neurospora) [48]; AOX1 (*Pp*, inducible) [48]; Ubiquitin [48]	polyA (CMV) [47, 57, 58]; Nos (*At*) [47, 57, 58]; CYC1 [47]; PFA3 [53]; SV40 [5]; Ubiquitin [48]; AOX1 (*Pp*) [48]	HR [5, 47]; Random [48, 53, 57, 58]
Schizochytrium sp. HX-308[a]	EF1α (*Sc*) [44, 45]; Ubiquitin (n/a) [44, 45]	CYC1 [44, 45]; Ubiquitin (n/a) [44, 45]	HR [44, 45]
Schizochytrium sp. PKU#Mn4[a]	poly-Ubiquitin [46]	CYC1 [46]	HR [46]; Random [46]
Schizochytrium sp. TIO01[a]	EF1α (*Sc*) [49]	CYC1 [49]	HR [49]
Schizochytrium sp. TIO1101[a]	EF1α (*Sc*) [50, 59]; 35S (CMV) [59]	CYC1 [50, 59] ; Nos (*At*) [59]	HR [50]; Random [59]
Schizochytrium sp. SEK 579	Ubiquitin (*T. aureum*) [27]	Ubiquitin (*T. aureum*) [27]	Random [27]
Schizochytrium sp. CB15-5[a]	Actin [51]; EF1α [51]; GAP [51]	Actin [51]; EF1α [51]; GAP [51]	HR [51]

Thraustochytrid strain 12B	EF1α [32]	EF1α [32]	HR [32]
T. aureum ATCC 34304[a]	Ubiquitin [27, 54]; EF-1α [27]; EF-1α (n/a) [54]	Ubiquitin [27, 54]; EF1α [27]; SV40 [54]; EF1α (n/a) [54]	HR [27, 54]; Random [54]
Thraustochytrium sp. ONC-T18[a]	Tubulin [55]	Tubulin [55]	HR [55]

The origins of each element were indicated in parentheses; *Sc*, *Saccharomyces cerevisiae*; All CYC1 originated from *Sc*; All SV40 originated from simian virus 40; Except CYC1 and SV40, all elements without indications are endogenous; EF1α (*Sc*), TEF1; PH, very-long-chain (3R)-3-hydroxyacyl-CoA dehydratase; DH, dehydrase/isomerase; Nos, nopaline synthase; 12B, Thraustochytrid strain 12B; RH-7A, *Aurantiochytrium* sp. RH-7A; SK4, *Aurantiochytrium* sp. SK4; *T. aureum, Thraustochytrium aureum* ATCC 34304; CMV, Cauliflower mosaic virus; *An*, *Aspergillus nidulans*; *Pp*, *Pichia pastoris*; *At*, *Agrobacterium tumefaciens; Hp, Hansenula polymorpha*; n/a, not available; n.r., not relevant (CRISPR-Cas9); [a]With GOIs expressed.

Table S4. The prevalence of constitutive promoters and terminators used in thraustochytrids genetic engineering.

	Endogenous	Non-endogenous			
		Thraustochytrids	***S. cerevisiae***	**Simian virus 40**	***H. polymorpha***
Promoter					
EF1α	4	3	7	0	0
Ubiquitin	4	5	0	0	0
Actin	4	1	0	0	0
Tubulin	4	1	0	0	0
GAP	2	0	0	0	1
Terminator					
CYC1	0	0	9	0	0
EF1α	4	2	0	0	0
Ubiquitin	2	4	0	0	0
SV40	0	0	0	5	0
Actin	3	1	0	0	0

The numbers show the number of strains that have used the promoter/terminator in at least one publication (Table S4).

Table S5. Antibiotics used for selecting transformants of thraustochytrids with detailed information regarding to the reference of each concentration.

Strain	Zeocin	Hygromycin	G418	Blasticidin	Other
A. limacinum F26-b		2000 [21-23]	500 [21, 22]		
A. limacinum mh0186	500* [27]	1000 [25]; 2000* [27]	500 [25-28]	1200 [27]	500 (neomycin) [24]
A. limacinum OUC168	5 [29]				100 (chloramphenicol) [29]
A. limacinum OUC88	5 [30]				100 (chloramphenicol) [30]
A. limacinum SR21	30 [35]; 50 [33, 35]; 100 [20, 34, 36, 52]	200 [20]	500 [20, 31, 32]		
Aurantiochytrium sp. KRS101					30 (cycloheximide) [37]
Aurantiochytrium sp. MP4	50 [38]				
Aurantiochytrium sp. PKU#SW7		500 [39]	500 [39]		
Aurantiochytrium sp. RH-7A	100 [36]				
Aurantiochytrium sp. SD116	30 [40]; 50 [42]; 100 [41]	500* [40]	50* [40]; 50 [41]		100* (anhydrotetracycline) [40]
Aurantiochytrium sp. SK4	50 [38, 43]				
Aurantiochytrium sp. YLH70	15 [56]				
Parietichytrium sp. TA04Bb		2000 [27]	500 [27]	800 [27]	
Schizochytrium sp. S31	40 [48]; 50 [5]		100 [47]		50(bleomycin) [47]; 250 (cefotaxime) [57, 58]; 50 (paromomycin) [53]
Schizochytrium sp. HX-308	1.5 [45]; 20 [44]				
Schizochytrium sp. PKU#Mn4			800 [46]		
Schizochytrium sp. TIO01	100 [49]				
Schizochytrium sp. TIO1101			300 [50, 59]		
Schizochytrium sp. SEK 579		2000 [27]	500 [27]		
Schizochytrium sp. CB15-5	20 [51]				
Thraustochytrid strain 12B			500 [32]		
T. aureum ATCC 34304		2000 [27, 54]	1000 [27]; 2000 [54]	200-400 [54]	
Thraustochytrium sp. ONC-T18	250 [55]	400 [55]			

Each number represent the minimal concentration (μg/mL) used on agar for transformant selection in the reference; *Minimum inhibitory concentration identified in the reference that was not used in transformant selection.

Paper III

Applied Microbiology and Biotechnology
https://doi.org/10.1007/s00253-021-11425-5

APPLIED GENETICS AND MOLECULAR BIOTECHNOLOGY

A non-canonical Δ9-desaturase synthesizing palmitoleic acid identified in the thraustochytrid *Aurantiochytrium* sp. T66

E-Ming Rau [1] · Inga Marie Aasen [2] · Helga Ertesvåg [1]

Received: 28 April 2021 / Revised: 14 June 2021 / Accepted: 22 June 2021

Abstract
Thraustochytrids are oleaginous marine eukaryotic microbes currently used to produce the essential omega-3 fatty acid docosahexaenoic acid (DHA, C22:6 n-3). To improve the production of this essential fatty acid by strain engineering, it is important to deeply understand how thraustochytrids synthesize fatty acids. While DHA is synthesized by a dedicated enzyme complex, other fatty acids are probably synthesized by the fatty acid synthase, followed by desaturases and elongases. Which unsaturated fatty acids are produced differs between different thraustochytrid genera and species; for example, *Aurantiochytrium* sp. T66, but not *Aurantiochytrium limacinum* SR21, synthesizes palmitoleic acid (C16:1 n-7) and vaccenic acid (C18:1 n-7). How strain T66 can produce these fatty acids has not been known, because BLAST analyses suggest that strain T66 does not encode any Δ9-desaturase-like enzyme. However, it does encode one Δ12-desaturase-like enzyme. In this study, the latter enzyme was expressed in *A. limacinum* SR21, and both C16:1 n-7 and C18:1 n-7 could be detected in the transgenic cells. Our results show that this desaturase, annotated T66Des9, is a Δ9-desaturase accepting C16:0 as a substrate. Phylogenetic studies indicate that the corresponding gene probably has evolved from a Δ12-desaturase-encoding gene. This possibility has not been reported earlier and is important to consider when one tries to deduce the potential a given organism has for producing unsaturated fatty acids based on its genome sequence alone.

Key points
- *In thraustochytrids, automatic gene annotation does not always explain the fatty acids produced.*
- *T66Des9 is shown to synthesize palmitoleic acid (C16:1 n-7).*
- *T66des9 has probably evolved from Δ12-desaturase-encoding genes.*

Keywords Delta-9 desaturase · Palmitoleic acid · Aurantiochytrium · Thraustochytrids · Delta-12 desaturase · Fatty acid

Introduction

Thraustochytrids are heterotrophic marine eukaryotes known for the ability to accumulate high levels of the omega-3 fatty acid DHA (Aasen et al. 2016; Morabito et al. 2019). They belong to the *Stramenopiles* group and are divided into several genera such as *Schizochytrium*, *Aurantiochytrium*, and *Thraustochytrium* (Marchan et al. 2018). Omega-3 fatty acids, including DHA, are beneficial to human health, and some thraustochytrid strains are used for commercial DHA production (Barclay et al. 2010; Guo et al. 2018). Due to the increasing demand for sustainable sources of fatty acids (FAs), such as DHA (Ghasemi Fard et al. 2019; Sprague et al. 2016), knowledge about how thraustochytrids synthesize FAs is important to be able to improve potential production strains by metabolic engineering.

Polyunsaturated fatty acids (PUFAs) can be produced by two distinct pathways. Usually, PUFAs are synthesized from C16:0, the main product of the fatty acid synthase (FAS), by the desaturase-elongase (DE) pathway (Sun et al. 2020; Thelen and Ohlrogge 2002) (Fig. 1). The desaturases of the DE pathway are mixed function oxidases, and the reaction is coupled to an electron flow

✉ Helga Ertesvåg
helga.ertesvag@ntnu.no

[1] Department of Biotechnology and Food Science, NTNU Norwegian University of Science and Technology, Trondheim, Norway

[2] Department of Biotechnology and Nanomedicine, SINTEF Industry, Trondheim, Norway

Published online: 22 July 2021

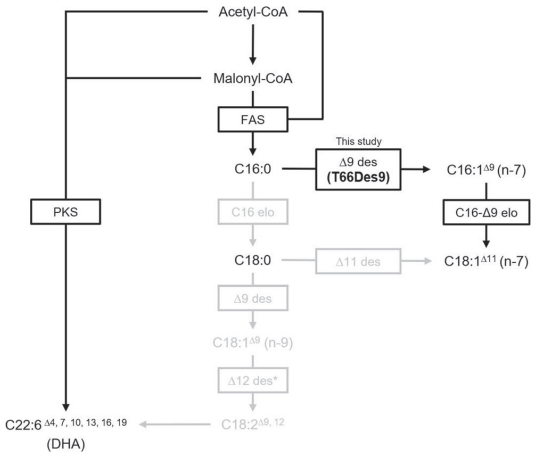

Fig. 1 Possible pathways for biosynthesis of unsaturated fatty acids in *Aurantiochytrium* sp. T66. des, desaturase; elo, elongase; FAS, fatty acid synthase; PKS, PKS pathway. Enzymes not found encoded in the *Aurantiochytrium* sp. T66 genome and FAs never detected in this strain are written in gray. Single asterisk indicates the automatic annotation for T66Des9.

involving cytochrome b5 and cytochrome b5 reductase. However, in thraustochytrids producing DHA and in bacteria producing omega-3 fatty acids, PUFAs are mostly synthesized by an alternative pathway, using a dedicated polyketide synthase (PKS) which synthesizes, e.g., DHA directly from malonyl-CoA and acetyl-CoA without the need for oxygen for desaturation (Hauvermale et al. 2006; Metz et al. 2001). Although some PUFAs are synthesized by the DE pathway in some thraustochytrids, this pathway has not been shown to contribute to DHA production (Matsuda et al. 2012; Sakaguchi et al. 2012). Even though both the FAS-DE and the PKS pathways share precursors such as acetyl-CoA, malonyl-CoA, and NADPH, the regulation of the relative activities of these pathways is still mostly unknown.

Different thraustochytrid genera or strains have different FA compositions, potentially related to the presence or absence of particular enzymes. In a comparative study, it was reported that the amount of linoleic acid (C18:2 n-6), stearic acid (C18:0), and oleic acid (C18:1 n-9) in *Schizochytrium* sp. SEK210 and *Thraustochytrium aureum* ATCC 24473 were significantly higher than those in the tested *Aurantiochytrium* sp. (Nagano et al. 2011). Moreover, *T. aureum* has been found to produce n-6 PUFAs by the DE pathway (Matsuda et al. 2012), while FAs like C20:4 have not been detected in *Aurantiochytrium* sp. (Heggeset et al. 2019). In addition, monounsaturated FA palmitoleic acid (C16:1 n-7) and vaccenic acid (C18:1 n-7) have been detected in *Aurantiochytrium* sp. T66., but not in *Aurantiochytrium limacinum* SR21 (Jakobsen et al. 2008; Yokochi et al. 1998). As indicated in Fig. 1, C16:0 can be desaturated to C16:1 n-7 by Δ9-desaturases. C16:1 n-7 can then be elongated to C18:1 n-7 by an elongase accepting C16-Δ9 as substrate. Alternatively, C18:1 n-7 could be synthesized from C18:0 by a Δ11-desaturase.

The genome of *Aurantiochytrium* sp. T66 encodes seven putative desaturases, including gene T66002957.1, which exhibits high homology to Δ12-desaturases that catalyze the conversion of oleic acid (C18:1 n-9) to linoleic acid (C18:2 n-6) (Heggeset et al. 2019). However, no C18:2 n-6 or C18:1 n-9 were detected in the FA profile of *Aurantiochytrium* sp. T66 (Jakobsen et al. 2008). In addition, T66002957.1 was highly expressed at the nitrogen-limited lipid accumulation stage in *Aurantiochytrium* sp. T66 cells and that is when the two monounsaturated FAs are synthesized (Heggeset et al. 2019). Moreover, in *Thraustochytrium* sp. ATCC 26185, a putative desaturase with the identical amino acid sequence of the T66002957.1 encoded a protein that displayed no Δ12-desaturase activity when expressed heterologously in *Escherichia coli* (Meesapyodsuk and Qiu 2016), suggesting that the function of the enzyme could be different from that predicted by sequence similarity.

In this study, we explored the hypothesis that although the T66002957.1 encoded protein shares Δ12-desaturase sequence characteristics, it might possess Δ9-desaturase activity. Since *A. limacinum* SR21 has not been reported to produce C16:1 or C18:1 FAs, and was found not to encode a homologous protein, we expressed T66002957.1 in *A. limacinum* SR21. The transgenic strain synthesized both C16:1 n-7 and C18:1 n-7. T66002957.1 is therefore named *T66des9* and the corresponding protein T66Des9 in the rest of this paper.

Materials and methods

Strains and medium

Aurantiochytrium limacinum SR21 (ATCC® MYA-1381™) was cultured in GPYS [3% glucose, 0.6% peptone, 0.2% yeast extract, 50 mM sucrose, 1.8% ocean salt (Tropic Marin® Sea Salt CLASSIC), 200 μg/ml ampicillin, 200 μg/ml streptomycin) at 28 °C with rotary shaking at 170 rpm. *Aurantiochytrium* sp. T66 (ATCC® PRA-276™) was cultured in YPDS (2% glucose, 2% peptone, 1% yeast extract, 1.75% ocean salt, 200 μg/ml ampicillin, 200 μg/ml streptomycin) at 25 °C with rotary shaking at 170 rpm (Supplemental Table S1). For plates, 20 g/L agar (LP0011, Oxoid Ltd, UK) was added. For long-term storage, cells were suspended in 15% glycerol and kept at −80 °C.

The fat accumulation medium was prepared as described: (in g/l) glucose (40), NH_4Cl (0.7), KH_2PO_4 (0.3), Na_2SO_4 (18), $MgSO_4x7H_2O$ (0.25), $CaCl_2x2H_2O$ (0.2), KCl (0.4), Tris-base (6.1), maleic acid (5.8), and yeast extract (0.3). The pH of medium was adjusted to 7 with NaOH.

Immediately before use, every liter of the medium was supplemented with 5 ml of trace mineral solution (in mg/l: 390 $CuSO_4x5H_2O$, 20 $CoCl_2x6H_2O$, 5000 $FeSO_4x7H_2O$, 150 $MnSO_4x7H_2O$, 10 $NaMoO_4x2H_2O$, and 440 $ZnSO_4x7H_2O$) and 1 ml of vitamin solution (in g/l: 0.05 thiamin HCl and 0.005 B12 cobalamin).

Phylogenetic analysis

The analyses were conducted in MEGA X (Kumar et al. 2018) by using the maximum likelihood method and JTT matrix-based model (Jones et al. 1992). The analysis involved 31 amino acid sequences. There were a total of 546 positions in the final dataset. Initial trees for the heuristic search were obtained automatically by applying Neighbor-Join and BioNJ algorithms to a matrix of pairwise distances estimated using the JTT model and then selecting the topology with superior log likelihood value.

Plasmid construction

PCRs were performed by Q5® High-Fidelity DNA Polymerase (New England Biolabs, USA). DNAs were digested by restriction enzymes (New England Biolabs, USA) and purified from gels by Monarch® DNA gel extraction kit (New England Biolabs, USA). Genomic DNAs were isolated by MasterPure™ Complete DNA and RNA Purification Kit (Lucigen, USA). Plasmids were extracted by ZR Plasmid Miniprep (Zymo Research, USA). DNAs were cloned into TOPO vectors by Zero Blunt™ TOPO™ PCR Cloning Kit (Invitrogen, USA). DNAs were ligated by T4 DNA Ligase (New England Biolabs, USA), followed by standard *E. coli* DH5α transformation and antibiotic selection. All PCR-originated regions of the clones are verified by Sanger sequencing (Eurofins Scientific, Luxembourg). Plasmids, primers, restriction enzymes, and antibiotic selection genes used were indicated in Supplemental Table S2, S3 and Fig. S1. Gene *T66des9* (T66002957.1) is the base pair position 4173-5426 of the T66 genome contig LNGJ01004217 (GenBank accession number) (Liu et al. 2016).

The scheme of the plasmid construction was illustrated in Supplemental Fig. S1. DNA fragment (r)*ble*-2A-*T66des9*-(f)GAPt was generated by overlap extension PCR. The 1st round PCR products A and C were amplified from pUC19-18GZG, and product B was amplified from *Aurantiochytrium* sp. T66 genomic DNA. PCR products A, B, and C were purified from gels and mixed as the 2nd round PCR template (Hilgarth and Lanigan 2020). DNA fragment GAPp-(f)*ble* and (r)GAPt were amplified from pUC19-18GZG. Upper and lower flanking were amplified from *A. limacinum* SR21 genomic DNA.

Transformation of *A. limacinum* SR21

The electrotransformation protocol of *A. limacinum* SR21 was adapted from Faktorová et al. (2020) and Rius (2021). Cell colonies were inoculated in GPY medium at 28 °C for 2 days with rotary shaking at 170 rpm, followed by sub-culturing cells with starting OD_{600}~0.02 in 50 ml GPY medium with 250 ml non-baffled flasks and 170 rpm rotary shaking at 28 °C until the OD_{600} reached around 3 (~24 h). Cells were then collected by centrifugation at 7,000 g for 5 min at 4 °C and washed by 10 ml of 1X BSS (10 mM KCl, 10 mM NaCl, and 3 mM $CaCl_2$) twice by 10 ml of 50 mM sucrose with the same centrifugation setting and resuspended in 2 ml of 50 mM sucrose to a final concentration of approximately 7.5×10^5 cells/μl. The cell suspensions were transferred to 2-mm-gap cuvettes (VWR, Belgium) on ice and adjusted to appropriate volumes (typically 150~300μl) with impedance (kΩ) between 0.9 and 1.5, measured by NEPA21 Electroporator (Nepa Gene Co., Ltd., Japan). DNA cassettes were linearized by *Sfo*I digestion at the plasmid backbone region and purified (Monarch® Kits for DNA Cleanup, New England Biolabs, USA). Ten μl DNA (3~5 μg) was added to the cell suspension in 2-mm-gap cuvettes, mixed by flicking, and incubated on ice for 5 min. Each cuvette was set on the NEPA21 Electroporator and pulsed with poring pulse parameters: 275 V, 8 milliseconds (ms) pulse length, two pulses, 50 ms length interval, 10% decay rate, "+" polarity and transfer pulse parameters: 20 V, 50 ms pulse length, 50 ms length interval, 1 pulse, 40% decay rate, "+/−" polarity. Two ml of GPYS medium was immediately added to the pulsed cells, which was then transferred to tubes and incubated overnight at 28 °C with rotary shaking at 170 rpm. The cells were collected by centrifugation and plated evenly to three GPYS agar plates (avoid over-dried) containing 100 μg/mL Zeocin (Thermo Fisher Scientific, USA) and incubated at room temperature for 3–5 days. Emerged colonies were re-streaked to new GPYS agar plates containing 100 μg/ml Zeocin. Colonies that grew after re-streaking were subjected to genomic DNA extraction (MasterPure™ Complete DNA and RNA Purification Kit, Lucigen, USA) and verified by PCR (Q5® High-Fidelity DNA Polymerase, New England Biolabs, USA).

RT-PCR analysis

Total RNA from *A. limacinum* SR21 cells cultivated overnight in GPY medium were isolated using Spectrum™ Plant Total RNA Kit (Sigma-Aldrich, USA) with DNase I treatment (DNA-free™ DNA Removal Kit, Thermo Fisher Scientific, USA), and the cDNA was synthesized using First-Strand cDNA Synthesis Kit (Cytiva, USA) with random hexamer primers. PCR was performed to amplify parts of *T66des9* cDNA by the primer pair 2957RT-f and 2957RT-r, *ble* cDNA by the primer pair zeo sjekk-f and zeoRT-r, and β-tubulin gene

(GenBank accession number: KX668278) cDNA as a reference gene by the primer pair SR21tubF2 and SR21tubR2 (Supplemental Table S3). PCR was performed by Q5® High-Fidelity DNA Polymerase (New England Biolabs, USA), with the parameters: 98 °C for 30 s, followed by 28 cycles of 98 °C for 10 s, 66 °C for 30 s, and 72 °C for 30 s, and followed by a final extension of 2 min at 72 °C.

Cultivations for determination of fatty acid profiles

Single colonies of *A. limacinum* SR21 were inoculated in tubes with GPY medium at 28 °C for 2 days with rotary shaking at 170 rpm, followed by sub-culturing cells with starting OD_{600}~0.02 in 100 ml fat accumulation medium with 500 ml baffled flasks and 170 rpm rotary shaking at 28 °C. For every collection time point, culture OD_{600} was recorded, and 2 ml of the culture was stored at −20 °C for FA analysis. For lipid extraction and determination of the FA isomers, 50 ml of the culture was centrifuged, and the pellet was stored at −20 °C until freeze-drying and analyses.

Fatty acid analyses

The FA concentrations were determined by LC-MS (Heggeset et al. 2019). For the determination of the FA isomers, total lipids were extracted from the freeze-dried pellets (Jakobsen et al. 2008). The extracted oil was diluted with isooctane (to ca. 80 μg/μl) and methylated (AOCS 2017a; AOCS 2017b), before analysis on an Agilent 8860 gas chromatograph (Agilent Technologies, USA) equipped with a flame ionization detector and a CP-Wax 52 CB capillary column (25 m × 250 μm × 0.2 μm, Agilent Technologies, USA). The FAs were identified based on the GLC Reference standard 68D (GCL-68D, Nu-Check, USA), which contains 20 fatty acid methyl esters (FAMEs).

Results

Sequence analysis of *T66des9*

We wanted to know if other species or strains encode homologs of T66Des9. The amino acid sequence of T66Des9 was first compared to the non-redundant protein sequences database at GenBank using BLAST. T66Des9 showed the highest degree of identity with proteins that are either annotated as Δ12-desaturase or hypothetical proteins, but no Δ9-desaturases (Supplemental Table S4). Phylogenetic analysis showed that T66Des9 is most closely related to proteins from other thraustochytrids, followed by diatoms and plants (Fig. 2). Two of the proteins most similar to T66Des9, TauΔ12des of *T. aureum* and PpDes12 of *Phaeodactylum tricornutum*, have both been verified to exhibit Δ12-desaturase activities (Domergue et al. 2003; Matsuda et al. 2012). To compare the sequence between T66Des9 and a functionally verified Δ9-desaturase, we added fD9des of *Fistulifera solaris* to the phylogenetic analysis (Muto et al. 2013). However, fD9des is substantially distant from the rest of the analyzed proteins, including a putative Δ12-desaturase from the same species. The structure of T66Des9 was then analyzed. Homology modeling using Phyre2 (Kelley et al. 2015) indicated that only the sequences of membrane-bound FA desaturases from mammals (Bai et al. 2015; Wang et al. 2015) were sufficiently similar to obtain a model. T66Des9 was found to have the four expected trans-membrane helixes (not shown). The protein contains the three histidine boxes with eight histidine residues and the single histidine residue after the last transmembrane helix (His302 in T66Des9), all of which are necessary for coordinating the di-iron molecule in the catalytic center (Nachtschatt et al. 2020; Nagao et al. 2019) (Fig. 3). The first histidine box has the consensus sequence HX_3H, not the consensus sequence HX_4H prevalent among Δ9-desaturases (Shanklin et al. 1994). We further compared the T66Des9 sequence to the *Labyrinthulomycetes* part of the whole genome shotgun database at NCBI and the sequenced *heterokonts* available at JGI. This identified a few additional thraustochytrid species encoding proteins closely related to T66Des9 (Supplemental Table S5). Notably, *A. limacinum* did not encode proteins closely related to T66Des9.

Generation of a *T66des9*-expressing *A. limacinum* SR21 mutant strain

It was decided to insert an expression cassette encoding T66Des9 into the *crtIBY* gene of *A. limacinum* SR21 by homologous recombination. The expression cassette contains a Zeocin resistance gene (*ble*) linked to *T66des9* by a 2A peptide-encoding DNA fragment, and gene expression was controlled by the endogenous glyceraldehyde 3-phosphate dehydrogenase (GAPDH) promoter and terminator (Fig. 4a and Supplemental Fig. S1). The 2A peptide can be cleaved off during protein translation, resulting in two separated proteins (Liu et al. 2017). The cassette was flanked by two DNA fragments from the β-carotene synthesis gene *crtIBY* (Iwasaka et al. 2018). Disruption of *crtIBY* will turn the colonies from brown to pale due to the lack of carotenoids, making this a convenient integration site since the site-specific genome integration does not affect viability or growth and can be verified by the color of the colonies (Rius 2021). The vector containing the *T66des9* knock-in cassette was designated pEMR24. Since the precursor of carotenoids is also acetyl-CoA, disruption of *crtIBY* could potentially affect FA synthesis. Moreover, the use of the endogenous GAPDH promoter might alter the expression of GAPDH and influence glycolysis, gluconeogenesis, and glycerol synthesis. Considering these potential side effects, we constructed plasmid pEMR26 to be able to create a control strain.

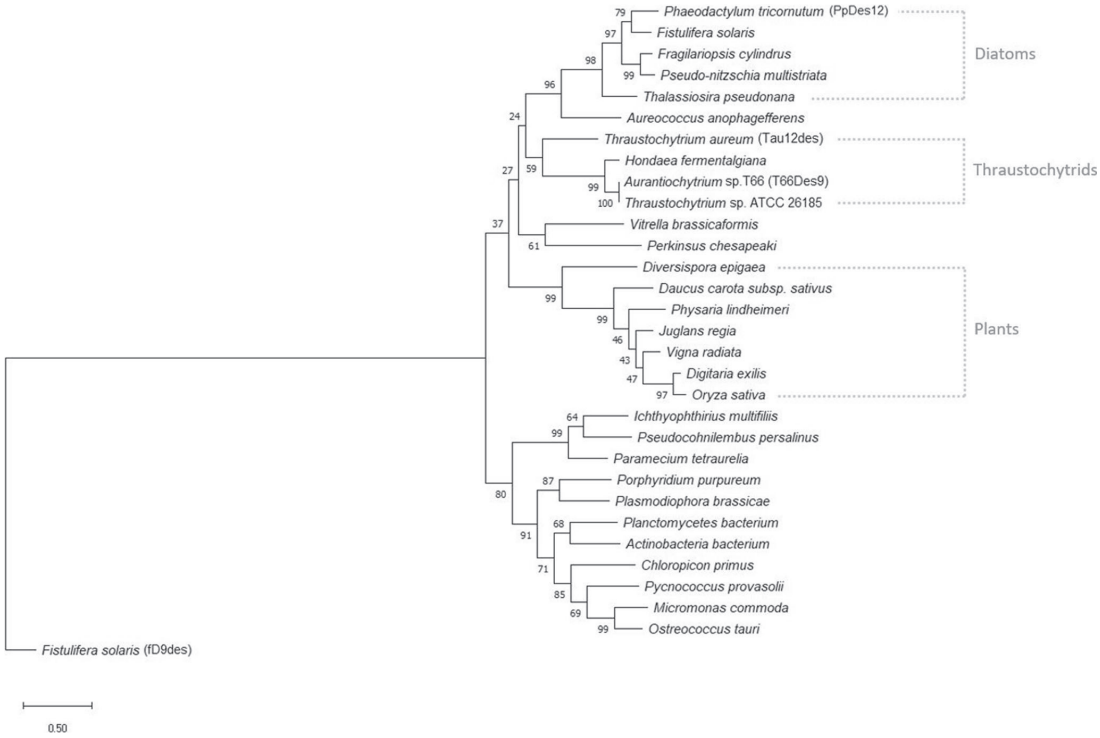

Fig. 2 Phylogenetic analysis of T66Des9 and its homologs from the GenBank search. The homologs' names and information were summarized in Supplemental Table S4 and shown here only with the species name unless selectively indicated with parentheses. The tree with the highest log likelihood (−20940.42) is shown. The tree is rooted with fD9des. The scale bar shows a distance of 0.5 substitutions per residue. The percentage of replicate trees in which the associated taxa clustered together in the bootstrap test (1000 replicates) are shown next to the branches (Felsenstein 1985)

pEMR26 is identical to pEMR24, except for it only encoding *ble* (Supplemental Fig. S1).

pEMR24 and pEMR26 were used to transform *A. limacinum* SR21 cells by electroporation. We obtained one colony (26-1) that could grow after re-streaking on a plate containing Zeocin after transformation by pEMR24 and five such colonies (30-1, 30-18, 30-21, 30-22, 30-23) after transformation by pEMR26. DNA from these colonies were then used in a PCR reaction that confirmed that 26-1 and three of the five transformants (30-1, 30-21, and 30-23) of pEMR26 had replaced parts of *crtIBY* with the plasmid inserts (Fig. 4a, b and Supplemental Fig. S2). Strains 26-1 and 30-1 encoding *ble*-2A-*T66des9* and *ble*, respectively, were chosen for further work. These strains also showed the expected pale phenotype which further supported that the expression cassette was correctly integrated (Fig. 4c).

While resistance to Zeocin indicated that the first part of the construct was expressed, we wanted to confirm that the *T66des9* gene transcripts were present in 26-1 strain. This was done by isolating RNA from the wild type (WT), strain 30-1 and 26-1, creating cDNA and then performing *T66des9* PCR. Samples without reverse transcriptase were used to rule out contamination of genomic DNA in the RNA samples. The results showed the presence of *T66des9* mRNA in 26-1 (Fig. 4d).

Analyses of the fatty acid compositions of the T66Des9-expressing transgenic *A. limacinum* SR21 strains

Given that the gene was expressed, it was likely that the protein also would be expressed. In that case, analyses of the FAs synthesized by the mutant strain could demonstrate the function of T66Des9.

A. limacinum SR21 WT and strains 30-1 and 26-1 were cultivated in shake flasks using glucose as the carbon source. The growth curves were similar for all three strains (Fig. 5). It should be mentioned that since the thraustochytrid cells accumulate lipids in the stationary phase, the optical density will still increase after they have stopped cell division. This becomes apparent in all studies plotting both optical density and lipid-free cell mass. We analyzed the FA composition of the

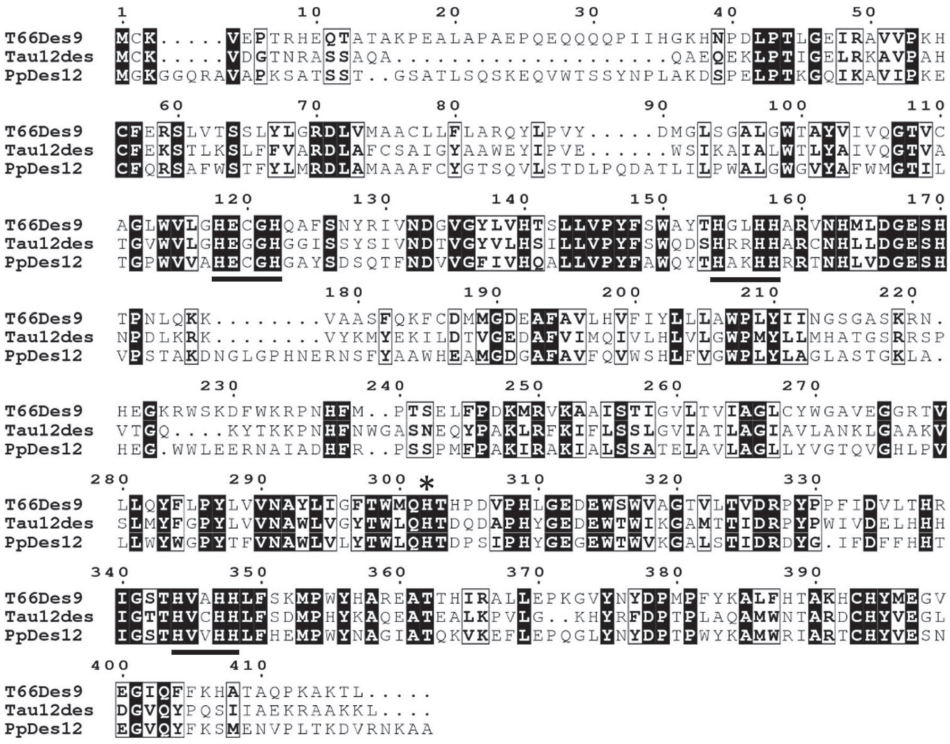

Fig. 3 Multiple sequence alignment of the amino acid sequence of T66Des9 with the two most homologous proteins with characterized enzyme activity found in our search was generated by ClustalW and drawn by ESPript 3.0 (Robert and Gouet 2014). Tau12des: TauΔ12des, a Δ12-desaturase of *T. aureum*; PpDes12: a Δ12-desaturase of *P. tricornutum*; white letters with a black background: identical residues; bold letters in a black box: similar residues; underline: the three conserved histidine boxes of membrane-bound FA desaturases; asterisk: the conserved His302

strains after cultivating for 16.5 (approximately at nitrogen-exhaustion), 36 (nitrogen-limited), and 60 h (late nitrogen-limited). Supplemental Table S6 shows the data for all time points and Table 1 the data for the last sampling of the two transgenic strains. As expected, neither C16:1 nor C18:1 was detected in WT or strain 30-1 at any time point. On the other hand, both C16:1 and C18:1 were detected in strain 26-1.

In order to determine the position of the double bond, methyl esters of the FAs produced by strain 26-1 and *Aurantiochytrium* sp. T66 WT as control were analyzed by GC-FID. The results showed that both C16:1 and C18:1 were the n-7 isomers (Fig. 6a and Supplemental Table S7). This indicated that T66Des9 is a Δ9-desaturase when C16:0 is the substrate.

Discussion

In the present study, expression of *T66Des9* resulted in the synthesis of C16:1 n-7 and C18:1 n-7 in *A. limacinum* SR21. Since the amount of C18:0 was lower than that of C18:1 n-7 and the amount of C16:1 n-7 and C18:1 n-7 accumulated nearly linearly at similar rates (Fig. 6 b and c), it is likely that C18:1 n-7 was synthesized from C16:1 n-7 by an elongase (Fig. 1). In *Aurantiochytrium* sp. T66, the putative protein encoded by T66003689.1 (ELO-1) is identical to the function-verified C16-Δ9 elongase TsELO2 from *Thraustochytrium* sp. ATCC 26185 (Heggeset et al. 2019; Ohara et al. 2013). The protein encoded by Aurli1_73494 of *A. limacinum* SR21 shows 72% identity to TsELO2, and this protein or other putative elongases might be able to accept C16:1 n-7 as substrate.

Our data cannot exclude the possibility that the enzyme T66Des9 is an ω-7 desaturase, counting from the methyl end instead of the carboxyl end indicated by the Δ-nomenclature. Still, we have not found any reports in literature on ω-type enzymes introducing the first double bond. Some plants also make n-7 fatty acids, and it has been shown that they do so by using Δ9 desaturases (see, e.g., Cahoon et al. 1998). However, since the plant enzymes utilize ACP-linked and not CoA-linked substrates, this merely is an indication. Taken together, the most likely interpretation of our data is that T66Des9 is a Δ9-desaturase that accepts C16:0 as a substrate.

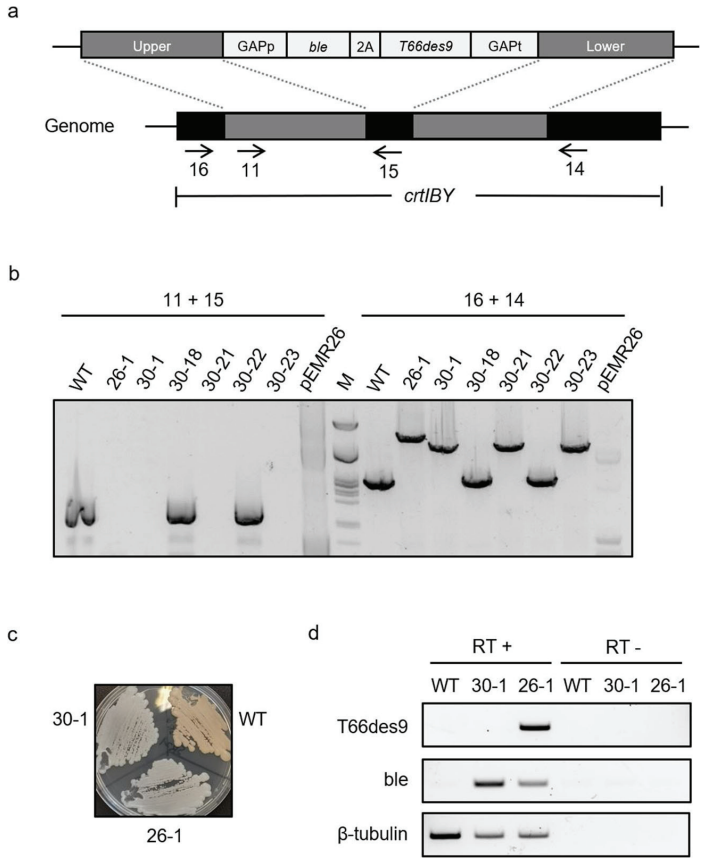

Fig. 4 **a** Scheme for linearized pEMR24 or pEMR26 (without 2A and *T66des9*) cassettes integrating into the genome of *A. limacinum* SR21 cells. Upper/lower, homologous regions; GAPp/t, GAPDH promoter/terminator; *ble*, Zeocin resistance gene; 2A, peptide self-cleavage sequence; arrows, primer annealing sites. **b** Genomic PCRs of indicated strains were performed with the primer pairs 11+15 and 16 + 14. M: lambda-PstI ladder. **c** Indicated strains were streaked on GPYS agar medium and incubated at room temperature for about 2 weeks. **d** The transcripts of the indicated strains were detected by RT-PCR using specific primers for the *T66des9*, *ble*, and β-tubulin gene; RT+/-, template RNA with/without reverse transcription

Table 1 Fatty acid composition of *A. limacinum* SR21 strains after cultivation for 60 h. (Data are expressed as the mean ± the variation of two replicates originating from two independent cultures. The data for each replicate are the mean of two separate runs of FA analysis. The FAs less than 0.01 g/l were considered as background signals and were not shown)

Strains	30-1		26-1	
FAs	g/l[a]	%[b]	g/l	%
C14:0	0.36±0.01	4.62±0.44	0.38±0.04	5.07±0.36
C16:0	4.35±0.3	55.18±0.92	3.99±0.19	52.94±0.02
C16:1	0.00	0.00	0.2±0.01	2.66±0.07
C18:0	0.09±0.04	1.1±0.54	0.1±0	1.4±0.09
C18:1	0.00	0.00	0.18±0	2.37±0.14
C20:5	0.02±0	0.3±0.01	0.02±0	0.29±0.02
C22:5	0.77±0.04	9.66±0.74	0.71±0.03	9.42±0.86
C22:6	2.31±0.18	29.11±0.82	2.05±0.14	27.13±0.57
Total	6.87±1.85		7.54±0.35	

[a] Grams per liter of the culture

[b] Percentage of total fatty acids

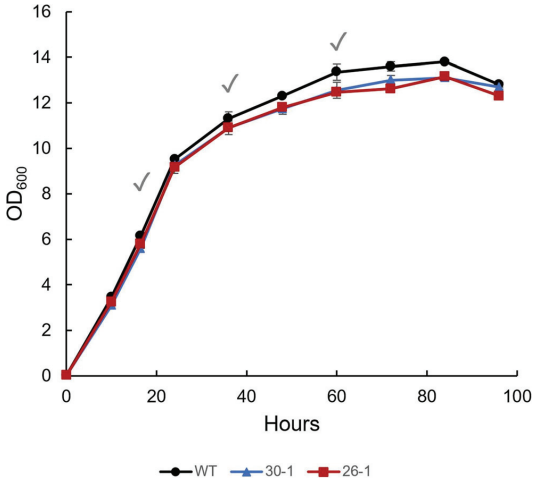

Fig. 5 The growth of *A. limacinum* SR21 strain WT, 30-1 and 26-1 in shake flasks using glucose as the carbon source, measured as optical density (OD_{600}); data are expressed as the mean of two replicates originating from two independent cultures; error bars represent the variation; checkmarks, sample collecting time points

Phylogenetic studies of desaturases have shown that Δ9-desaturases and Δ12-desaturases are well separated (Sperling et al. 2003; Wilding et al. 2017). However, the same papers also point out that since the assumed gene duplication and subsequent functional change to Δ9-desaturases or Δ12-desaturases took place fairly early in evolution, much of the amino acids now found to be specific for Δ9-desaturases or Δ12-desaturases might not really be necessary for their specific functions. Still, Fig. 1 shows that T66Des9 belongs to the clade identified as Δ12-desaturases (Wilding et al. 2017). A possible explanation could be that the Δ12-desaturase gene in an ancestral thraustochytrid cell became duplicated. Then, one of the duplicate genes evolved, possibly through the step of encoding a bifunctional Δ9/Δ12-desaturase into a Δ9-desaturase gene. In the ancestral T66 cell, the Δ12-desaturase gene was then lost. One similar incident has been described earlier in the house cricket (*Acheta domesticus*) (Zhou et al. 2008). This insect encodes a bifunctional Δ12/Δ9-desaturase AdD9des with low Δ9 desaturation activity that presumably evolved from a Δ9-desaturase (Zhou et al. 2008). The Δ9 desaturation activity of AdD9des could also be enhanced by point mutations, identified

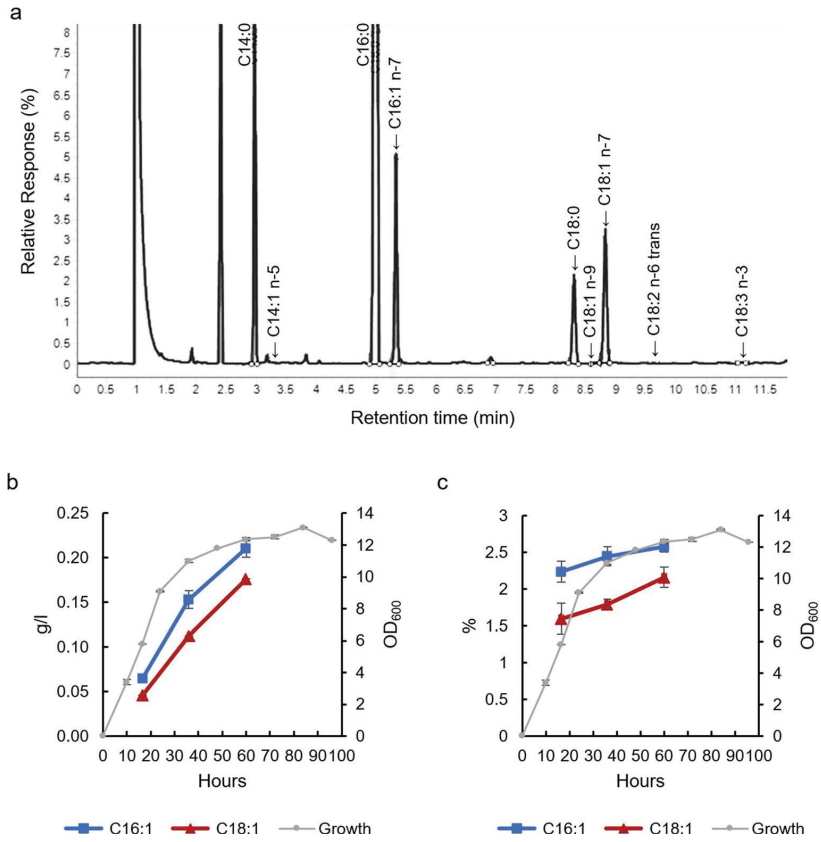

Fig. 6 **a** Partial gas chromatography chromatogram of FAMEs from *A. limacinum* SR21 strain 26-1 cultured for 60 hours. The positions of the FAs were based on the standard GCL-68D. The time course accumulation of C16:1 and C18:1 from *A. limacinum* SR21 strain 26-1 is shown by grams per liter of culture (**b**) and the percentage of total fatty acids (**c**). Data are the mean of two replicates originating from two independent cultures. The data for each replicate are the mean of two separate runs of FA analysis; cell growth is the mean of two replicates originating from two independent cultures and indicated as OD_{600}; error bars represent the variation

via directed evolution approaches, indicating that the Δ12 regioselectivity of AdD9des could gradually have been obtained by an ancestral Δ9-desaturase (Vanhercke et al. 2011). No diunsaturated FA were identified in our experiments, indicating that T66Des9 is not a bifunctional enzyme.

One of the reasons that thraustochytrids may not usually generate DHA through the DE pathway is that many strains are missing one or more of the expected DE pathway desaturases and elongases (Dellero et al. 2018; Liang et al. 2020; Meesapyodsuk and Qiu 2016). For example, here we demonstrated that *Aurantiochytrium* sp. T66 lacks the Δ12-desaturase annotated previously, because the gene instead encodes the Δ9-desaturase T66Des9 synthesizing C16:1 n-7, a FA that is not considered as a DHA precursor. Our findings are consistent with the possibility described in previous reports that *Aurantiochytrium* sp. T66 does not possess an intact FAS-DE pathway to produce DHA (Heggeset et al. 2019; Jakobsen et al. 2008).

C16:1 n-7 and a non-oleic C18:1 FA can be produced in *Thraustochytrium* sp. ATCC 26185 (Weete et al. 1997). It has earlier been demonstrated that C18:1 n-7 can be synthesized from C16:1 n-7 by TsELO2 of this strain (Ohara et al. 2013), while it was not known which enzyme produces C16:1 n-7. Since *Thraustochytrium* sp. ATCC 26185 has an identical protein to T66Des9, our discovery seems to be fitting the last piece into the puzzle of how *Thraustochytrium* sp. ATCC 26185 can produce the C18:1 n-7, presumably the non-oleic C18:1 found in the strain. Conjugated linoleic acid, the downstream product of C18:1 n-7, is substantially beneficial to human metabolism (Koba and Yanagita 2014). The potential values of C18:1 n-7 itself on health are also expanding (Blewett et al. 2009; Jacome-Sosa et al. 2016). The knowledge gained from this study demonstrates the potential of utilizing thraustochytrids to produce C18:1 n-7 by metabolic strain engineering.

Supplementary Information The online version contains supplementary material available at https://doi.org/10.1007/s00253-021-11425-5.

Acknowledgements We are grateful to Jackie L. Collier, Mariana Rius, and Joshua Rest (Stony Brook University, Stony Brook, NY, USA) for the help with suggesting the gene expression approach, sharing unpublished methods, and reviewing the manuscript. We thank Huong Bui and Janne Beate Øiaas (SINTEF Industry, Trondheim, Norway) for carrying out the fatty acid analyses.

Author contribution E-MR, IMA, and HE conceived and designed the experiments. E-MR and IMA performed the experiments. E-MR, IMA, and HE interpreted the results. E-MR, IMA, and HE wrote the manuscript. All authors read and approved the manuscript.

Funding Open access funding provided by NTNU Norwegian University of Science and Technology (incl St. Olavs Hospital - Trondheim University Hospital). The work was funded by a grant from the Research Council of Norway.

Availability of data and material The strains developed in this study are available upon request. All data generated or analyzed during this study are included in this published article and its supplementary information files.

Code availability Not applicable.

Declarations

Ethics approval This article does not contain any studies performed with human participants or animals by any of the authors.

Consent to participate Not applicable.

Consent for publication Not applicable.

Conflict of interest The authors declare no competing interests.

References

Aasen IM, Ertesvåg H, Heggeset TM, Liu B, Brautaset T, Vadstein O, Ellingsen TE (2016) Thraustochytrids as production organisms for docosahexaenoic acid (DHA), squalene, and carotenoids. Appl Microbiol Biotechnol 100:4309–4321. https://doi.org/10.1007/s00253-016-7498-4

AOCS (2017a) Fatty acid composition by GLC: marine oils. Official method Ce 1b-89. In: Official methods and recommended practices of the AOCS 7th ed. American Oil Chemists Society, Champaign, IL, pp 1b–89

AOCS (2017b) Preparation of methyl esters of long-chain fatty acids. Official method Ch 1-91. In: Official methods and recommended practices of the AOCS, 7th edn. American Oil Chemists Society, Champaign, IL, pp 1–91

Bai Y, McCoy JG, Levin EJ, Sobrado P, Rajashankar KR, Fox BG, Zhou M (2015) X-ray structure of a mammalian stearoyl-CoA desaturase. Nature 524:252–256. https://doi.org/10.1038/nature14549

Barclay W, Weaver C, Metz J, Hansen J (2010) Development of a docosahexaenoic acid production technology using *Schizochytrium*: historical perspective and update. In: Cohen Z, Ratledge C (eds) Single cell oils, microbial and algal oils, 2nd edn. AOCS Press, Urbana, IL, pp 75–96

Blewett HJ, Gerdung CA, Ruth MR, Proctor SD, Field CJ (2009) Vaccenic acid favourably alters immune function in obese JCR: LA-*cp* rats. Br J Nutr 102:526–536. https://doi.org/10.1017/S0007114509231722

Cahoon EB, Shah S, Shanklin J, Browse J (1998) A determinant of substrate specificity predicted from the acyl-acyl carrier protein

desaturase of developing cat's claw seed. Plant Physiol 117:593–598. https://doi.org/10.1104/pp.117.2.593

Dellero Y, Cagnac O, Rose S, Seddiki K, Cussac M, Morabito C, Lupette J, Aiese Cigliano R, Sanseverino W, Kuntz M, Jouhet J, Maréchal E, Rébeillé F, Amato A (2018) Proposal of a new thraustochytrid genus *Hondaea* gen. nov. and comparison of its lipid dynamics with the closely related pseudo-cryptic genus *Aurantiochytrium*. Algal Res 35:125–141. https://doi.org/10.1016/j.algal.2018.08.018

Domergue F, Spiekermann P, Lerchl J, Beckmann C, Kilian O, Kroth PG, Boland W, Zähringer U, Heinz E (2003) New insight into *Phaeodactylum tricornutum* fatty acid metabolism. Cloning and functional characterization of plastidial and microsomal Δ12-fatty acid desaturases. Plant Physiol 131:1648–1660. https://doi.org/10.1104/pp.102.018317

Faktorová D, Nisbet RER, Fernández Robledo JA, Casacuberta E, Sudek L, Allen AE, Ares M Jr, Aresté C, Balestreri C, Barbrook AC, Beardslee P, Bender S, Booth DS, Bouget FY, Bowler C, Breglia SA, Brownlee C, Burger G, Cerutti H, Cesaroni R, Chiurillo MA, Clemente T, Coles DB, Collier JL, Cooney EC, Coyne K, Docampo R, Dupont CL, Edgcomb V, Einarsson E, Elustondo PA, Federici F, Freire-Beneitez V, Freyria NJ, Fukuda K, Garcia PA, Girguis PR, Gomaa F, Gornik SG, Guo J, Hampl V, Hanawa Y, Haro-Contreras ER, Hehenberger E, Highfield A, Hirakawa Y, Hopes A, Howe CJ, Hu I, Ibañez J, Irwin NAT, Ishii Y, Janowicz NE, Jones AC, Kachale A, Fujimura-Kamada K, Kaur B, Kaye JZ, Kazana E, Keeling PJ, King N, Klobutcher LA, Lander N, Lassadi I, Li Z, Lin S, Lozano JC, Luan F, Maruyama S, Matute T, Miceli C, Minagawa J, Moosburner M, Najle SR, Nanjappa D, Nimmo IC, Noble L, Novák Vanclová AMG, Nowacki M, Nuñez I, Pain A, Piersanti A, Pucciarelli S, Pyrih J, Rest JS, Rius M, Robertson D, Ruaud A, Ruiz-Trillo I, Sigg MA, Silver PA, Slamovits CH, Smith GJ, Sprecher BN, Stern R, Swart EC, Tsaousis AD, Tsypin L, Turkewitz A, Turnšek J, Valach M, Vergé V, von Dassow P, von der Haar T, Waller RF, Wang L, Wen X, Wheeler G, Woods A, Zhang H, Mock T, Worden AZ, Lukeš J (2020) Genetic tool development in marine protists: emerging model organisms for experimental cell biology. Nat Methods 17:481–494. https://doi.org/10.1038/s41592-020-0796-x

Felsenstein J (1985) Confidence limits on phylogenies: an approach using the bootstrap. Evolution 39:783–791. https://doi.org/10.2307/2408678

Ghasemi Fard S, Wang F, Sinclair AJ, Elliott G, Turchini GM (2019) How does high DHA fish oil affect health? A systematic review of evidence. Crit Rev Food Sci Nutr 59:1684–1727. https://doi.org/10.1080/10408398.2018.1425978

Guo D-S, Ji X-J, Ren L-J, Li G-L, Sun X-M, Chen K-Q, Gao S, Huang H (2018) Development of a scale-up strategy for fermentative production of docosahexaenoic acid by *Schizochytrium* sp. Chem Eng Sci 176:600–608. https://doi.org/10.1016/j.ces.2017.11.021

Hauvermale A, Kuner J, Rosenzweig B, Guerra D, Diltz S, Metz JG (2006) Fatty acid production in *Schizochytrium* sp.: involvement of a polyunsaturated fatty acid synthase and a type I fatty acid synthase. Lipids 41:739–747. https://doi.org/10.1007/s11745-006-5025-6

Heggeset TMB, Ertesvåg H, Liu B, Ellingsen TE, Vadstein O, Aasen IM (2019) Lipid and DHA-production in *Aurantiochytrium* sp. - responses to nitrogen starvation and oxygen limitation revealed by analyses of production kinetics and global transcriptomes. Sci Rep 9:19470. https://doi.org/10.1038/s41598-019-55902-4

Hilgarth RS, Lanigan TM (2020) Optimization of overlap extension PCR for efficient transgene construction. MethodsX 7:100759. https://doi.org/10.1016/j.mex.2019.12.001

Iwasaka H, Koyanagi R, Satoh R, Nagano A, Watanabe K, Hisata K, Satoh N, Aki T (2018) A possible trifunctional β-carotene synthase gene identified in the draft genome of *Aurantiochytrium* sp. strain KH105. Genes 9:200. https://doi.org/10.3390/genes9040200

Jacome-Sosa M, Vacca C, Mangat R, Diane A, Nelson RC, Reaney MJ, Shen J, Curtis JM, Vine DF, Field CJ, Igarashi M, Piomelli D, Banni S, Proctor SD (2016) Vaccenic acid suppresses intestinal inflammation by increasing anandamide and related N-acylethanolamines in the JCR:LA-cp rat. J Lipid Res 57:638–649. https://doi.org/10.1194/jlr.M066308

Jakobsen AN, Aasen IM, Josefsen KD, Strøm AR (2008) Accumulation of docosahexaenoic acid-rich lipid in thraustochytrid *Aurantiochytrium* sp. strain T66: effects of N and P starvation and O_2 limitation. Appl Microbiol Biotechnol 80:297–306. https://doi.org/10.1007/s00253-008-1537-8

Jones DT, Taylor WR, Thornton JM (1992) The rapid generation of mutation data matrices from protein sequences. Comput Appl Biosci 8:275–282. https://doi.org/10.1093/bioinformatics/8.3.275

Kelley LA, Mezulis S, Yates CM, Wass MN, Sternberg MJE (2015) The Phyre2 web portal for protein modeling, prediction and analysis. Nat Protoc 10:845–858. https://doi.org/10.1038/nprot.2015.053

Koba K, Yanagita T (2014) Health benefits of conjugated linoleic acid (CLA). Obes Res Clin Pract 8:e525–e532. https://doi.org/10.1016/j.orcp.2013.10.001

Kumar S, Stecher G, Li M, Knyaz C, Tamura K (2018) MEGA X: molecular evolutionary genetics analysis across computing platforms. Mol Biol Evol 35:1547–1549. https://doi.org/10.1093/molbev/msy096

Liang L, Zheng X, Fan W, Chen D, Huang Z, Peng J, Zhu J, Tang W, Chen Y, Xue T (2020) Genome and transcriptome analyses provide insight into the omega-3 long-chain polyunsaturated fatty acids biosynthesis of *Schizochytrium limacinum* SR21. Front Microbiol 11:687. https://doi.org/10.3389/fmicb.2020.00687

Liu B, Ertesvåg H, Aasen IM, Vadstein O, Brautaset T, Heggeset TM (2016) Draft genome sequence of the docosahexaenoic acid producing thraustochytrid *Aurantiochytrium* sp. T66. Genom Data 8:115–116. https://doi.org/10.1016/j.gdata.2016.04.013

Liu Z, Chen O, Wall JBJ, Zheng M, Zhou Y, Wang L, Ruth Vaseghi H, Qian L, Liu J (2017) Systematic comparison of 2A peptides for cloning multi-genes in a polycistronic vector. Sci Rep 7:2193. https://doi.org/10.1038/s41598-017-02460-2

Marchan LF, Chang KJL, Nichols PD, Mitchell WJ, Polglase JL, Gutierrez T (2018) Taxonomy, ecology and biotechnological applications of thraustochytrids: a review. Biotechnol Adv 36:26–46. https://doi.org/10.1016/j.biotechadv.2017.09.003

Matsuda T, Sakaguchi K, Hamaguchi R, Kobayashi T, Abe E, Hama Y, Hayashi M, Honda D, Okita Y, Sugimoto S, Okino N, Ito M (2012) Analysis of Δ12-fatty acid desaturase function revealed that two distinct pathways are active for the synthesis of PUFAs in *T. aureum* ATCC 34304. J Lipid Res 53:1210–1222. https://doi.org/10.1194/jlr.M024935

Meesapyodsuk D, Qiu X (2016) Biosynthetic mechanism of very long chain polyunsaturated fatty acids in *Thraustochytrium* sp. 26185. J Lipid Res 57:1854–1864. https://doi.org/10.1194/jlr.M070136

Metz JG, Roessler P, Facciotti D, Levering C, Dittrich F, Lassner M, Valentine R, Lardizabal K, Domergue F, Yamada A, Yazawa K, Knauf V, Browse J (2001) Production of polyunsaturated fatty acids by polyketide synthases in both prokaryotes and eukaryotes. Science 293:290–293. https://doi.org/10.1126/science.1059593

Morabito C, Bournaud C, Maës C, Schuler M, Aiese Cigliano R, Dellero Y, Maréchal E, Amato A, Rébeillé F (2019) The lipid metabolism in thraustochytrids. Prog Lipid Res 76:101007. https://doi.org/10.1016/j.plipres.2019.101007

Muto M, Kubota C, Tanaka M, Satoh A, Matsumoto M, Yoshino T, Tanaka T (2013) Identification and functional analysis of delta-9 desaturase, a key enzyme in PUFA Synthesis, isolated from the oleaginous diatom *Fistulifera*. PLoS One 8:e73507. https://doi.org/10.1371/journal.pone.0073507

Nachtschatt M, Okada S, Speight R (2020) Integral membrane fatty acid desaturases: a review of biochemical, structural, and

biotechnological advances. Eur J Lipid Sci Technol 122:2000181. https://doi.org/10.1002/ejlt.202000181

Nagano N, Sakaguchi K, Taoka Y, Okita Y, Honda D, Ito M, Hayashi M (2011) Detection of genes involved in fatty acid elongation and desaturation in thraustochytrid marine eukaryotes. J Oleo Sci 60: 475–481. https://doi.org/10.5650/jos.60.475

Nagao K, Murakami A, Umeda M (2019) Structure and function of Δ9-fatty acid desaturase. Chem Pharm Bull (Tokyo) 67:327–332. https://doi.org/10.1248/cpb.c18-01001

Ohara J, Sakaguchi K, Okita Y, Okino N, Ito M (2013) Two fatty acid elongases possessing C18-Δ6/C18-Δ9/C20-Δ5 or C16-Δ9 elongase activity in *Thraustochytrium* sp. ATCC 26185. Mar Biotechnol (NY) 15:476–486. https://doi.org/10.1007/s10126-013-9496-1

Rius M (2021) Evolutionary origins, regulation, and function of carotenoid biosynthesis in the marine heterotrophic eukaryote, *Aurantiochytrium limacinum*. Stony Brook University, Doctoral dissertation

Robert X, Gouet P (2014) Deciphering key features in protein structures with the new ENDscript server. Nucleic Acids Res 42:W320–W324. https://doi.org/10.1093/nar/gku316

Sakaguchi K, Matsuda T, Kobayashi T, Ohara J, Hamaguchi R, Abe E, Nagano N, Hayashi M, Ueda M, Honda D, Okita Y, Taoka Y, Sugimoto S, Okino N, Ito M (2012) Versatile transformation system that is applicable to both multiple transgene expression and gene targeting for thraustochytrids. Appl Environ Microbiol 78:3193–3202. https://doi.org/10.1128/aem.07129-11

Shanklin J, Whittle E, Fox BG (1994) Eight histidine residues are catalytically essential in a membrane-associated iron enzyme, stearoyl-CoA desaturase, and are conserved in alkane hydroxylase and xylene monooxygenase. Biochemistry 33:12787–12794. https://doi.org/10.1021/bi00209a009

Sperling P, Ternes P, Zank TK, Heinz E (2003) The evolution of desaturases. Prostaglandins Leukot Essent Fat Acids 68:73–95. https://doi.org/10.1016/s0952-3278(02)00258-2

Sprague M, Dick JR, Tocher DR (2016) Impact of sustainable feeds on omega-3 long-chain fatty acid levels in farmed Atlantic salmon, 2006–2015. Sci Rep 6:21892. https://doi.org/10.1038/srep21892

Sun XM, Xu YS, Huang H (2020) Thraustochytrid cell factories for producing lipid compounds. Trends Biotechnol 39:648–650. https://doi.org/10.1016/j.tibtech.2020.10.008

Thelen JJ, Ohlrogge JB (2002) Metabolic engineering of fatty acid biosynthesis in plants. Metab Eng 4:12–21. https://doi.org/10.1006/mben.2001.0204

Vanhercke T, Shrestha P, Green AG, Singh SP (2011) Mechanistic and structural insights into the regioselectivity of an acyl-CoA fatty acid desaturase via directed molecular evolution. J Biol Chem 286: 12860–12869. https://doi.org/10.1074/jbc.M110.191098

Wang H, Klein MG, Zou H, Lane W, Snell G, Levin I, Li K, Sang BC (2015) Crystal structure of human stearoyl-coenzyme A desaturase in complex with substrate. Nat Struct Mol Biol 22:581–585. https://doi.org/10.1038/nsmb.3049

Weete JD, Kim H, Gandhi SR, Wang Y, Dute R (1997) Lipids and ultrastructure of *Thraustochytrium* sp. ATCC 26185. Lipids 32: 839–845. https://doi.org/10.1007/s11745-997-0107-z

Wilding M, Nachtschatt M, Speight R, Scott C (2017) An improved and general streamlined phylogenetic protocol applied to the fatty acid desaturase family. Mol Phylogenet Evol 115:50–57. https://doi.org/10.1016/j.ympev.2017.07.012

Yokochi T, Honda D, Higashihara T, Nakahara T (1998) Optimization of docosahexaenoic acid production by *Schizochytrium limacinum* SR21. Appl Microbiol Biotechnol 49:72–76. https://doi.org/10.1007/s002530051139

Zhou XR, Horne I, Damcevski K, Haritos V, Green A, Singh S (2008) Isolation and functional characterization of two independently-evolved fatty acid Δ12-desaturase genes from insects. Insect Mol Biol 17:667–676. https://doi.org/10.1111/j.1365-2583.2008.00841.x

Supplementary Information

Applied Microbiology and Biotechnology

A non-canonical Δ9-desaturase synthesizing palmitoleic acid identified in the thraustochytrid *Aurantiochytrium* sp. T66

Authors

E-Ming Rau[1], Inga Marie Aasen[2], Helga Ertesvåg[1*]

[1]Department of Biotechnology and Food Science, NTNU Norwegian University of Science and Technology, Trondheim, Norway

[2]Department of Biotechnology and Nanomedicine, SINTEF Industry, Trondheim, Norway

* Correspondence to: helga.ertesvag@ntnu.no

Supplemental Table S1 Strains used in this study

Strain	Description	Reference
T66	Wild-type *Aurantiochytrium* sp. T66	ATCC®
SR21	Wild-type *Aurantiochytrium limacinum* SR21	ATCC®
#26-1	Transgenic strain derived from SR21 with *crtIBY* disrupted by *ble*-2A-*T66des9* expression cassette	this study
#30-1	Transgenic strain derived from SR21 with *crtIBY* disrupted by *ble* expression cassette	this study

Supplemental Table S2 Plasmids used in this study

Plasmids	Description	Reference
pUC19-18GZG	Amp^R, *ble* flanked by SR21 endogenous GAPDH promoter and terminator	Addgene
pEMR15	Kan^R, pCR™Blunt II-TOPO® containing *ble* (rear part)-2A-*T66des9*-GAPDH terminator (front part)	This study
pEMR19	Kan^R, pCR™Blunt II-TOPO® containing *crtIBY* homologous flanking sequence (upper)	This study
pEMR20	Kan^R, pCR™Blunt II-TOPO® containing GAPDH promoter-*Ble* (front part)	This study
pEMR21	Kan^R, pCR™Blunt II-TOPO® containing GAPDH terminator (rear part)	This study
pEMR22	Kan^R, pCR™Blunt II-TOPO® containing *crtIBY* homologous flanking sequence (lower)	This study
pEMR23	Amp^R, containing GAPDH terminator (rear part)-*crtIBY* homologous flanking sequence (lower)	This study
pEMR24	Amp^R, GAPDH promoter-*ble*-2A-*T66des9*-GAPDH terminator expression cassette flanked by *crtIBY* homologous sequences	This study
pEMR26	Amp^R, GAPDH promoter-*ble*-GAPDH terminator expression cassette flanked by *crtIBY* homologous sequences	This study

Supplemental Table S3 Primers used in this study

Primer short name	Primer	Sequence 5'→3'	Underlined region
1	KI2957-1-SmaI	CTCCCGGGACTTCGTG	*Xma*I/*Sma*I
2	KI2957-2-2a	GTCTCCTGCTTGCTTGAGCAGAGAGAAGTTCGTG GCTCCGGATCCGTCCTGCTCCTCGGC	partial 2A sequence
3	KI2957-3-2a	GCCACGAACTTCTCTCTGCTCAAGCAAGCAGGAG ACGTGGAAGAAAACCCCGGTCCTTGCAAGGTGG AGCCC	partial 2A sequence
4	KI2957-4	TACATGTCGACTCTAGAGGATCCCCTTAGAGCGT CTTGGCCTTG	
5	KI2957-5	GGGGATCCTCTAGAGTCGAC	
6	KI2957-6	CAGAAATACTAGTTTTGTGAATGAAAAGAGATG ATAAAAG	*Spe*I
7	GAPDHpro_SbfI-F	ATACCTGCAGGGAGACGAGCATATGACTACTG	*Sbf*I
8	Ble_inside_SmaI-R	ACGAAGTCCCGGGAGAAC	*Xma*I/*Sma*I
9	GAPDHter_inside-SpeI-F	CATTCACAAAACTAGTATTTCTGCATTAGAAATC	*Spe*I
10	GAPDHter-NotI-R	ATAGCGGCCGCAGCGGATAACAATTTCACACAG G	*Not*I
11	SR21 CrtUF	GGTACCTGGATGCCTGAGGTCTTC	*Kpn*I
12	SR21 CrtUR	GGGCCCATTAATCCTGCAGGGAATACATGGCTGC GCTAC	*Sbf*I
13	SR21 CrtD-NotI-F	ATAGCGGCCGCCGCTCGCTTTCTTGGATACTG	*Not*I
14	SR21 CrtDR	ATTGTCACAGGGCGAACG	
15	21crt-midR	CGGCCGTGTTCATATAAGAG	
16	21CrtUFcheck	TGGCAGAGCTCATCAGTTTG	
	zeo sjekk-f	AGTTGACCAGTGCCGTTCC	
	zeoRT-r	CGAAGTCGTCCTCCACGAAG	
	SR21tubF2	TGTTGAGAACGCTGATGAGG	
	SR21tubR2	CGAGCTTACGGAGGTCAGAG	
	2957RT-f	GTCAACGCCTACCTCATTGGG	
	2957RT-r	CTTGGAGAAGAGGTGGTGCG	

Supplemental Table S4 T66Des9 homologs that showed the highest degree of identity with proteins encoded by different genera or thraustochytrids species using BLAST in the non-redundant protein sequences database at Genbank

Accession	Description	Species	Query Cover	E value	Per. Ident
AOG21009.1	delta12 desaturase	*Thraustochytrium* sp. ATCC 26185	100%	0	100.00%
GBG24140.1	Delta12-fatty-acid desaturase	*Hondaea fermentalgiana*	100%	0	80.65%
BAM37464.1	delta12-fatty acid desaturase (TauΔ12des)	*Thraustochytrium aureum*	99%	1.00E-124	44.12%
AAO23564.1	delta 12 fatty acid desaturase (PpDes12)	*Phaeodactylum tricornutum*	97%	8.00E-119	44.34%
BAO27791.1	delta12 desaturase-b	*Fistulifera solaris*	90%	1.00E-110	44.19%
OEU07512.1	delta 12 fatty acid desaturase	*Fragilariopsis cylindrus* CCMP1102	91%	2.00E-109	44.25%
XP_002292071.1	predicted protein	*Thalassiosira pseudonana* CCMP1335	91%	3.00E-106	41.67%
VEU44279.1	unnamed protein product	*Pseudo-nitzschia multistriata*	90%	2.00E-103	42.57%
CEM11741.1	unnamed protein product	*Vitrella brassicaformis* CCMP3155	88%	1.00E-101	43.32%
XP_009035621.1	hypothetical protein AURANDRAFT_24467	*Aureococcus anophagefferens*	87%	2.00E-100	42.01%
MBC8351339.1	fatty acid desaturase	*Planctomycetes bacterium*	86%	7.00E-93	42.12%
KAA8495721.1	Omega-6 fatty acid desaturase, endoplasmic reticulum isozyme 2	*Porphyridium purpureum*	96%	8.00E-93	38.69%
NLA37757.1	fatty acid desaturase	*Actinobacteria bacterium*	85%	7.00E-87	41.32%
XP_002507091.1	fatty acid desaturase	*Micromonas commoda*	94%	6.00E-85	38.06%
CEO99628.1	hypothetical protein PBRA_007361	*Plasmodiophora brassicae*	90%	7.00E-84	37.99%
XP_001454547.1	hypothetical protein	*Paramecium tetraurelia* strain d4-2	85%	2.00E-83	39.28%
NLD75814.1	fatty acid desaturase	*Acidimicrobiales bacterium*	92%	2.00E-82	39.19%
HBU37186.1	TPA: fatty acid desaturase	*Planctomycetaceae bacterium*	91%	8.00E-82	37.98%
KAF4668261.1	linoleoyl-CoA desaturase activity	*Perkinsus chesapeaki*	87%	2.00E-81	38.92%
XP_003075374.1	Fatty acid desaturase, type 1	*Ostreococcus tauri*	86%	1.00E-80	38.21%
RHZ75025.1	hypothetical protein Glove_218g3	*Diversispora epigaea*	95%	6.00E-80	34.91%

QDZ17765.1	delta(12)-fatty-acid desaturase	*Chloropicon primus*	84%	2.00E-78	38.72%
ABQ01458.1	oleate 12-hydroxylase	*Physaria lindheimeri*	84%	2.00E-78	38.14%
XP_018860212.1	delta(12)-fatty-acid desaturase FAD2-like	English walnut	93%	3.00E-78	38.78%
XP_004025050.1	hypothetical protein IMG5_193510	*Ichthyophthirius multifiliis*	91%	6.00E-78	37.28%
KRX08182.1	hypothetical protein PPERSA_12337	*Pseudocohnilembus persalinus*	88%	7.00E-78	36.19%
GHP07573.1	linoleoyl-CoA desaturase	*Pycnococcus provasolii*	84%	9.00E-78	40.77%
XP_022640459.1	omega-6 fatty acid desaturase, endoplasmic reticulum isozyme 2 isoform X2	mung bean	91%	2.00E-77	39.16%
KAF8643095.1	hypothetical protein HU200_066967	*Digitaria exilis*	95%	2.00E-77	38.00%
KAB8088627.1	hypothetical protein EE612_013286	rice	89%	3.00E-77	38.96%
XP_017220518.1	PREDICTED: delta(12)-fatty-acid desaturase FAD2-like	Daucus carota subsp. sativus	90%	4.00E-77	37.86%

Supplemental Table S5 List of thraustochytrid species encoding proteins closely related to T66Des9 by using BLAST in the databases[a] at Genbank

	nr[b]		wgs[c]	
Species	**Accession**	**Identity (%)**	**Accession**	**Identity (%)**
Aurantiochytrium sp. KH105			BGKB01000047.1	87
Aurantiochytrium sp. KH105			BGKB01000033.1	80
Hondaea fermentalgiana strain FCC1311	GBG24140.1	80.65	NPFB01000004.1	81
Schizochytrium sp. CCTCC M209059			JTFK01001013.1	86
Thraustochytrium aureum ATCC 34304	BAM37464.1	44.12	BLSG01000191.1	43
Thraustochytrium sp. ATCC 26185	AOG21009.1	100		

[a] No relevant results were obtained from the sequenced *heterokonts* available at JGI database. [b] The non-redundant protein sequences database at Genbank. [c] The *Labyrinthulomycetes* part of the whole genome shotgun database at Genbank

Supplemental Table S6 Fatty acid compositions of *A. limacinum* SR21 strains: all analyzed timepoints [a]

					g/l[b]				
Strain		**WT**			**30-1**			**26-1**	
Hr FA	16.5	36	60	16.5	36	60	16.5	36	60
C14:0	0.11±0.01	0.28±0.01	0.34±0.01	0.11±0.01	0.31±0.01	0.36±0.01	0.13±0.01	0.34±0.03	0.38±0.04
C15:0	0	0	0	0	0	0	0	0	0
C16:0	1.53±0.06	3.46±0.1	4.71±0.3	1.36±0.12	3.36±0.21	4.35±0.3	1.37±0.23	3.32±0.07	3.99±0.19
C16:1	0	0	0	0	0	0	0.06±0	0.15±0.01	0.2±0.01
C17:0	0	0	0	0	0	0	0	0	0
C18:0	0.02±0.03	0.05±0.07	0.12±0	0.04±0	0.06±0.03	0.09±0.04	0.04±0	0.09±0	0.1±0
C18:1	0	0	0	0	0	0	0.05±0	0.12±0	0.18±0
C20:5	0.02±0	0.02±0	0	0.01±0	0.02±0	0.02±0	0.01±0	0.02±0	0.02±0
C22:5	0.24±0.04	0.58±0.06	0.79±0.08	0.21±0	0.6±0.02	0.77±0.04	0.21±0.01	0.58±0.05	0.71±0.03
C22:6	0.74±0.11	1.8±0.12	2.63±0.48	0.64±0.02	1.78±0.01	2.31±0.18	0.66±0.08	1.66±0.02	2.05±0.14
Total	2.64±0.2	6.18±0.22	8.61±0.72	2.37±0.15	5.32±1.28	6.87±1.85	2.51±0.34	6.21±0.05	7.54±0.35

					%[c]				
Strain		**WT**			**30-1**			**26-1**	
Hr FA	16.5	36	60	16.5	36	60	16.5	36	60
C14:0	4.18±0.17	4.48±0.26	3.93±0.23	4.51±0.02	5.11±0.22	4.62±0.44	5.01±0.15	5.47±0.45	5.07±0.36
C15:0	0	0	0	0	0	0	0	0	0
C16:0	58.04±2.27	55.98±0.32	54.72±1.02	57.43±1.47	54.81±2.13	55.18±0.92	54.69±1.63	53.51±0.66	52.94±0.02
C16:1	0	0	0	0	0	0	2.36±0.14	2.42±0.13	2.66±0.07
C17:0	0	0	0	0	0	0	0	0	0
C18:0	0.78±1.1	0.74±1.04	1.36±0.06	1.78±0.1	1.03±0.51	1.1±0.54	1.71±0.14	1.44±0.02	1.4±0.09
C18:1	0	0	0	0	0	0	2.08±0.21	1.89±0.07	2.37±0.14
C20:5	0.29±0.01	0.26±0.01	0	0.3±0.01	0.27±0.02	0.3±0.01	0.28±0.01	0.26±0.01	0.29±0.02
C22:5	8.89±0.99	9.37±1.38	9.19±1.65	8.69±0.58	9.75±0.61	9.66±0.74	8.52±0.61	9.31±0.82	9.42±0.86
C22:6	27.82±2.2	29.18±0.93	30.47±3.07	27.26±0.79	29±0.75	29.11±0.82	26.57±0.5	26.73±0.45	27.13±0.57

[a]Data are expressed as the mean ±variation of two replicates originated from two independent cultures. The data of each replicate of strain 30-1 and 26-1 are the mean of two separate runs of FA analysis. [b]Grams per liter of the culture. [c]Percentage of total fatty acids. The FAs less than 0.01 g/l were considered as background signals and were not shown

Supplemental Table S7 Fatty acid compositions of *A. limacinum* SR21 strain 26-1 and *Aurantiochytrium* sp. T66 WT with the isomers distinguished

	Peak Area % of identified FAMEs	
Fatty acid	**26-1**	**T66**
C14:0	3.76	13.75
C14:1 n-5	< 0.1	< 0.1
C16:0	55.67	32.82
C16:1 n-7	2.64	13.62
C18:0	1.57	1.23
C18:1 n-9	< 0.1	< 0.1
C18:1 n-7	2.45	8.17
C18:3 n-3	< 0.1	< 0.1
C20:0	0.20	< 0.1
C20:4 n-6	0.23	0.15
C20:5 n-3 (EPA)	0.26	0.48
C22:0	0.11	< 0.1
C22:5 n-3 (DPA)	5.99	7.97
C24:0	< 0.1	0.17
C22:6 n-3 (DHA)	26.99	21.42
Sum identified FAMEs (%)	99.40	98.19
Sum unknown peaks (%)	0.60	1.65
LOQ 0.1%		

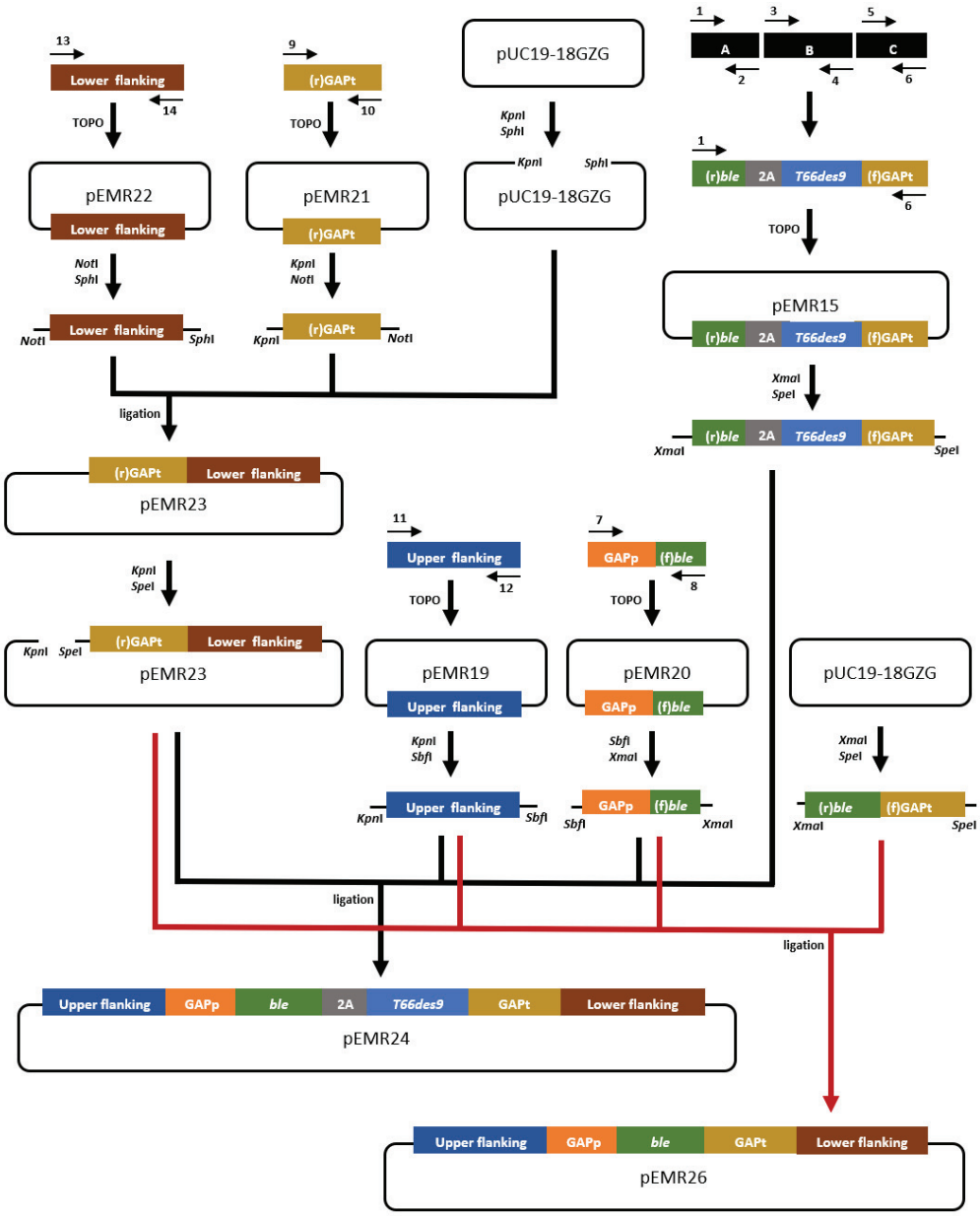

Supplemental Fig. S1 Scheme of constructing pEMR24 and pEMR26. Upper/Lower flanking: *crtIBY* homologous regions; GAPp: GAPDH promoter; GAPt: GAPDH terminator; (f)/(r)GAPt: the front/rear of GAPt ; *ble*: Zeocin resistance gene; (f)/(r)*ble*: the front/rear of *ble*; 2A: peptide self-cleavage sequence; 1~12: PCR primers

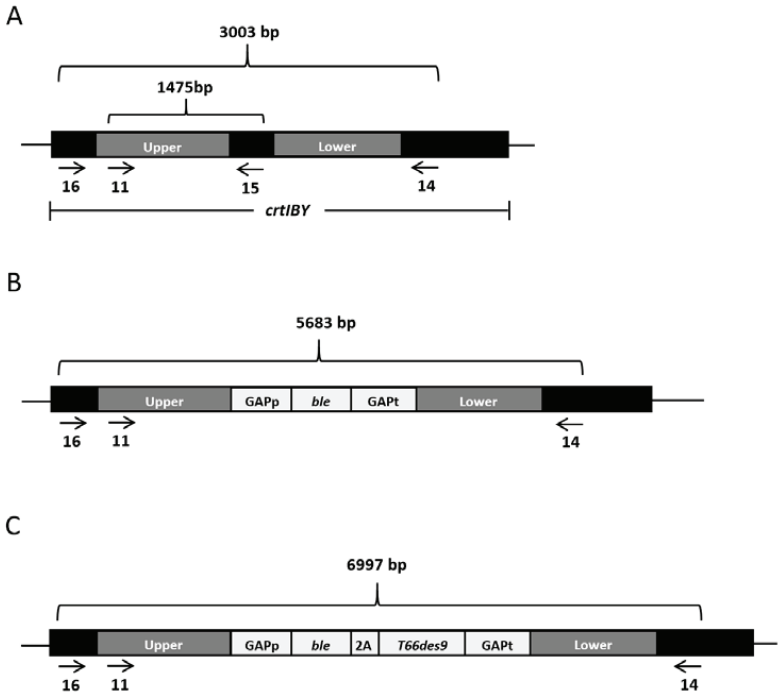

Supplemental Fig. S2 Illustration of the sizes of PCR products amplified from the gnomic DNA of (A) WT and non-transformants (30-18 and 30-22), (B) strain 30-1, 30-21 and 30-23, (C) strain 26-1. Primer pair 11+15 amplified fragments of 1475bp only from WT, 30-18 and 30-22. Primer pair 16 + 14 amplified larger PCR fragments of 6997bp and 5683bp from 26-1, and the three strains (30-1, 30-21 and 30-23), respectively. Primer pair 16 and 14 amplified a shorter fragment of 3003bp from WT, 30-18 and 30-22. Upper/Lower: *crtIBY* homologous regions; GAPp/t: GAPDH promoter/terminator; *ble*: Zeocin resistance gene; 2A: peptide self-cleavage sequence; Arrows: primer annealing sites

Paper IV

Aurantiochytrium species encode two acyl-CoA:diacylglycerol acyltransferase 2 like acyl-CoA:sterol acyltransferases whose overexpression facilitate squalene accumulation

E-Ming Rau[1], Zdenka Bartosova[1], Kåre Andre Kristiansen[1], Inga Marie Aasen[2], Per Bruheim[1], Helga Ertesvåg[1*]

[1]Department of Biotechnology and Food Science, NTNU Norwegian University of Science and Technology, Trondheim, Norway

[2]Department of Biotechnology and Nanomedicine, SINTEF Industry, Trondheim, Norway

*** Correspondence:**
Helga Ertesvåg
helga.ertesvag@ntnu.no

ISBN 978-82-326-5984-5 (printed ver.)
ISBN 978-82-326-5272-3 (electronic ver.)
ISSN 1503-8181 (printed ver.)
ISSN 2703-8084 (online ver.)

NTNU

Norwegian University of
Science and Technology